UNIVERSIDADE FEDERAL DE CIÊNCIAS DA SAÚDE DE PORTO ALEGRE
PROGRAMA DE PÓS-GRADUAÇÃO EM CIÊNCIAS DA SAÚDE

Thaís Casagrande Paim

Análise de biomateriais inovadores para regeneração óssea, cardiovascular e dérmica

Porto Alegre
2024

UNIVERSIDADE FEDERAL DE CIÊNCIAS DA SAÚDE DE PORTO ALEGRE

PROGRAMA DE PÓS-GRADUAÇÃO EM CIÊNCIAS DA SAÚDE

Thaís Casagrande Paim

Avaliação da biocompatibilidade de biomateriais inovadores para aplicação na medicina regenerativa

Tese submetida ao Programa de Pós-Graduação em Ciências da Saúde da Universidade Federal de Ciências da Saúde de Porto Alegre como requisito para a obtenção do grau de Doutora.

Porto Alegre
2024

Catalogação na Publicação

Casagrande Paim, Thaís
Análise de biomateriais inovadores para regeneração óssea, cardiovascular e dérmicaAnálise de biomateriais inovadores para regeneração óssea, cardiovascular e dérmica / Thaís Casagrande Paim. -- 2024.
123 f. : 30 cm.

Tese (doutorado) -- Universidade Federal de Ciências da Saúde de Porto Alegre, Programa de Pós-Graduação em Ciências da Saúde, 2024.

Orientador(a): Márcia Rosângela Wink.

1. Células Tronco Mesenquimais. 2. Biomateriais. 3. Regeneração óssea. 4. Ferro. 5. Substituto dérmico. I. Título.

Sistema de Geração de Ficha Catalográfica da UFCSPA com os dados fornecidos pelo(a) autor(a).

AGRADECIMENTOS

Gostaria de expressar minha gratidão a todos que contribuíram de alguma forma para a conclusão desta etapa acadêmica.

Agradeço à minha orientadora, Márcia Wink, por sua orientação e inspiração ao longo de todo o processo. Sua sabedoria, dedicação e apoio foram fundamentais para o desenvolvimento deste trabalho e para o meu crescimento acadêmico e profissional.

Aos meus colaboradores Diego e Rafaela, que foram parceiros essenciais na realização deste trabalho.

Ao PPGCS pelo apoio constante durante toda a minha pós-graduação.

À UFCSPA, seus professores, alunos, técnicos e funcionários, cuja contribuição foi inestimável para o meu trabalho.

Aos colegas do laboratório de biologia celular, em especial Alicce, Carla, Iago, Lili, Isa, Rafa, Sofia, meu sincero agradecimento pela troca de experiências, apoio e pelo ambiente colaborativo que tornou esta jornada mais enriquecedora e gratificante.

Aos membros da banca examinadora por dedicarem seu tempo para avaliá-lo, em especial à Professora Katya que fez relatoria deste trabalho.

Às agências de fomento pelo suporte financeiro.

Às minhas "roommates" ao longo deste período, Gabi, Meiski e Sami, pelos momentos de apoio e descontração.

À minha supervisora no exterior, Dra. Véronique Moulin, pela oportunidade de eu fazer doutorado sanduiche em seu laboratório no Canadá.

Aos colegas do centro de pesquisa CHU de Québec, pela acolhida durante esta experiência, Elodie, Sophie, Israël, Emilie, Syrine e Sébastien.

Aos meus pais, Domingas e Valdecir, pelo amor incondicional, apoio emocional e incentivo constante ao longo de toda a jornada acadêmica.

Ao Renan, pelo companheirismo, apoio emocional e incentivo ao longo destes anos.

Finalmente, gostaria de expressar minha gratidão a Deus. Minha fé foi fundamental para manter-me forte em meio às adversidades.

Dedico à minha nona Severina (In Memoriam)

SUMÁRIO

RESUMO

A engenharia de tecidos integra *scaffolds*, células e moléculas biologicamente ativas em substitutos biológicos de tecidos ou órgãos, desempenhando um papel crucial na regeneração de órgãos e tecidos danificados. Essa abordagem evolui em paralelo com os avanços na busca de novos biomateriais e na investigação do potencial das células tronco mesenquimais (MSCs). Os biomateriais têm sido aplicados em três áreas cruciais da medicina regenerativa: regeneração óssea, cardiovascular e dérmica. Para aplicação na regeneração óssea, biocerâmicas foram sintetizadas a partir de geopolímeros empregando uma mistura de metacaulinita (MK) e hidroxiapatita (HA). A metacaulinita, conhecida por suas propriedades mecânicas e a hidroxiapatita destacada pela sua biocompatibilidade foram testadas *in vitro* para verificar a sua biocompatibilidade utilizando MSCs derivadas do tecido adiposo humano (ADSCs). Os resultados demonstraram que os extratos de MK-HA não são citotóxicos para as ADSCs, que foram aptas a aderir e proliferar sobre o biomaterial. Na área cardiovascular, materiais metálicos biodegradáveis são candidatos promissores para uso em stents vasculares, uma vez que podem proporcionar um suporte estrutural temporário para o vaso durante o processo de remodelação das paredes. Entre esses materiais, o ferro destaca-se devido às suas propriedades mecânicas e biocompatibilidade. Utilizando a moldagem de pós-metálicos por injeção (MPI) e um novo ligante ecológico e nacional, a borracha extraída da seringueira (*Hevea brasiliensis*), amostras de ferro puro foram avaliadas e testadas quanto à biocompatibilidade *in vitro* com ADSCs e células endoteliais da veia umbilical humana, assim como *in vivo* foi testada por meio de implantes subcutâneos em ratos Wistar. Os resultados demonstraram a biocompatibilidade do ferro moldado por injeção. Além disso, foi desenvolvido um substituto dérmico com inibição da expressão de CD73 em queratinócitos e fibroblastos, proporcionando uma nova ferramenta para estudar o papel dessa molécula na regeneração tecidual e trazendo perspectivas para o desenvolvimento de novas terapias. Dessa forma, este trabalho contribui para o avanço da medicina regenerativa no que tange o desenvolvimento de terapias eficazes na regeneração de tecidos.

Palavras-Chave: Ferro Puro; Células tronco mesenquimais; Materiais Metálicos Biodegradáveis; Metacaulinita; Hidroxiapatita; Medicina Regenerativa

ABSTRACT

Tissue engineering integrates scaffolds, cells and biologically active molecules into biological tissue or organ substitutes, playing a crucial role in the regeneration of damaged organs and tissues. This approach evolves in parallel with advances in the search for new biomaterials and the investigation of the potential of mesenchymal stem cells (MSCs). Biomaterials have been applied in three crucial areas of regenerative medicine: bone, cardiovascular and dermal regeneration. For application in bone regeneration, bioceramics were synthesized from geopolymers using a mixture of metakaolinite (MK) and hydroxyapatite (HA). Metakaolinite, known for its mechanical properties, and hydroxyapatite highlighted for its biocompatibility were tested in vitro to verify their biocompatibility using MSCs derived from human adipose tissue (ADSCs). The results demonstrated that MK-HA extracts are not cytotoxic to ADSCs, which were able to adhere and proliferate on the biomaterial. In the cardiovascular area, biodegradable metallic materials are promising candidates for use in vascular *stents*, as they can provide temporary structural support for the vessel during the wall remodeling process. Among these materials, iron stands out due to its mechanical properties and biocompatibility. Using powder metal injection molding (MPI) and a new ecological and national binder, rubber extracted from the rubber tree (*Hevea brasiliensis*), pure iron samples were evaluated and tested for in vitro biocompatibility with ADSCs and vein endothelial cells human umbilical implant, as well as in vivo, was tested using subcutaneous implants in Wistar rats. The results demonstrated the biocompatibility of injection molded iron. Furthermore, a dermal substitute was developed with inhibition of CD73 expression in keratinocytes and fibroblasts, providing a new tool to study the role of this molecule in tissue regeneration and bringing perspectives for the development of new therapies. In this way, this work contributes to the advancement of regenerative medicine in terms of the development of effective therapies for tissue regeneration.

Key words: Pure Iron; Mesenchymal stem cells; Biodegradable Metallic Materials; Metakaolinite; Hydroxyapatite; Regenerative Medicine

1. REFERENCIAL TEÓRICO

1.1 MEDICINA REGENERATIVA E ENGENHARIA DE TECIDOS

A engenharia de tecidos e a medicina regenerativa destacam-se como campos biomédicos que trazem abordagens avançadas para a regeneração e cicatrização de tecidos danificados. O campo da engenharia de tecidos e da medicina regenerativa cresceu significativamente nas últimas décadas, e seus avanços envolveram diferentes áreas de pesquisa, incluindo design e processamento de biomateriais, modificação de superfícies e funcionalização para melhorar as interações célula-material (1).

Ainda que os termos sejam usados de maneira intercambiável, há diferenças entre eles. A engenharia de tecidos refere-se à prática de combinar *scaffolds*, células e moléculas biologicamente ativas em substitutos biológicos de tecidos ou órgãos que podem ser transplantados para o paciente (1–3). Esta abordagem tem evoluído em conjunto com os grandes avanços em biomateriais, células-tronco e tecnologias de manufatura aditiva (4).

Por outro lado, a medicina regenerativa é um campo mais amplo que inclui a engenharia de tecidos, mas também foca na regeneração dos tecidos diretamente no organismo. Isso envolve os próprios sistemas do corpo, algumas vezes combinados com materiais biológicos externos para recriar células e reconstruir tecidos e órgãos. Podem ser utilizadas estratégias como terapias celulares, imunomodulação, terapia genética, nanomedicina além da própria engenharia de tecidos (5). As células tronco constituem uma frente estratégica da medicina regenerativa (6).

O presente trabalho visa explorar novos biomateriais para dispositivos e implantes médicos, bem como o emprego de células-tronco, a fim de promover a regeneração tecidual e a restauração das funções afetadas.

1.2 CÉLULAS TRONCO MESENQUIMAIS

As MSCs têm sido amplamente estudadas nos últimos 30 anos, sua biologia celular e potencial clínico fazem delas um elemento central do desenvolvimento da engenharia de tecidos (7). Elas constituem uma população heterogênea de células

presentes em diferentes tecidos (Figura 5) e órgãos, tais como: medula óssea, sangue periférico, tecido adiposo, sinovial, derme, periósteo e dentes decíduos e em órgãos sólidos, como fígado e o pulmão. Os critérios para a caracterização das MSCs foram estabelecidos em 2006 pela Sociedade Internacional para a Pesquisa em Células-tronco (ISSCR). As células devem ter adesão ao plástico, capacidade de diferenciação em pelo menos três linhagens (ex.: osteogênica, condrogênica e adipogênica). Além disso, devem apresentar marcação fenotípica positiva para as proteínas de membrana CD105, CD73 e CD90 e negativa para CD45, CD34, CD11b, CD14, CD79a e HLA-DR (8).

As MSCs têm propriedades anti-inflamatórias, angiogênicas e imunomoduladoras que desempenham um papel crucial na cicatrização e regeneração tecidual (9). Em 11 de janeiro de 2023, um total de 1034 ensaios clínicos com os termos *mesenchymal stromal/stem cell-based* foram registrados nos Institutos Nacionais de Saúde dos EUA (https://clinicaltrials.gov/), incluindo testes em andamento, suspensos, completos e desconhecidos. Pesquisas indicam o uso promissor delas no tratamento de doenças neurodegenerativas, tais como o Alzheimer, doenças autoimunes, doenças ósseas e cartilaginosas, bem como doenças respiratórias, cardiovasculares, renais e hepáticas, além de neoplasias malignas, e a doença do enxerto contra hospedeiro (GvHD) (10).

Os efeitos terapêuticos das MSCs podem ser creditados a três principais mecanismos de ação: 1) a capacidade *homing,* que direciona as células para o local da lesão; 2) a capacidade de diferenciação celular que favorece a reparação do tecido lesado; e 3) a secreção de fatores bioativos (9,11). Essas características os tornam atraentes para aplicações em engenharia de tecidos (9)

No decorrer da inflamação aguda as MSCs são mobilizadas para a produção de fatores imunorreguladores. Nessas condições, as células T ativadas secretam citocinas pró-inflamatórias, tais como: IFNγ, TNF-α, IL-1 ou IL-17, que ativam as MSCs, iniciando a modulação das respostas imunes pela liberação de moléculas anti-inflamatórias, como prostaglandina E2, IL-10, HLA-G, indoleamina-2,3-dioxigenase, fator de crescimento de hepatócitos, fator de crescimento beta, NO, galectinas, semaforina-3A ou heme-oxigenase e quimiocinas (12,13). Os fatores de crescimento e quimiocinas liberados pelas MSCs têm a capacidade de induzir a migração e a proliferação celular na população adjacente, além de estimular a formação de novos vasos sanguíneos (14–16).

Atualmente, o tecido adiposo é uma das principais fontes de células tronco devido à sua acessibilidade, abundância e procedimento de coleta menos doloroso quando comparado a outras fontes (9,17). As células-tronco adiposo derivadas (ADSCs) são consideradas ferramentas promissoras para substituir, reparar e regenerar células mortas ou danificadas. Elas são usadas em diversas estratégias terapêuticas aplicadas em investigações clínicas. Estudos indicam que terapias celulares baseadas em ADSCs possuem eficácia e eficiência ideais em algumas condições clínicas, tanto para aplicação autóloga quanto alogênica (17,18).

Biomateriais podem apresentar diferentes aspectos bioquímicos e biomecânicos que influenciam a proliferação, migração e diferenciação de ADSCs (19). O uso de MSCs e sua associação com biomateriais é abordado no capítulo 1.

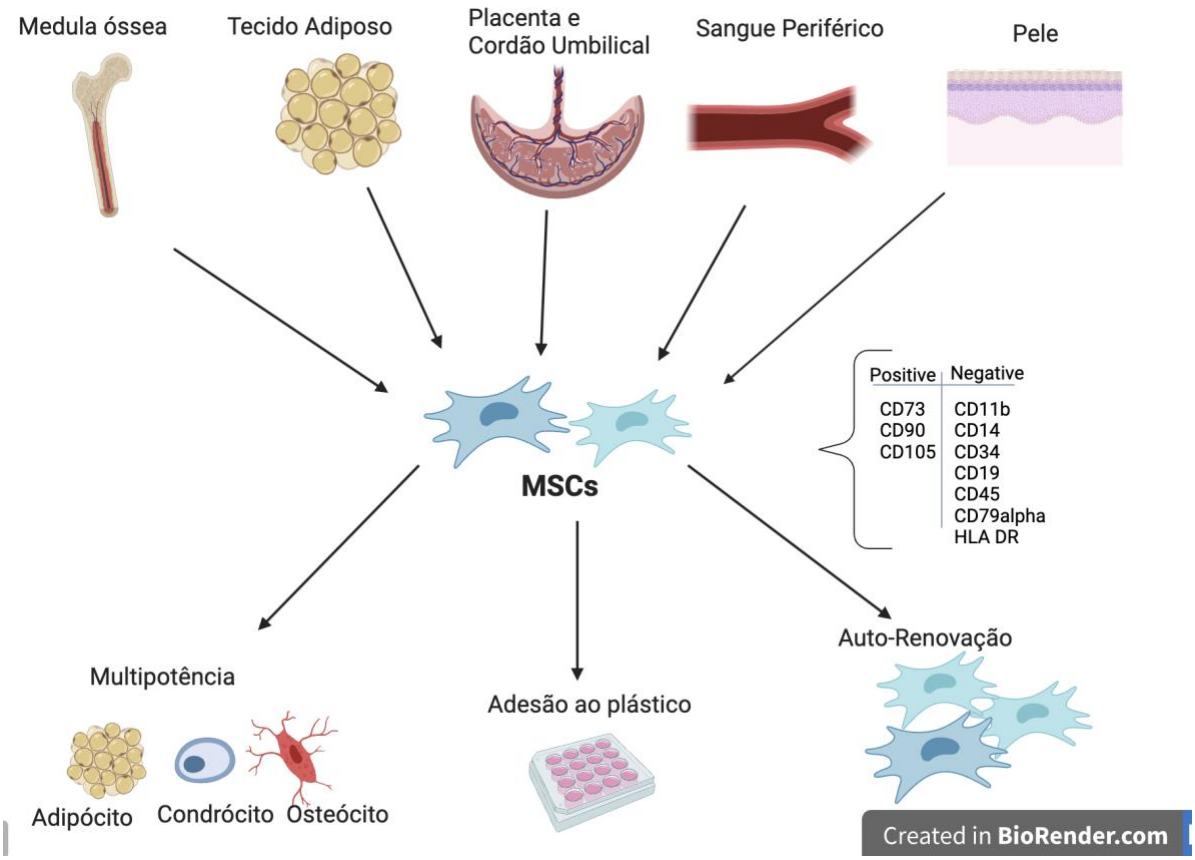

Figura 5. Principais fontes e características das MSCs. As MSCs estão presentes na medula óssea, tecido adiposo, placenta, cordão umbilical, sangue periférico, pele e diversos outros tecidos/órgãos. Elas possuem multipotência, podendo diferenciar-se, após estímulo químico ou físico, em qualquer célula especializada de origem mesodérmica. *In vitro,* elas são capazes de aderir ao plástico e autorrenovar-se, Fonte: Criado no BioRender.com. Adaptado de (20)

1.3 BIOMATERIAIS

Civilizações antigas empregavam materiais para fins médicos. Ossos, dentes de animais e até madeira eram utilizados para a substituição de dentes. Deformidades cranianas eram corrigidas utilizando ouro e marfim, enquanto as suturas eram realizadas com o uso de linho, crina de cavalo e algodão (21,22). Além de ossos e dentes, os enxertos de pele também têm uma história que remonta a milênios. O médico indiano Sushruta, que provavelmente viveu entre os séculos 12 e 6 a.C., em sua enciclopédia médica, a *Sushruta Samhita*, mencionou a primeira reconstrução nasal, realizada com enxerto de pele da própria bochecha do paciente. Os médicos daquela época, sem qualquer conhecimento sobre técnicas assépticas e mecânicas, conseguiam manter uma ferida aberta, limpa e viável, retirando uma parte da pele e recolocando-a para que pudesse ser revascularizada (23,24).

Com o desenvolvimento tecnológico e o aumento da expectativa de vida, a demanda por serviços de saúde de alta qualidade e acessíveis cresce. Por isso, hoje no âmbito da medicina regenerativa, um dos focos é o desenvolvimento de novos biomateriais e a exploração de métodos e técnicas inovadoras de fabricação (25).

Os biomateriais desempenham um papel fundamental na promoção da restauração de funções e no processo de cicatrização após lesões teciduais ou doenças (26). Eles são geralmente constituídos de múltiplos componentes que podem ser naturais ou sintéticos, vivos ou sem vida, os quais interagem com os sistemas biológicos e são frequentemente usados em aplicações médicas para melhorar ou substituir funções naturais do organismo (27).

Os biomateriais podem ser classificados quanto a sua estrutura química (metal, cerâmica, polímero e compósitos) (28,29) e conforme a interação que ocorre com o tecido: biotolerantes, bioativos e bioinertes (30). Os materiais biotolerantes, como o vidro e o silicone, não são rejeitados quando implantados no organismo, sendo envolvidos por uma camada de tecido fibroso em forma de cápsula composta principalmente por colágeno e fibroblastos. Os materiais bioinertes, como aço inoxidável, zircônia estabilizada, titânio, polietileno de ultra-alto peso molecular e alumina têm mínima interação com o tecido ao seu redor e não induzem o organismo a reagir contra o corpo estranho. Em contraste, os materiais bioativos, como as cerâmicas de fosfato de cálcio, permitem a interação direta do biomaterial com o

tecido, estimulando ou retardando funções celulares específicas. A troca iônica que ocorre entre a hidroxiapatita e os fluidos corporais ao seu redor, estabelece uma camada ativa de hidroxiapatita de carbonato sobre o implante, semelhante à fase mineral no osso (30) (31). Os biomateriais biodegradáveis, como a hidroxiapatita e o ferro, constituem uma classe de biomateriais bioativos que fornecem um suporte temporário para o processo de cicatrização de um tecido doente e se degrada progressivamente a partir de então (30,32).

Atualmente, os principais materiais utilizados na produção de dispositivos médicos incluem polímeros naturais e sintéticos, tais como proteínas, polissacarídeos, glicosaminoglicanos, ácido poliglicólico, ácido polilático (PLA), poli-ε-caprolactona. Além deles são empregados metais como, magnésio, ferro, titânio e suas ligas; cerâmicas, como alumina, zircônia, cimentos de fosfato de cálcio, e compósitos, os quais constituem a combinação de dois ou mais materiais distintos em suas propriedades físicas para obter um material com propriedades melhores que seus componentes individuais (33).

Os biomateriais servem como estruturas para direcionar a regeneração dos tecidos, alterar o microambiente ou atuar como transportadores para a liberação contínua de fatores biológicos. Suas propriedades físicas, biológicas e químicas distintas, resultam em variações na capacidade de promover a regeneração tecidual (34).

A aprovação de um novo biomaterial destinado ao desenvolvimento de um dispositivo biomédico requer várias etapas. Inicialmente é necessário identificar a necessidade de tratar alguma condição patológica ou substituir parcial ou totalmente um órgão ou tecido. Em seguida, o material é projetado e sintetizado, sendo submetido a diferentes testes (composição, estrutura, propriedades mecânicas, toxicologia, imunorreação, bioestabilidade etc.). Os materiais aprovados são produzidos em maior escala, esterilizados e encaminhados para testes mais específicos de biocompatibilidade em modelos *in vitro* e *in vivo*. Sendo os resultados obtidos promissores, é iniciado o processo regulatório referente à pré-aprovação, o qual compreende as etapas da pesquisa clínica em humanos que se estende mesmo após a liberação para uso clínico (35).

O processo de implantação de um biomaterial provoca lesões nos tecidos ou órgãos, desencadeando respostas inflamatórias, reações corporais e cicatrização. A resposta à lesão depende de inúmeros fatores como a extensão da área lesionada,

necrose celular, resposta inflamatória, perda de estruturas da membrana basal, interações sangue-material e formação de matriz provisória. Esses eventos podem afetar a formação de tecido de granulação, reação ao corpo estranho e desenvolvimento de fibrose ou cápsula fibrosa. Estas reações são consideradas normais e fornecem perspectivas sobre a biocompatibilidade. Elas ocorrem dentro de 2 a 3 semanas após a implantação e normalmente são solucionadas rapidamente, levando a fibrose ou formação de cápsula fibrótica (28,36).

Os biomateriais e as novas tecnologias estão sendo aplicados em três áreas cruciais da medicina regenerativa: a regeneração óssea, cardiovascular e dérmica.

1.4 REGENERAÇÃO ÓSSEA

As fraturas ósseas são uma das mais comuns injúrias teciduais e normalmente são causadas por traumas como acidentes de trânsito e esportivos, infecções, neoplasias, condições congênitas ou simplesmente pelo envelhecimento. A cicatrização de fraturas ósseas é um processo complexo, orquestrado e regenerativo que envolve células progenitoras, inflamatórias, endoteliais e hematopoiéticas (37). Embora o osso tenha uma excelente capacidade de reparação, a sua capacidade de corrigir defeitos maiores é limitada (38).

Os enxertos são necessários para substituir o tecido lesionado, materiais utilizados neste processo devem fornecer um ambiente estrutural ideal para as células que participam do processo de cicatrização óssea. O osso autógeno é considerado o “padrão ouro” para a regeneração óssea devido às suas propriedades osteogênicas, osteocondutoras e osteoindutoras. Porém, seu uso depende da disponibilidade óssea, apresentando desvantagens como risco de lesões vasculares-nervosas e morbidade no leito receptor. Uma alternativa menos invasiva são os enxertos ósseos xenogênicos, alogênicos e aloplásticos (39).

As limitações dos enxertos xenógenos, obtidos de diferente espécie, residem na sua capacidade limitada de serem completamente integrados ao osso, permanecendo na área implantada por longos períodos, além do risco de rejeição e transmissão de doenças. Enxertos ósseos alogênicos são obtidos de diferentes indivíduos da mesma espécie, eles possuem propriedades osteoindutoras reduzidas, além de apresentar maior risco de imunorreações e infecções.

Enxertos aloplásticos, substitutos ósseos naturais ou sintéticos como cerâmicas, polímeros e metais, têm sido empregados na engenharia de tecidos isoladamente ou em associação a fatores de crescimento ou células. As principais vantagens deste tipo de enxerto são a facilidade de manuseio, maior disponibilidade de formatos, tamanhos e de recursos para sua produção. Além disso, a ausência de risco de transmissão de doenças infecciosas (39) constitui outra vantagem. Dessa forma, objetiva-se criar biomateriais sintéticos que possuam as qualidades dos autos enxertos, mas sem suas restrições. Os novos biomateriais, além de regenerar tecidos, devem fornecer suporte mecânico durante o processo de cicatrização e evitar potenciais processos infecciosos causados por intervenções cirúrgicas (40).

Diferentes biomateriais têm sido propostos como substitutos sintéticos de enxertos ósseos, desde metais, até polímeros. Porém, os mais utilizados na reparação de partes danificadas ou doentes do músculo esquelético são as biocerâmicas e, entre elas, os ortofosfatos de cálcio, devido à sua semelhança com à fase mineral do osso (41).

1.4.1.1 Hidroxiapatita

A hidroxiapatita (HA)- tris(ortofosfato)hidróxido de pentacálcio (conhecido como Ca10(PO4)6(OH)2), é um fosfato de cálcio bioativo e biodegradável amplamente utilizado que tem similaridade química com o componente inorgânico da matriz óssea. Ela pode aumentar a concentração de Ca^{2+} local, ativando a proliferação de osteoblastos e promovendo o crescimento e diferenciação de MSCs. Devido às propriedades não imunogênicas, biocompatibilidade, bioatividade e boa condutividade óssea da HA, ela vem sendo utilizada na engenharia de tecidos ósseos e cada vez mais estudos exploram maneiras de melhorar suas propriedades físicas e funções biológicas (42)

No entanto, a hidroxiapatita não pode ser utilizada como único material protético devido à sua fragilidade e baixa tenacidade à fratura. Para aumentar a sua resistência ela já foi associada com óxido de alumínio, nanotubos de carbono, quitosana e colágeno, e outros materiais (43–45). Nós propomos no Capítulo II, associá-la a geopolímeros a fim de ter um biomaterial com as propriedades mecânicas dos geopolímeros, mas com a biocompatibilidade e características químicas da hidroxiapatita.

1.4.1.2 Geopolímeros

Os geopolímeros são uma classe de materiais cimentícios formados pela mistura de um sólido seco, um aluminossilicato (ex: metacaulinita, argila calcinada, entre outros) com uma solução alcalina que contém hidróxidos alcalinos, silicatos, aluminatos, carbonatos e/ou sulfatos. Eles apresentam boas propriedades mecânicas, devido a sua resistência e durabilidade (46,47).

A dissolução de materiais aluminossilicatos, que formam uma fase em gel, é a etapa dominante na geopolimerização. Durante a dissolução da matéria-prima são liberados alumínio (Al) e silício (Si), que passam pelo processo de polimerização, gerando um gel rico em Al. Posteriormente, o Si na solução reage com este gel, formando o gel final rico em Si. O principal produto da geopolimerização é o gel $Na_2O{-}Al_2O3\text{-}SiO_2{-}H_2O$. Os geopolímeros são formados com uma estrutura policristalina compacta (46).

Dentre os materiais aluminossilicatos que podem ser utilizados na geopolimerização, a metacaulinita se destaca como um material natural barato. MK é a fase amorfa da caulinita - que é o principal componente do caulim. O caulim é um mineral argiloso formado principalmente pela decomposição de feldspatos, granito e silicatos de alumínio (48). A caulinita é bastante utilizada em vidro e cerâmica devido às suas propriedades mecânicas.

Atualmente a pesquisa de novos geopolímeros para diversas aplicações está se expandindo, entre elas a regeneração óssea. No entanto, a baixa bioatividade dos geopolímeros é um desafio para a utilização destes materiais em aplicações biológicas. Nesse sentido, a hidroxiapatita pode ser incorporada à fase gel para aumentar a biocompatibilidade dos geopolímeros, agregando também suas características bioativas (46,49).

1.5 REGENERAÇÃO CARDIOVASCULAR

As doenças cardiovasculares são a principal causa de morte a nível mundial, elas corresponderam a 32% das mortes em 2019. Ataques cardíacos e acidente vascular cerebral (AVCs) constituem 85% dessas mortes (50,51). A angioplastia,

seguida da colocação de *stent* vascular, é o tratamento padrão para ataques cardíacos e é utilizada para tratamento e prevenção de AVCs (52).

No entanto, um obstáculo são as taxas de reestenose pós-colocação de *stent* que são significativas, 26-35% dos pacientes apresentam reestenose dentro de quatro anos (53,54) e *stents* de artérias periféricas apresentam 18-40% de reestenose após 12 anos (55,56). Por isso, para melhorar o desempenho do *stent*, há um enfoque em biomateriais reabsorvíveis e abordagens de engenharia avançadas com foco na regeneração vascular, especialmente através do uso de materiais metálicos

1.5.1 Materiais Metálicos

Os metais têm propriedades que os tornam adequados para aplicação em implantes biomédicos, principalmente em parafusos, pinos para fixação óssea e *stents* cardiovasculares. Eles possuem alta resistência tanto ao impacto quanto ao desgaste, além de uma alta capacidade para absorver energia de deformação em comparação a outros materiais (30,57,58).

Ao contrário do passado, quando o foco era a criação de implantes metálicos resistentes à corrosão, atualmente, um dos objetivos é desenvolver próteses que sejam não apenas mais fortes e duráveis, mas também biocompatíveis e biodegradáveis (59). Os metais biodegradáveis têm sido propostos mais comumente para aplicações cardiovasculares e ortopédicas, sendo esperado que eles se degradem por corrosão após providenciar o suporte estrutural pelo tempo necessário para a regeneração do tecido afetado (60,61). Contudo, novos usos estão sendo explorados, tal como filmes finos condutores de dispositivos eletrônicos bioabsorvíveis. Técnicas de microfabricação possibilitam a padronização desses metais biodegradáveis em uma variedade de componentes essenciais, como antenas, transistores, diodos, sensores e baterias que podem ser integrados em implantes médicos, sensores ambientais e dispositivos descartáveis para fins diagnóstico e terapêutico (62–66).

Apesar das inúmeras vantagens dos metais biodegradáveis, é imprescindível se atentar aos produtos de degradação liberados no organismo. Os produtos de corrosão devem provocar a menor resposta e toxicidade possível no organismo hospedeiro. Assim deve-se evitar ou utilizar apenas o mínimo necessário de componentes conhecidos por induzir tais efeitos. Além disso, os subprodutos de

degradação devem ser eficientemente transportados e excretados do corpo e não causar acúmulo local ou sistêmico (30,67–69).

1.5.1.1 Aplicação de biomateriais metálicos: *Stent* Vasculares

Metais suscetíveis à corrosão representam candidatos promissores para serem utilizados em *stents* cardiovasculares. Um *stent* cardiovascular é um pequeno tubo em formato de "malha" projetado para abrir uma artéria estreitada ou bloqueada (Figura 1), geralmente devido a placas de ateromas ou decorrente de doenças congênitas (58,70,71).

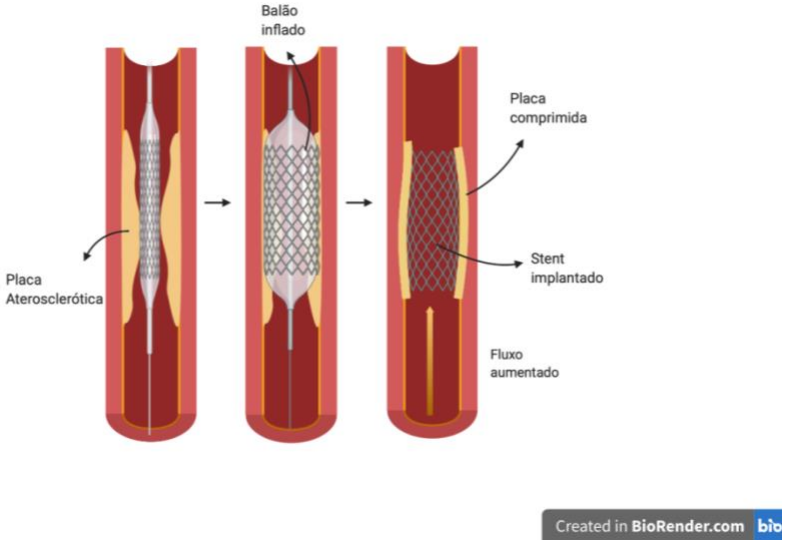

Figura 1. Angioplastia e implantação do *stent* em um vaso obstruído por placa aterosclerótica. Fonte: (20)(Criado no BioRender.com).

Na prática clínica, utiliza-se mais comumente *stents* permanentes, produzidos com metais resistentes à corrosão, tais como o aço inoxidável 316L, níquel-titânio e liga de cromo-cobalto (72–74). No entanto, em geral, os *stent*s são necessários apenas temporariamente, até que o processo de cicatrização e a re endotelização sejam alcançados. A longo prazo, os *stents* permanentes podem ocasionar complicações. Para mitigar efeitos adversos como inflamação crônica, reestenose, trombose e incompatibilidade de tamanho dos vasos, *stents* biodegradáveis estão sendo cada vez mais propostos.

Os *stents* metálicos biodegradáveis apresentam perspectivas promissoras, pois tem o objetivo de dar suporte a abertura das artérias até o remodelamento das suas paredes, o que normalmente ocorre entre 6 a 12 meses após o implante. Após 12 a 24 meses, esses *stents* devem desaparecer progressivamente do organismo pelo processo de corrosão (Figura 2) (61,75,76).

Polímeros como PLA; ácido poli-DL-láctico ácido poli-L-láctico; ácido poliglicólico; ácido poli-DL-lactídeo-co-glicólido; ácido co-glicólido poli-láctico; policaprolactona; ácido polilático/policaprolactona e policarbonatos e metais como ligas de magnésio com diferentes composições são exemplos de materiais mais utilizados em *stents* biodegradáveis, inclusive alguns deles já estão presentes na prática clínica (77) (78–80).

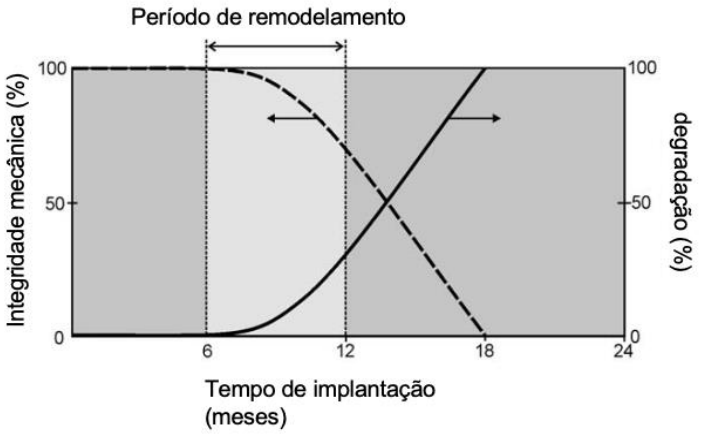

Figura 2. *Stent* biodegradável. Relação entre o tempo de degradação e de implantação de um *sten*t biodegradável ideal. Fonte: (HERMAWAN; DUBÉ; MANTOVANI, 2010)

Um *stent* biodegradável e os seus produtos de degradação devem ser biocompatíveis; o dispositivo deve permanecer no local de implantação por alguns meses antes de ser completamente bioabsorvido, deve garantir a integridade dinâmica funcional do vaso durante a sua degradação e a força radial deve manter o suporte estrutural do vaso pelo tempo necessário à terapia (76,81). Ademais, os materiais candidatos ao uso em *stents* metálicos biodegradáveis devem possuir propriedades mecânicas similares ao aço 316L, que é considerado o padrão de referência (58,82). Uma comparação entre os *stents metálicos* biodegradáveis e os permanentes pode ser observada na Tabela 1 (70,83).

Tabela 1. Comparação entre os *stents* biodegradáveis e os permanentes.

Características	***Stents* biodegradáveis**	***Stents* permanentes**
Suporte radial	Transitório	Permanente
Stress mecânico	Transitório	Permanente
Necessidade de prolongada terapia antiplaquetária	Não	Sim
Risco de trombose tardia	Não	Sim
Acompanhamento com técnicas não invasivas	Sim	Não
Ramos laterais presos permanentemente	Não	Sim
Facilidade de intervenção no segmento tratado	Sim	Não
Potencial recuperação da função endotelial	Sim	Não
Possível remodelação expansiva	Sim	Não
Inflamação	Alta	Baixa

Fonte:(20,70)

1.6 FERRO COMO BIOMATERIAL PARA STENTS BIODEGRADÁVEIS

O ferro puro pode ser um material apropriado para aplicações biomédicas, pois possui grande resistência radial devido ao seu alto módulo de elasticidade e é biocompatível. Ele é um dos melhores candidatos para *stents* metálicos biodegradáveis graças à sua biocompatibilidade, ductilidade, conformabilidade e alta resistência. As propriedades mecânicas destes são semelhantes aos já tradicionais *stents* de aço. Uma vantagem adicional é que o ferro é rádioopaco, não se fazendo

necessária adição de marcadores de fluorescência para localizar a endoprótese após o seu implante (84–87).

Em 2001, foi realizado o primeiro implante de um *stent* de ferro (Fe > 99,8%) na aorta descendente de coelhos. Os resultados indicaram uma resposta inflamatória moderada do vaso submetido à desobstrução e ausência de hiperplasia pronunciada. Após 6, 12 e 18 meses de implantação do *sten*t, não foram observados sinais de restenose do vaso ou formação de trombos. A avaliação histopatológica não identificou acúmulo do material degradado nos órgãos, nem toxicidade sistêmica (88). Em um estudo adicional do mesmo grupo de pesquisa, *stents* de ferro (Fe > 99,5%) e de aço 316L, foram implantados na aorta descendente de miniporcos, os quais foram acompanhados por 360 dias. A análise histopatológica dos órgãos também não indicou sinais de acúmulo de ferro ou toxicidade relacionada ao metal, nem se constatou diferença na proliferação celular neointimal vascular entre os materiais usados (89). Esses resultados indicam a segurança e a compatibilidade de *stents* de ferro durante longos períodos no ambiente biológico.

Os efeitos a curto prazo do implante de *stents* de ferro e de cromo-cobalto foram avaliados em artérias coronárias porcinas. Após 28 dias, havia sinais de degradação nos *stents* de ferro, a superfície deles apresentava uma coloração preta amarronzada e a parede vascular estava acastanhada, sem sinais de embolização ou trombose, nem deposição de fibrina. Não houve diferenças entre os animais que receberam o *stents* de ferro e os que receberam o de cobalto-cromo em nenhum dos parâmetros mensurados: Vasos (área do vaso, área do *stent*, área do lúmen e área medial), inflamação (injúria, inflamação, fibrina íntima e fibrose) e cicatrização (endotelização e células musculares lisas da íntima). Embora estatisticamente não significante, houve menor formação neointimal nos animais com o *stent* de ferro (87).

Em um estudo para elucidar os efeitos da deposição de fibrina na endotelização de *stents* de ferro, *stents* do material com focos de corrosão e de aço 316L foram implantados nas bifurcações das artérias carótida e ilíaca de coelhos. Após 15 dias, havia deposição de fibrina na superfície do *stent* e em 30 dias observou-se uma monocamada endotelial na superfície corroída do *stent* de ferro. Por outro lado, no *stent* de aço 316L, foram notadas poucas deposições de fibrinas e monocamadas endoteliais. Após 60 dias o *stent* estava totalmente coberto por células endoteliais. Os achados indicam que com a corrosão, numerosas fibrilas são depositadas no *stent* de

ferro o que facilita a adesão e proliferação de células endoteliais, o que, por sua vez, promove a endotelização após a colocação do *stent* (90).

Recentemente, a implantação de *stents* de ferro em animais hiperglicêmicos e normoglicêmicos revelou que a diabetes aumentou a degradação dos *stents* de ferro, contudo, isso resultou na inibição da reendotelização. Adicionalmente, a degradação dos *stents* de ferro teve um efeito positivo na regulação da resposta inflamatória. É importante destacar que os *stents* de ferro mesmo mais degradados em animais diabéticos exibiram uma hemocompatibilidade satisfatória (91).

1.5.1.2 Estratégias para aumentar a biodegradabilidade do Ferro

Ainda que o ferro seja biodegradável, os estudos indicam que o processo de corrosão de dispositivos de ferros é lento no organismo, por isso estratégias têm sido usadas para otimizar *stents* de ferro e aumentar sua biodegradabilidade. Um estudo de longo prazo (53 meses de acompanhamento) comparou a implantação de um *stent* de ferro puro com uma modificação no material feita com ferro nitretado. O dispositivo com ferro nitretado corroeu significativamente mais rápido do que o de ferro puro. A tecnologia se mostrou eficaz por obter o equilíbrio entre resistência à biocorrosão e plasticidade sem afetar a biocompatibilidade (92). Modificação de superfície também emerge como uma alternativa promissora.

O revestimento é um dos métodos para modificar as propriedades superficiais dos biomateriais. O PLA pode ser associado ao ferro puro na produção de *stents* em porcos o revestimento de PLA acelerou a corrosão do dispositivo. Cobertura íntima e respostas inflamatórias moderadas foram observadas juntamente com degradação do *stent*. O stent composto pelo polímero, apresentou excelente operabilidade no tratamento intervencionista de doenças cardiovasculares; sua segurança e eficácia também foram confirmadas preliminarmente. Apesar das vantagens apresentadas pelo novo *stent* biodegradável, a taxa de estenose de diâmetro do *stent* de ferro puro não foi melhor do que a do ferro com o PLA. Todavia, as taxas de estenose de diâmetro de ambos os *stents* foram inferiores a 50% são considerados aceitáveis (93)

Outra estratégia para aumentar a degradabilidade é alterar a densidade do material, uma vez que ela tem um papel importante na corrosão de implantes metálicos biodegradáveis. O processo de moldagem pós-metálicos por injeção (MPI) permite o controle da porosidade que impacta na densidade. A MPI consiste em 4

etapas principais: 1. Mistura: do ligante (polímero + ceras + ácidos) com o pó metálico para formar a matéria-prima. 2. Moldagem por injeção: a matéria-prima é aquecida e fornece a fluidez ao ligante permitindo a moldagem da peça verde em uma máquina de injeção. 3. *Debinding:* o ligante é retirado e a estrutura restante, chamada de peça marrom, é constituída apenas por pó metálico. 4. Sinterização: a estrutura metálica é aquecida e a união dos pós-metálicos ocorre por difusão. Nesta etapa é alcançada a resistência da peça sinterizada. A MPI permite o desenvolvimento de formas complexas de alta densidade, promovendo grande precisão dimensional. Além disso, este processo pode reduzir custos de produção e permitir a produção em larga escala (86).

Os *stents* de ferro têm sido implantados em animais, mostrando promissora aplicação médica. Contudo, ensaios clínicos em seres humanos ainda não foram conduzidos, e a literatura necessita de mais informações para avaliar a segurança e eficácia desses dispositivos.

1.5.1.3 Metabolismo do Ferro no organismo e implicação no desenvolvimento de dispositivos médicos

O ferro é essencial para o organismo humano, sendo o íon central no heme, o componente não protéico da hemoglobina, da mioglobina e dos citocromos. Ele tem facilidade em participar de reações de transferência de elétrons, podendo doar ou receber elétrons através da interconversão entre o íon férrico (Fe^{2+}) e o ferroso (Fe^{3+}) o que o torna um componente importante aos citocromos e as outras moléculas que se ligam ao oxigênio (94)

No intestino, a maioria do ferro da dieta é absorvida pelos enterócitos duodenais. No pH fisiológico, o ferro está no estado férrico oxidado (Fe^{3+}); para absorção, ele precisa estar no estado ferroso (Fe^{2+}) ou ligado a proteínas como o heme. O baixo pH do ácido gástrico no duodeno proximal permite que o citocromo B duodenal (converta íons férricos insolúveis (Fe^{3+}) em íons ferrosos absorvíveis (Fe^{2+}) na borda em escova dos enterócitos. Depois que o ferro férrico é reduzido a ferro ferroso, o transportador de cátions metálicos divalentes 1 (DMT1) transporta o ferro para os enterócitos. Uma vez dentro do enterócito, o ferro pode ser armazenado como ferritina ou transportado através para a circulação ligado à ferroportina (95).

O corpo humano tem em média 4 g de ferro, dos quais 2,5 g está presente na hemoglobina das hemácias; 1 g está armazenado nos macrófagos esplênicos e hepáticos, os quais reciclam a hemoglobina, e o restante está distribuído em proteínas como a mioglobina, citocromos e outras ferro proteínas. Apenas cerca de 3 mg está ligada a transferrina e constituem o compartimento de ferro móvel que supre os estoques intracelulares de ferro (96,97). O organismo necessita em média 20 mg de ferro para manter a eritropoiese. A maior parte dessa demanda é suprida pela recuperação do ferro das hemácias senescentes fagocitadas pelo retículo endotelial (98).

Carnes, aves, alguns frutos do mar, cereais prontos para o consumo e lentilhas são fontes importantes de ferro para o organismo. O ferro proveniente da dieta pode ser ingerido na forma do íon Fe^{2+} no grupo heme de fontes animais e Fe^{3+} de fontes vegetais não heme. O ferro de origem animal é menos abundante, mas é mais bem absorvido pelo organismo. Aproximadamente 10% do ferro ingerido é absorvido, o que equivale a aproximadamente 1 a 2 mg por dia, quantidade compensada pelas perdas naturais do corpo, principalmente pela descamação entérica e cutânea, além de pequenas perdas sanguíneas (99). O organismo não possui um mecanismo ativo para excretar o ferro do corpo. Por isso, uma carga contínua excedente de 1 a 2 mg por dia resulta em uma sobrecarga que pode afetar órgãos como o fígado, coração, tireóide, cérebro e pâncreas (100).

Apesar de ser fundamental para as funções biológicas, o excesso de ferro leva ao aumento da produção de espécies reativas de oxigênio (EROs) através da reação de Fenton. Nessa reação o Fe^{+2} reage com peróxido de hidrogênio (H_2O_2), e forma um radical hidroxila ($^{\bullet}OH$) e um íon hidróxido (OH^-), de acordo com a reação 1 (101).

$$Fe^{+2} + H_2O_2 \rightarrow Fe^{+3} + {}^{\bullet}OH + OH^-$$

Reação 1: Reação de Fenton

O radical hidroxila, é uma das mais agressivas EROs, pode induzir danos ao DNA e outras biomoléculas (102). As EROs induzem lesões no DNA e em proteínas e causam peroxidação de lipídeos (99). A exposição intensa a EROS pode resultar em mutações e outras alterações celulares levando a carcinogênese (103). O acúmulo de ferro e estresse oxidativo podem também induzir a agregação de algumas

proteínas, tais como Aβ e α-sinucleina, que possuem um papel crítico no Mal de Alzheimer e de Parkinson, respectivamente (104,105).

1.5.2 Estrutura dos vasos sanguíneos

Os *stents* são geralmente inseridos no interior de artérias e veias para restabelecer o fluxo sanguíneo. Assim como os demais componentes do sistema circulatório, coração, artérias, capilares, veias e linfáticos, as artérias e veias apresentam uma estrutura básica semelhante. Eles são revestidos internamente pelo endotélio e sua lâmina basal, que se apoiam na íntima. Em sequência existe a média, a músculo elástica e, mais externamente, a adventícia, constituída por tecido conjuntivo frouxo, contendo quantidades variáveis de tecido adiposo (Figura 3).

Nas paredes dos vasos sanguíneos há uma população de células-tronco vasculares (VSCs) capaz de se diferenciar em todos os tipos de células. Elas estão distribuídas por todo o sistema vascular, e atuam na manutenção da integridade dos vasos e na regulação da vasculogênese pós-natal. Com base nas propriedades antigênicas e diferenciação capacidade, as VSCs são divididas em quatro populações principais, conforme suas propriedades antigênicas e capacidade de diferenciação celular: MSCs, células progenitoras endoteliais , células progenitoras do músculo liso e células perivasculares (106,107).

As artérias possuem a túnica média mais espessa constituída por colágeno e quantidades variáveis de fibras elásticas e musculares lisas. Diferente das artérias, as veias possuem menor quantidade de fibras elásticas e musculares, porém apresentam válvulas na túnica interna que auxiliam o fluxo correto do sangue de volta ao coração (107,108).

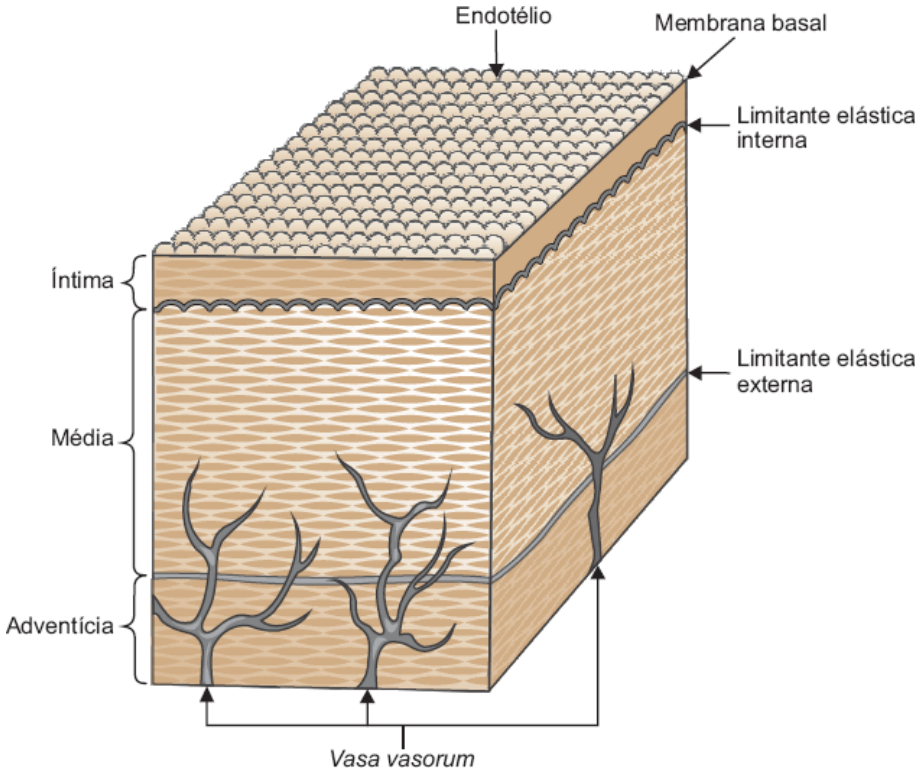

Figura 3. Estrutura de um grande vaso Sanguíneo Fonte: Alberts, 2017

As células endoteliais revestem internamente todos os vasos, formando uma camada trombo resistente que separa o sangue dos tecidos abaixo do endotélio, altamente trombogênicos. A camada endotelial é responsável pelas trocas entre o sangue e a parede dos vasos se comportando como uma membrana semipermeável capaz de selecionar aquilo que por ela passa. Além de revestirem os vasos e o coração, as células endoteliais secretam diferentes substâncias, tais como colágeno, elastina, proteoglicanas, citocinas vasodilatadoras e vasoconstritoras, moléculas de adesão, radicais livres, óxido nítrico, endotelinas, fatores de crescimento (107).

As células endoteliais vasculares organizam-se uma monocamada celular, o endotélio, que reveste o lúmen de todos os vasos sanguíneos. Ele atua no controle de trocas gasosas a nível pulmonar, regula o fluxo de células sanguíneas circulantes e moléculas bioativas como fatores de crescimento e proteínas da coagulação. O modelo clássico para o estudo dos diferentes aspectos das funções e alterações do endotélio utiliza as Células Endoteliais da Veia Umbilical Humana (HUVECs). Elas são importantes no estudo da toxicidade e trombogenicidade dos *stents* cardiovasculares, uma vez que atuam na endotelização do vaso após a implantação da prótese (109,110).

1.6 REGENERAÇÃO DÉRMICA

A pele, o maior e um dos órgãos mais complexos do corpo humano, é composta por duas principais camadas: a epiderme (queratinócitos, células de Langerhans, células de Merkel e melanócitos) e a derme (fibroblastos/células tronco mesenquimais, unidades pilossebáceas, glândulas sudoríparas, mastócitos e leucócitos infiltrantes). A pele possui funções complexas e insubstituíveis; lesões neste órgão podem ocasionar um desequilíbrio no ambiente interno corporal, além de danos externos (119).

A principal função da pele é proteger o corpo de estímulos do ambiente externo, como produtos químicos, luz, calor, lesões mecânicas e infecções. A pele também participa da regulação da temperatura, da detecção de informações, do armazenamento de energia/água e da regulação imunológica do corpo, o que torna o tecido da pele vital para a sobrevivência humana (111).

A cicatrização de feridas é uma resposta inerente que visa restaurar a integridade do tecido, sendo um processo complexo que envolve migração, proliferação e diferenciação celular, além da apoptose, síntese e remodelação da matriz extracelular. Feridas causadas por queimaduras ou traumas podem não cicatrizar adequadamente sem intervenção. A derme, ao contrário do fígado, ossos e da epiderme não pode se regenerar completamente após ser destruída, tornando difícil evitar cicatrizes durante o processo de cura natural. A reconstrução perfeita da derme representaria um avanço significativo nos métodos utilizados para a cicatrização de feridas (112).

Novas abordagens de engenharia para tratar feridas cutâneas têm sido desenvolvidas, incluindo células-tronco e substitutos dérmicos. A utilização de células mesenquimais de diferentes fontes facilita a regeneração da pele, tanto pela diferenciação em células locais, quanto pela secreção de fatores de crescimento. A incorporação de células na matriz extracelular resulta em substitutos de pele, utilizando diferentes abordagens, como membranas sintéticas para culturas mono ou multicamadas e matrizes tridimensionais (3D). Essas matrizes 3D podem estimular o fechamento funcional da ferida e são especialmente úteis em pacientes queimados (111).

Modelos de pele humana reconstruída são alternativas promissoras para a cicatrização de feridas e regeneração de tecidos. Substitutos de pele produzidos por engenharia de tecidos têm sido desenvolvidos e otimizados com base em condições de cultura, fontes celulares, tipos de células e substratos dérmicos sintéticos ou naturais, visando mimetizar a composição da pele (113). Os substitutos de pele automontados (SASS) possuem duas camadas altamente funcionais que compartilham muitas propriedades com a pele humana e são úteis para estudar a cicatrização de feridas cutâneas (114). Estes modelos são ferramentas valiosas em pesquisas experimentais para estudar a biologia da pele, permitindo avaliar a função das diferentes moléculas envolvidas no processo de regeneração tecidual.

1.7 SINALIZAÇÃO PURINÉRGICA

A sinalização purinérgica tem demonstrado um papel importante na via de reparo tecidual (115,116). Os nucleotídeos extracelulares (ATP, ADP, AMP, UTP) são moléculas sinalizadoras da cascata purinérgica e influenciam uma variedade de processos fisiológicos, como secreções endócrinas e exócrinas, respostas imunes, inflamação, proliferação, diferenciação, migração, morte celular e regeneração (117). Nucleotídeos e nucleosídeos podem ser liberados do meio intracelular por exocitose, ou devido a dano celulares para serem degradados e/ou atuarem sobre diferentes receptores no meio extracelular (118,119).

A molécula adenosina trifosfato (ATP) desempenha um papel central na sinalização durante condições injúria ou dano celular, sendo liberada no meio extracelular por células ativadas ou danificadas. No espaço extracelular, o ATP atua como uma molécula sinalizadora de perigo, desencadeando a cascata da sinalização purinérgica, composta por receptores purinérgicos e ectoenzimas. Os receptores purinérgicos são divididos em receptores metabotrópicos P1 (A1, A2A, A2B e A3) associados à adenosina (ADO), receptores ionotrópicos P2X (P2X1-7) e receptores metabotrópicos P2Y (P2Y1, P2Y2, P2Y4, P2Y6 e P2Y11-14) (120). A hidrólise dos nucleotídeos ocorre principalmente pela ação das ectoenzimas E-NTPDase1/CD39 (catalisa a hidrólise de ATP e ADP em AMP e da ecto-5’-nucleotidase/CD73 (catalisa a hidrólise de AMP em ADO) (121).

É crucial que a liberação fisiológica e a degradação dos nucleotídeos sejam reguladas para evitar uma resposta imune prolongada que pode desencadear um

aumento de mediadores inflamatórios, induzir o recrutamento excessivo de células imunes e estabelecer as condições inflamatórias crônicas, frequentemente acompanhadas de fibrose (122). A liberação de ATP nos locais de trauma pode estimular fibroblastos a aumentarem sua produção de matriz extracelular no processo cicatricial, resultando em fibrose tecidual (123). Além disso, segundo Nassani, ectoenzimas NTPDase1 e NPP1 parecem estar envolvidas na cicatrização de feridas e o UTP age promovendo a reepitelização e a proliferação de queratinócitos e fibroblastos (119).

No sistema vascular, a ruptura da parede do vaso, que atua como uma barreira integral separando o sangue dos elementos altamente reativos do subendotélio, como o colágeno e o fator tecidual, por estímulos bioquímicos ou físicos resulta na rápida ativação do endotélio, agregação plaquetária e acúmulo de leucócitos. A liberação secundária de nucleotídeos atua como um potente promotor de trombose e inflamação. O endotélio mantém a integridade vascular e a fluidez sanguínea através de mecanismos tromborreguladores endógenos, incluindo liberação de eicosanóides, geração de óxido nítrico, expressão de sulfato de heparano e catabolismo dos nucleotídeos purinérgicos (124).

Os nucleotídeos são liberados das células vasculares em taxas baixas, que aumentam quando as células são lesionadas ou estressadas. Esses nucleotídeos funcionam como moléculas sinalizadoras parácrinas potentes para ativar programas pró-trombóticos e pró-inflamatórios na vasculatura, exercendo sinalização mediada por receptores purinérgicos em plaquetas, células endoteliais, células musculares lisas e leucócitos.

Neste contexto, o aumento da expressão de enzimas e receptores purinérgicos podem ser utilizados como marcadores precoces de dano tecidual e afetar a agregação plaquetária, fatores importantes no processo de aterosclerose e remodelação do vaso após a inserção do *stent (124)*.

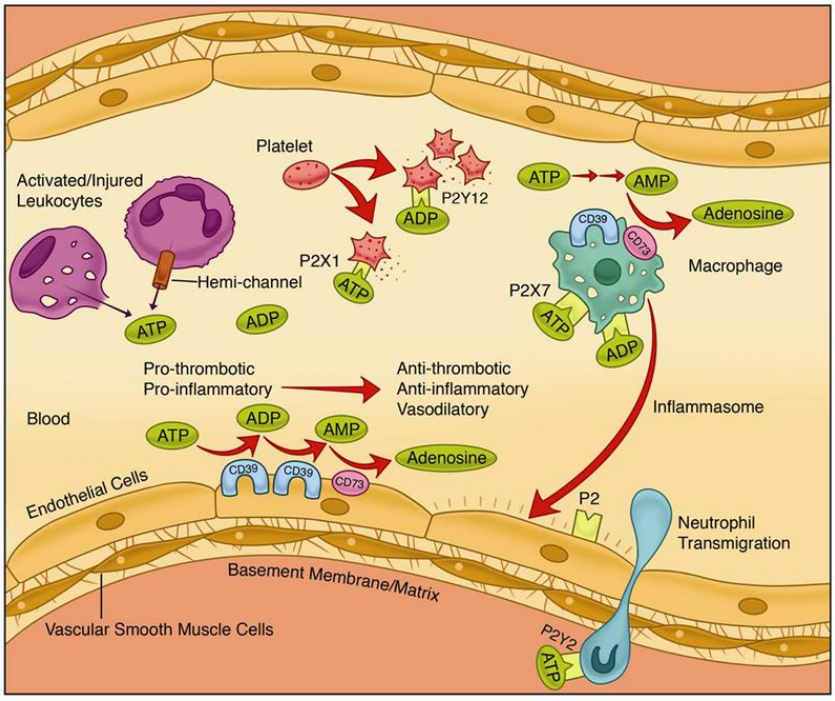

Figura 4 :Modulação da inflamação vascular e da trombose em resposta à lesão pelas enzimas purinérgicas CD39/CD73.

A via CD39/CD73 modula a inflamação vascular e a trombose em resposta à lesão (Figura 4). Os nucleotídeos liberados durante a ativação/lesão celular ligam-se aos receptores P2 para ativar eventos tromboinflamatórios na vasculatura, ligando-se aos receptores no endotélio, plaquetas e leucócitos. Os leucócitos endoteliais e células circulantes possuem a maquinaria catabólica que converte ATP/ADP em adenosina para extinguir os sinais pró-inflamatórios e pró-trombóticos e exercer um efeito vascular protetor potente (125).

A CD73 destaca-se como um marcador de superfície presente em diversos tipos celulares, como fibroblastos, queratinócitos e células tronco mesenquimais. Ela desempenha um papel fundamental na sinalização purinérgica, sendo uma das principais enzimas responsáveis por controlar os níveis de Adenosina Monofosfato (AMP) e adenosina (ADO) no meio extracelular, convertendo AMP em ADO (126). Essa atividade enzimática desempenha um papel essencial na homeostase celular e nas respostas fisiológicas da pele.

A importância da adenosina na regeneração de tecidos tem sido cada vez mais reconhecida. Estudos in vitro e in vivo sugerem que a geração excessiva de adenosina e a estimulação de seus receptores (P1) estão relacionadas ao aumento de lesões

ulcerativas e fibrose (123). Foi demonstrado que há um acúmulo de adenosina no fluido de bolhas formadas em queimaduras, podendo exercer efeitos variados dependendo de sua concentração, como efeitos anti-inflamatórios e disfunção do sistema imune (127). No entanto, apesar das evidências do envolvimento da adenosina na regeneração tecidual, a atividade enzimática da CD73 e seus efeitos no microambiente da lesão ainda não foram completamente elucidados.

2. JUSTIFICATIVA

Os avanços na medicina regenerativa são impulsionados por diversos fatores, como o aumento da expectativa de vida que eleva a suscetibilidade a doenças ósseas, cartilaginosas, dermatológicas, ortopédicas e neurológicas. Além disso, os desafios associados ao envelhecimento acarretam um maior número de lesões musculoesqueléticas. Em resposta a esses desafios, novas terapias para reparar e regenerar órgãos danificados e doentes estão sendo desenvolvidas, com destaque ao uso de células tronco mesenquimais e biomateriais como principais recursos terapêuticos utilizados.

No campo cardiovascular, o ferro é um dos elementos que se destaca para o uso em *stents* biodegradáveis, devido às suas características mecânicas e biocompatibilidade. O uso moldagem de pós-metálicos por injeção para a fabricação de dispositivos médicos biodegradáveis, se mostra uma opção. Na área de regeneração óssea a associação de biomateriais se mostra promissora. A hidroxiapatita que tem boa biocompatibilidade pode ser combinada com a metacaulinita que confere propriedades mecânicas adequadas.

Na área da regeneração dérmica o desenvolvimento de novos substitutos dérmicos surge como uma alternativa promissora no tratamento de lesões de pele e como ferramenta para o estudo das moléculas envolvidas na cicatrização. Ao inibir a expressão de CD73, podemos compreender melhor o processo de regeneração, criando abordagens terapêuticas mais eficazes e personalizadas para a cicatrização da pele.

Portanto, a análise das propriedades físico-químicas desses materiais, bem como sua biocompatibilidade com células e tecidos, é fundamental para o avanço dessas terapias regenerativas. No contexto da regeneração dérmica, o desenvolvimento de novos substitutos dérmicos surge como uma alternativa promissora no tratamento de lesões de pele, aproveitando-se dos avanços em biomateriais e na compreensão das moléculas envolvidas na cicatrização.

3. OBJETIVOS

3.1 OBJETIVO GERAL

Analisar a biocompatibilidade de biomateriais visando aplicações potenciais em regeneração tecidual e terapias regenerativas, com foco na regeneração óssea, cardiovascular e dérmica.

3.2 OBJETIVOS ESPECÍFICOS

a. Revisar, o potencial regenerativo das células-tronco mesenquimais e sua aplicabilidade em associação com biomateriais.
b. Desenvolver e avaliar ensaios de biocompatibilidade *in vitro* para biocerâmica de hidroxiapatita e metacaulinita proposta para regeneração óssea
c. Desenvolver e avaliar ensaios de biocompatibilidade *in vitro* e *in vivo* para o ferro 99,95% P.A produzido por moldagem de pós-metálicos por injeção para aplicação em *stents* cardiovasculares.
d. Avaliar o comportamento das células endoteliais da veia umbilical humana, após contato com ferro puro proposto como biomaterial para uso em *stents* cardiovasculares.
e. Desenvolver um substituto dérmico sem a expressão da CD73 (ecto-5′-nucleotidase) em fibroblastos e queratinócitos para avaliar o papel da enzima na regeneração dérmica.

REFERÊNCIAS BIBLIOGRÁFICAS

1. Pina S, Ribeiro VP, Marques CF, Maia FR, Silva TH, Reis RL, et al. Scaffolding Strategies for Tissue Engineering and Regenerative Medicine Applications. Materials . 2019 Jun 5;12(11):1824.

2. National Institute of Biomedical Imaging and Bioengineering [Internet]. [cited 2024 Jan 25]. Tissue Engineering and Regenerative Medicine. Available from: https://www.nibib.nih.gov/science-education/science-topics/tissue-engineering-and-regenerative-medicine

3. Berthiaume F, Maguire TJ, Yarmush ML. Tissue engineering and regenerative medicine: history, progress, and challenges. Annu Rev Chem Biomol Eng. 2011;2:403–30.

4. Şeker Ş, Elçin AE, Elçin YM. Advances in Regenerative Medicine and Biomaterials. Methods Mol Biol. 2023;2575:127–52.

5. Tissue Engineering and Regenerative Medicine: Past, Present, and Future. In: International Review of Neurobiology. Academic Press; 2013. p. 1–33.

6. Bijukumar DR, McGeehan C, Mathew MT. Regenerative Medicine Strategies in Biomedical Implants. Curr Osteoporos Rep. 2018 Jun;16(3):236–45.

7. Pittenger MF, Discher DE, Péault BM, Phinney DG, Hare JM, Caplan AI. Mesenchymal stem cell perspective: cell biology to clinical progress. NPJ Regen Med. 2019 Dec 2;4:22.

8. Dominici M, Le Blanc K, Mueller I, Slaper-Cortenbach I, Marini F, Krause D, et al. Minimal criteria for defining multipotent mesenchymal stromal cells. The International Society for Cellular Therapy position statement. Cytotherapy. 2006;8(4):315–7.

9. Casagrande T. The versatility of mesenchymal stem cells: From regenerative medicine to COVID, what is next? Biocell. 2021 Dec 15;46(4):913–22.

10. Brown C, McKee C, Bakshi S, Walker K, Hakman E, Halassy S, et al. Mesenchymal stem cells: Cell therapy and regeneration potential. J Tissue Eng Regen Med. 2019 Sep;13(9):1738–55.

11. Vizoso FJ, Eiro N, Cid S, Schneider J, Perez-Fernandez R. Mesenchymal Stem Cell Secretome: Toward Cell-Free Therapeutic Strategies in Regenerative Medicine. Int J Mol Sci [Internet]. 2017 Aug 25;18(9). Available from: http://dx.doi.org/10.3390/ijms18091852

12. Jimenez-Puerta GJ, Marchal JA, López-Ruiz E, Gálvez-Martín P. Role of Mesenchymal Stromal Cells as Therapeutic Agents: Potential Mechanisms of Action and Implications in Their Clinical Use. J Clin Med Res [Internet]. 2020 Feb 6;9(2). Available from: http://dx.doi.org/10.3390/jcm9020445

13. García-Bernal D, García-Arranz M, Yáñez RM, Hervás-Salcedo R, Cortés A, Fernández-García M, et al. The Current Status of Mesenchymal Stromal Cells: Controversies, Unresolved Issues and Some Promising Solutions to Improve Their Therapeutic Efficacy. Front Cell Dev Biol. 2021 Mar 16;9:650664.

14. Meirelles L da S, da Silva Meirelles L, Fontes AM, Covas DT, Caplan AI. Mechanisms involved in the therapeutic properties of mesenchymal stem cells [Internet].

Vol. 20, Cytokine & Growth Factor Reviews. 2009. p. 419–27. Available from: http://dx.doi.org/10.1016/j.cytogfr.2009.10.002

15. Zimmerlin L, Park TS, Zambidis ET, Donnenberg VS, Donnenberg AD. Mesenchymal stem cell secretome and regenerative therapy after cancer. Biochimie. 2013 Dec;95(12):2235–45.

16. Sharma P, Kumar A, Dey AD, Behl T, Chadha S. Stem cells and growth factors-based delivery approaches for chronic wound repair and regeneration: A promise to heal from within. Life Sci. 2021 Mar 1;268:118932.

17. Mazini L, Rochette L, Amine M, Malka G. Regenerative Capacity of Adipose Derived Stem Cells (ADSCs), Comparison with Mesenchymal Stem Cells (MSCs). Int J Mol Sci [Internet]. 2019 May 22;20(10). Available from: http://dx.doi.org/10.3390/ijms20102523

18. Soltani A, Moradi M, Nejad AR, Moradi S, Javandoost E, Nazari H, et al. Adipose-derived Stem Cells: Potentials, Availability and Market Size in Regenerative Medicine. Curr Stem Cell Res Ther. 18(3):347–79.

19. Alonso-Goulart V, Carvalho LN, Marinho ALG, de Oliveira Souza BL, de Aquino Pinto Palis G, Lage HGD, et al. Biomaterials and Adipose-Derived Mesenchymal Stem Cells for Regenerative Medicine: A Systematic Review. Materials [Internet]. 2021 Aug 18;14(16). Available from: http://dx.doi.org/10.3390/ma14164641

20. Paim TC. Análise in vitro e in vivo da biocompatibilidade de amostras de Ferro com pureza absoluta (P.A.) de 99,95% e 99,5% produzidas por metalurgia do pó para uso em dispositivos médicos. 2020 [cited 2024 Feb 4]; Available from: https://repositorio.ufcspa.edu.br/handle/123456789/1666

21. Migonney V. History of Biomaterials [Internet]. Biomaterials. 2014. p. 1–10. Available from: http://dx.doi.org/10.1002/9781119043553.ch1

22. Stumpf A de SG, Bergmann C, Prietsch JR, Vicenzi J. Shear bond strength of metallic and ceramic brackets using color change adhesives. Dental Press J Orthod. 2013 Mar;18(2):76–80.

23. Bath K, Aggarwal S, Sharma V. Sushruta: Father of plastic surgery in Benares. J Med Biogr. 2019 Feb;27(1):2–3.

24. Pandit A. Development of Naturally-Derived Biomaterials and Optimization of Their Biomechanical Properties. In: N Ashammakhi RR, Chiellini E, editors. Topics in Tissue Engineering. 2007.

25. Ashammakhi N, GhavamiNejad A, Tutar R, Fricker A, Roy I, Chatzistavrou X, et al. Highlights on Advancing Frontiers in Tissue Engineering. Tissue Eng Part B Rev. 2022 Jun;28(3):633–64.

26. Biomaterials [Internet]. 2017 [cited 2020 Jan 18]. Available from: https://www.nibib.nih.gov/science-education/science-topics/biomaterials

27. Springer Nature [Internet]. 2020 [cited 2020 Mar 5]. Biomaterials - Latest research and news | Nature. Available from: https://www.nature.com/subjects/biomaterials

28. Ajmal S. Recent progress in development and applications of biomaterials. Materials Today: Proceedings. 2022 Jan 1;62(1):385–91.

29. Bharadwaj A. An Overview on Biomaterials and Its Applications in Medical Science. In: IOP Conference Series: Materials Science and Engineering [Internet]. 2021 [cited 2024 Feb 1]. Available from: https://iopscience.iop.org/article/10.1088/1757-899X/1116/1/012178

30. Hermawan H. Biodegradable Metals: State of the Art. 2012.

31. Eftekhar Ashtiani R, Alam M, Tavakolizadeh S, Abbasi K. The Role of Biomaterials and Biocompatible Materials in Implant-Supported Dental Prosthesis. Evid Based Complement Alternat Med. 2021 Aug 5;2021:3349433.

32. Godavitarne C, Robertson A, Peters J, Rogers B. Biodegradable materials. Orthop Trauma. 2017 Oct 1;31(5):316–20.

33. Festas AJ, Ramos A, Davim JP. Medical devices biomaterials – A review. Proc Inst Mech Eng Part L J Mat Des Appl [Internet]. 2019 Oct 20 [cited 2024 Jan 24]; Available from: https://journals.sagepub.com/doi/10.1177/1464420719882458

34. Wang YH, Wang DR, Guo YC, Liu JY, Pana J. The application of bone marrow mesenchymal stem cells and biomaterials in skeletal muscle regeneration. Regenerative Therapy. 2020 Dec 1;15:285–94.

35. Pires ALR, Bierhalz ACK, Moraes ÂM. BIOMATERIALS: TYPES, APPLICATIONS, AND MARKET [Internet]. Química Nova. 2015. Available from: http://dx.doi.org/10.5935/0100-4042.20150094

36. Anderson JM. Biocompatibility and Bioresponse to Biomaterials. In: Principles of Regenerative Medicine. Academic Press; 2019. p. 675–94.

37. Ho-Shui-Ling A, Bolander J, Rustom LE, Johnson AW, Luyten FP, Picart C. Bone regeneration strategies: Engineered scaffolds, bioactive molecules and stem cells current stage and future perspectives. Biomaterials. 2018 Oct;180:143–62.

38. Kiernan C, Knuth C, Farrell E. Endochondral Ossification: Recapitulating Bone Development for Bone Defect Repair. In: Developmental Biology and Musculoskeletal Tissue Engineering. Academic Press; 2018. p. 125–48.

39. Girón J, Kerstner E, Medeiros T, Oliveira L, Machado GM, Malfatti CF, et al. Biomaterials for bone regeneration: an orthopedic and dentistry overview. Braz J Med Biol Res. 2021 Jun 14;54(9):e11055.

40. Vallet-Regí M. Evolution of Biomaterials. Front Mater Sci. 2022 Mar 18;9:864016.

41. Ginebra MP, Espanol M, Maazouz Y, Bergez V, Pastorino D. Bioceramics and bone healing. EFORT Open Rev. 2018 May;3(5):173–83.

42. Shi H, Zhou Z, Li W, Fan Y, Li Z, Wei J. Hydroxyapatite Based Materials for Bone Tissue Engineering: A Brief and Comprehensive Introduction. Crystals. 2021 Feb 1;11(2):149.

43. Xiao Y, Gong T, Zhou S. The functionalization of multi-walled carbon nanotubes by in situ deposition of hydroxyapatite. Biomaterials. 2010 Jul;31(19):5182–90.

44. Balani K, Lahiri D, Keshri AK, Bakshi SR, Tercero JE, Agarwal A. The nano-scratch behavior of biocompatible hydroxyapatite reinforced with aluminum oxide and

carbon nanotubes. JOM. 2009 Sep 9;61(9):63–6.

45. Becerra J, Rodriguez M, Leal D, Noris-Suarez K, Gonzalez G. Chitosan-collagen-hydroxyapatite membranes for tissue engineering. J Mater Sci Mater Med. 2022 Jan 24;33(2):1–16.

46. Castillo H, Collado H, Droguett T, Vesely M, Garrido P, Palma S. State of the art of geopolymers: A review. E-polymers. 2022 Jan 1;22(1):108–24.

47. Ricciotti L, Apicella A, Perrotta V, Aversa R. Geopolymer Materials for Bone Tissue Applications: Recent Advances and Future Perspectives. Polymers [Internet]. 2023 Feb 22;15(5). Available from: http://dx.doi.org/10.3390/polym15051087

48. Bhuiya AW, Hu M, Sankar K, Keane PF, Ribero D, Kriven WM. Bone ash reinforced geopolymer composites. J Am Ceram Soc. 2021 Jun 1;104(6):2767–79.

49. de Andrade R, Paim TC, Bertaco, Isadora, Naasani L, Buchner S, et al. Hierarchically porous bioceramics based on geopolymer-hydroxyapatite composite as a novel biomaterial: Structure, mechanical properties and biocompatibility evaluation. Applied Materials Today. 2023 Aug 1;33:101875.

50. Cardiovascular diseases [Internet]. [cited 2024 Jun 11]. Available from: https://www.who.int/health-topics/cardiovascular-diseases/#tab=tab_1

51. CGHE. GACD. [cited 2024 Jun 11]. Cardiovascular diseases. Available from: https://www.gacd.org/about/what-we-do/what-are-ncds/heart-disease

52. Selvakumar PP, Rafuse MS, Johnson R, Tan W. Applying Principles of Regenerative Medicine to Vascular Stent Development. Front Bioeng Biotechnol. 2022 Mar 7;10:826807.

53. Taniwaki M, Stefanini GG, Silber S, Richardt G, Vranckx P, Serruys PW, et al. 4-year clinical outcomes and predictors of repeat revascularization in patients treated with new-generation drug-eluting stents: a report from the RESOLUTE All-Comers trial (A Randomized Comparison of a Zotarolimus-Eluting Stent With an Everolimus-Eluting Stent for Percutaneous Coronary Intervention). J Am Coll Cardiol. 2014 Apr 29;63(16):1617–25.

54. Cassese S, Byrne RA, Schulz S, Hoppman P, Kreutzer J, Feuchtenberger A, et al. Prognostic role of restenosis in 10 004 patients undergoing routine control angiography after coronary stenting. Eur Heart J. 2015 Jan 7;36(2):94–9.

55. Schillinger M, Sabeti S, Loewe C, Dick P, Amighi J, Mlekusch W, et al. Balloon angioplasty versus implantation of nitinol stents in the superficial femoral artery. N Engl J Med. 2006 May 4;354(18):1879–88.

56. Laird JR, Katzen BT, Scheinert D, Lammer J, Carpenter J, Buchbinder M, et al. Nitinol stent implantation versus balloon angioplasty for lesions in the superficial femoral artery and proximal popliteal artery: twelve-month results from the RESILIENT randomized trial. Circ Cardiovasc Interv. 2010 Jun 1;3(3):267–76.

57. Purnama A, Hermawan H, Champetier S, Mantovani D, Couet J. Gene expression profile of mouse fibroblasts exposed to a biodegradable iron alloy for stents. Acta Biomater. 2013 Nov;9(10):8746–53.

58. Moravej M, Mantovani D. Biodegradable metals for cardiovascular stent application: interests and new opportunities. Int J Mol Sci. 2011 Jun 29;12(7):4250–70.

59. Webster TJ, editor. Nanotechnology Enabled In situ Sensors for Monitoring Health. 2011.

60. Fagali NS, Grillo CA, Puntarulo S, Fernández Lorenzo de Mele MA. Cytotoxicity of corrosion products of degradable Fe-based stents: relevance of pH and insoluble products. Colloids Surf B Biointerfaces. 2015 Apr 1;128:480–8.

61. Hermawan H, Purnama A, Dube D, Couet J, Mantovani D. Fe-Mn alloys for metallic biodegradable stents: degradation and cell viability studies. Acta Biomater. 2010 May;6(5):1852–60.

62. Yu KJ, Kuzum D, Hwang SW, Kim BH, Juul H, Kim NH, et al. Bioresorbable silicon electronics for transient spatiotemporal mapping of electrical activity from the cerebral cortex. Nat Mater. 2016 Jul;15(7):782–91.

63. Lu D, Liu TL, Chang JK, Peng D, Zhang Y, Shin J, et al. Transient Light-Emitting Diodes Constructed from Semiconductors and Transparent Conductors that Biodegrade Under Physiological Conditions. Adv Mater. 2019 Oct;31(42):e1902739.

64. Singh R, Bathaei MJ, Istif E, Beker L. A Review of Bioresorbable Implantable Medical Devices: Materials, Fabrication, and Implementation. Adv Healthc Mater. 2020 Sep;9(18):e2000790.

65. Ryu H, Seo MH, Rogers JA. Bioresorbable Metals for Biomedical Applications: From Mechanical Components to Electronic Devices. Adv Healthc Mater. 2021 Sep;10(17):e2002236.

66. Salvatore GA, Sülzle J, Valle FD, Cantarella G, Robotti F, Jokic P, et al. Biodegradable and Highly Deformable Temperature Sensors for the Internet of Things. Adv Funct Mater. 2017 Sep 1;27(35):1702390.

67. Gu X, Zheng Y, Cheng Y, Zhong S, Xi T. In vitro corrosion and biocompatibility of binary magnesium alloys. Biomaterials. 2009 Feb;30(4):484–98.

68. Zhu D, Cockerill I, Su Y, Zhang Z, Fu J, Lee KW, et al. Mechanical Strength, Biodegradation, and in Vitro and in Vivo Biocompatibility of Zn Biomaterials. ACS Appl Mater Interfaces. 2019 Feb 20;11(7):6809–19.

69. Mantovani D, Witte F. Acta Biomaterialia Special Issue: 4th Biometal 2012, Maratea, Italy: August 27-September 1, 2012. Acta Biomater. 2013 Nov;9(10):8474.

70. Gonzalo N, Macaya C. Absorbable stent: focus on clinical applications and benefits. Vascular Health and Risk Management. 2012;125.

71. Toong, Daniel W, Ng, Jaryl C. K., Huang, Y., Wong, P. E. H., Leo, Hwa L., S. S. V., Ang, Hui Y. Bioresorbable metals in cardiovascular stents: Material insights and progress. Materialia. 2020 Aug 1;12:100727.

72. Saraf AR, Yadav SP. Fundamentals of bare-metal stents. In: Functionalised Cardiovascular Stents. Woodhead Publishing; 2018. p. 27–44.

73. Kapoor D. Nitinol for Medical Applications: A Brief Introduction to the Properties and Processing of Nickel Titanium Shape Memory Alloys and their Use in Stents [Internet]. Vol. 61, Johnson Matthey Technology Review. 2017. p. 66–76. Available from: http://dx.doi.org/10.1595/205651317x694524

74. Mori H, Atmakuri DR, Torii S, Braumann R, Smith S, Jinnouchi H, et al. Very

Late Pathological Responses to Cobalt–Chromium Everolimus-Eluting, Stainless Steel Sirolimus-Eluting, and Cobalt–Chromium Bare Metal Stents in Humans [Internet]. Vol. 6, Journal of the American Heart Association. 2017. Available from: http://dx.doi.org/10.1161/jaha.117.007244

75. Erne P, Schier M, Resink TJ. The Road to Bioabsorbable Stents: Reaching Clinical Reality? [Internet]. Vol. 29, CardioVascular and Interventional Radiology. 2006. p. 11–6. Available from: http://dx.doi.org/10.1007/s00270-004-0341-9

76. Saito S. New horizon of bioabsorbable stent. Catheter Cardiovasc Interv. 2005 Dec;66(4):595–6.

77. Scafa Udriște A, Niculescu AG, Grumezescu AM, Bădilă E. Cardiovascular Stents: A Review of Past, Current, and Emerging Devices. Materials [Internet]. 2021 May 12;14(10). Available from: http://dx.doi.org/10.3390/ma14102498

78. Magmaris [Internet]. [cited 2024 Jan 24]. Available from: https://www.biotronik.com/en-ch/products/coronary/magmaris

79. www.bostonscientific.com [Internet]. [cited 2024 Jan 24]. Sistema de stent cardíaco de polímero bioabsorvível - SYNERGY Stent. Available from: https://www.bostonscientific.com/pt-BR/produtos/stents-coronarios/sistema-de-stent-cardiaco-de-polimero-bioabsorvivel-synergy-stent.html

80. ABSORB GT1™ BIORESORBABLE VASCULAR SCAFFOLD SYSTEM [Internet]. [cited 2024 Feb 2]. Available from: https://www.fda.gov/media/96307/download

81. Narayan R, Wang M, Laurencin C, Yu X, Hellmich C, Krishnan S, et al. Encyclopedia of Biomedical Engineering. Narayan R, editor. Vol. 2. United States: Elsevier; 2019.

82. Fu J, Su Y, Qin YX, Zheng Y, Wang Y, Zhu D. Evolution of metallic cardiovascular stent materials: A comparative study among stainless steel, magnesium and zinc. Biomaterials. 2020 Feb;230:119641.

83. Zong J, He Q, Liu Y, Qiu M, Wu J, Hu B. Advances in the development of biodegradable coronary stents: A translational perspective. Mater Today Bio. 2022 Dec;16:100368.

84. Gąsior G, Szczepański J, Radtke A. Biodegradable Iron-Based Materials—What Was Done and What More Can Be Done? Materials . 2021 Jun 18;14(12):3381.

85. Paim TC, Wermuth DP, Bertaco I, Zanatelli C, Naasani LIS, Slaviero M, et al. Evaluation of in vitro and in vivo biocompatibility of iron produced by powder metallurgy. Mater Sci Eng C Mater Biol Appl. 2020 Oct;115:111129.

86. Wermuth DP, Paim TC, Bertaco I, Zanatelli C, Naasani LIS, Slaviero M, et al. Mechanical properties, in vitro and in vivo biocompatibility analysis of pure iron porous implant produced by metal injection molding: A new eco-friendly feedstock from natural rubber (Hevea brasiliensis). Mater Sci Eng C Mater Biol Appl. 2021 Dec;131:112532.

87. Waksman R, Pakala R, Baffour R, Seabron R, Hellinga D, Tio FO. Short-term effects of biocorrodible iron stents in porcine coronary arteries. J Interv Cardiol. 2008 Feb;21(1):15–20.

88. Peuster M, Wohlsein P, Brügmann M, Ehlerding M, Seidler K, Fink C, et al. A

novel approach to temporary stenting: degradable cardiovascular stents produced from corrodible metal-results 6-18 months after implantation into New Zealand white rabbits. Heart. 2001 Nov;86(5):563–9.

89. Peuster M, Hesse C, Schloo T, Fink C, Beerbaum P, von Schnakenburg C. Long-term biocompatibility of a corrodible peripheral iron stent in the porcine descending aorta. Biomaterials. 2006 Oct;27(28):4955–62.

90. Deng Y, Wen Y, Yin J, Huang J, Zhang R, Zhang G, et al. Corroded iron stent increases fibrin deposition and promotes endothelialization after stenting. Bioeng Transl Med. 2023 May;8(3):e10469.

91. Qiu D, Yin J, Wen Y, Huang J, Lei T, Changqing, et al. Diabetes-induced iron stent degradation but preventing re-endothelialization after implantation. Mater Des. 2023 May 1;229:111930.

92. Long-term in vivo corrosion behavior, biocompatibility and bioresorption mechanism of a bioresorbable nitrided iron scaffold. Acta Biomater. 2017 May 1;54:454–68.

93. Li X, Zhang W, Lin W, Qiu H, Qi Y, Ma X, et al. Long-Term Efficacy of Biodegradable Metal–Polymer Composite Stents After the First and the Second Implantations into Porcine Coronary Arteries. ACS Appl Mater Interfaces [Internet]. 2020 Mar 11 [cited 2024 Jan 23]; Available from: https://pubs.acs.org/doi/abs/10.1021/acsami.0c00971

94. Murphy MJ. Bioquímica Clinica [Internet]. Grupo GEN; 2019 [cited 2024 Jan 27]. Available from: https://app.minhabiblioteca.com.br/#/books/9788595150751/

95. Ems T, St Lucia K, Huecker MR. Biochemistry, Iron Absorption. In: StatPearls. Treasure Island (FL): StatPearls Publishing; 2023.

96. Wijayanti N, Katz N, Immenschuh S. Biology of heme in health and disease. Curr Med Chem. 2004 Apr;11(8):981–6.

97. Waldvogel-Abramowski S, Waeber G, Gassner C, Buser A, Frey BM, Favrat B, et al. Physiology of iron metabolism. Transfus Med Hemother. 2014 Jun;41(3):213–21.

98. Rodgers GP, Young NS. Manual Bethesda de hematologia clínica. Thieme Revinter Publicações LTDA; 2018. 502 p.

99. Ferrier DR. Bioquímica Ilustrada - 7.ed. Artmed Editora; 2018. 576 p.

100. Kohgo Y, Ikuta K, Ohtake T, Torimoto Y, Kato J. Body iron metabolism and pathophysiology of iron overload [Internet]. Vol. 88, International Journal of Hematology. 2008. p. 7–15. Available from: http://dx.doi.org/10.1007/s12185-008-0120-5

101. Aguiar A, Ferraz A, Contreras D, Rodríguez J. Mecanismo e aplicações da reação de fenton assistida por compostos fenólicos redutores de ferro [Internet]. Vol. 30, Química Nova. 2007. p. 623–8. Available from: http://dx.doi.org/10.1590/s0100-40422007000300023

102. Barbosa KBF, Costa NMB, de Cássia Gonçalves Alfenas R, De Paula SO, Minim VPR, Bressan J. Estresse oxidativo: conceito, implicações e fatores modulatórios. Revista de Nutrição. 2010;23(4):629–43.

103. Vahidian F, Duijf PHG, Safarzadeh E, Derakhshani A, Baghbanzadeh A, Baradaran B. Interactions between cancer stem cells, immune system and some environmental components: Friends or foes? Immunol Lett. 2019 Apr;208:19–29.

104. Yarjanli Z, Ghaedi K, Esmaeili A, Rahgozar S, Zarrabi A. Iron oxide nanoparticles may damage to the neural tissue through iron accumulation, oxidative stress, and protein aggregation. BMC Neurosci. 2017 Jun 26;18(1):51.

105. Tvrdá E, Benko F. Free radicals: what they are and what they do. In: Pathology. Academic Press; 2020. p. 3–13.

106. Avolio E, Madeddu P. Discovering cardiac pericyte biology: From physiopathological mechanisms to potential therapeutic applications in ischemic heart disease. Vascul Pharmacol. 2016 Nov;86:53–63.

107. Maffei FH de A, Yoshida WB, Rollo HA, Moura R, Sobreira ML, Giannini M, et al. Doenças Vasculares Periféricas - 2 Vols [Internet]. Grupo GEN; 2015. Available from: https://books.google.com/books/about/Doen%C3%A7as_Vasculares_Perif%C3%A9ricas_2_Vols.html?hl=&id=s-73zwEACAAJ

108. Alberts B, Johnson A, Lewis J, Morgan D, Raff M, Roberts K, et al. Biologia Molecular da Célula. Artmed Editora; 2017. 1464 p.

109. Cao Y, Gong Y, Liu L, Zhou Y, Fang X, Zhang C, et al. The use of human umbilical vein endothelial cells (HUVECs) as an in vitro model to assess the toxicity of nanoparticles to endothelium: a review. J Appl Toxicol. 2017 Dec;37(12):1359–69.

110. Baudin B, Bruneel A, Bosselut N, Vaubourdolle M. A protocol for isolation and culture of human umbilical vein endothelial cells. Nat Protoc. 2007;2(3):481–5.

111. Wang L, Liu X, Shen K. New Prospects in Skin Tissue Engineering and Fabrication. In: Biofabrication for Orthopedics. John Wiley & Sons, Ltd; 2022. p. 423–59.

112. Zhou H, You C, Wang X, Jin R, Wu P, Li Q, et al. The progress and challenges for dermal regeneration in tissue engineering. J Biomed Mater Res A. 2017 Apr;105(4):1208–18.

113. Choudhury S, Das A. Advances in generation of three-dimensional skin equivalents: pre-clinical studies to clinical therapies. Cytotherapy. 2021 Jan;23(1):1–9.

114. Laplante AF, Germain L, Auger FA, Moulin V. Mechanisms of wound reepithelialization: hints from a tissue-engineered reconstructed skin to long-standing questions. FASEB J. 2001 Nov;15(13):2377–89.

115. Burnstock G, Knight GE, Greig AVH. Purinergic signaling in healthy and diseased skin. J Invest Dermatol. 2012 Mar;132(3 Pt 1):526–46.

116. Naasani LIS, Pretto L, Zanatelli C, Paim TC, Souza AFD, Pase PF, et al. Bioscaffold developed with decellularized human amniotic membrane seeded with mesenchymal stromal cells: assessment of efficacy and safety profiles in a second-degree burn preclinical model. Biofabrication [Internet]. 2022 Nov 23;15(1). Available from: http://dx.doi.org/10.1088/1758-5090/ac9ff4

117. Burnstock G. Physiology and pathophysiology of purinergic neurotransmission. Physiol Rev. 2007 Apr;87(2):659–797.

118. Abbracchio MP, Burnstock G, Verkhratsky A, Zimmermann H. Purinergic

signalling in the nervous system: an overview. Trends Neurosci. 2009 Jan;32(1):19–29.

119. Naasani LIS, Sévigny J, Moulin VJ, Wink MR. UTP increases wound healing in the self assembled skin substitute (SASS). J Cell Commun Signal. 2023 Sep;17(3):827–44.

120. Bertoni APS, de Campos RP, Tamajusuku ASK, Stefani GP, Braganhol E, Battastini AMO, et al. Biochemical analysis of ectonucleotidases on primary rat vascular smooth muscle cells and in silico investigation of their role in vascular diseases. Life Sci. 2020 Sep 1;256:117862.

121. Gachet C, Hechler B. Platelet Purinergic Receptors in Thrombosis and Inflammation. Hamostaseologie. 2020 May;40(2):145–52.

122. Ferrari D, Gambari R, Idzko M, Müller T, Albanesi C, Pastore S, et al. Purinergic signaling in scarring. FASEB J. 2016 Jan;30(1):3–12.

123. Lu D, Insel PA. Cellular mechanisms of tissue fibrosis. 6. Purinergic signaling and response in fibroblasts and tissue fibrosis. Am J Physiol Cell Physiol. 2014 May 1;306(9):C779–88.

124. Müller CE, Baqi Y, Namasivayam V. Agonists and Antagonists for Purinergic Receptors. Methods Mol Biol. 2020;2041:45–64.

125. Kanthi YM, Sutton NR, Pinsky DJ. CD39: Interface between vascular thrombosis and inflammation. Curr Atheroscler Rep. 2014 Jul;16(7):425.

126. Galgaro BC, Beckenkamp LR, van den M Nunnenkamp M, Korb VG, Naasani LIS, Roszek K, et al. The adenosinergic pathway in mesenchymal stem cell fate and functions. Med Res Rev. 2021 Jul;41(4):2316–49.

127. Shaked G, Gurfinkel R, Czeiger D, Douvdevani A, Sufaro Y. Adenosine in burn blister fluid. Burns. 2007 May;33(3):352–4.

4 CAPÍTULO 1

A engenharia de tecidos combina *scaffolds*, células e moléculas biologicamente ativas para criar substitutos biológicos de tecidos ou órgãos, que podem ser transplantados ao paciente. Este capítulo versa sobre as células tronco mesenquimais, visando explorar suas características biológicas e o potencial uso delas na engenharia de tecidos tanto em terapias celulares quanto na associação com biomateriais.

BIOCELL
2022 46(4): 913-922

Tech Science Press

The versatility of mesenchymal stem cells: From regenerative medicine to COVID, what is next?

Thaís CASAGRANDE PAIM; Márcia Rosângela WINK*

Laboratório de Biologia Celular, Universidade Federal de Ciências da Saúde de Porto Alegre (UFCSPA), Porto Alegre, 90050-170, Brazil

Key words: Mesenchymal stem cells, Regenerative medicine, Secretome, Biomaterials, Extracellular vesicles

Abstract: Mesenchymal stem cells (MSCs) play key roles in regenerative medicine by promoting tissue healing. MSCs can be isolated from different adult tissues and they are able to differentiate into several lineages. Due to their anti-inflammatory, angiogenic and immune-modulatory properties, MSCs are suitable for tissue engineering applications and, when associated with biomaterials, their benefits can be improved. Moreover, recently, MSCs have been studied for new clinical applications, such as in the treatment of patients with COVID-19. MSCs regenerative potential has been attributed to their secretome, which comprises extracellular matrix, soluble proteins and several elements, including the release of extracellular vesicles. Even though, in order to explore all their therapeutic potential, it is still necessary to advance in the investigation of their basic cell biology characteristics.

Viewpoint

Mesenchymal stem cells (MSCs) are multipotent cells found in adult tissues. They are characterized by their adherence to plastic, multilineage differentiation, and immunophenotype (Dominici *et al.*, 2006; Galgaro *et al.*, 2021; Song *et al.*, 2020). Since their discovery, MSCs have been extensively studied, mainly in the last decade. A brief timeline of the main highlights of the MSCs research can be observed in Fig. 1. MSCs were initially isolated from bone marrow, but they can actually be isolated from virtually all tissues (da Silva *et al.*, 2006). This represents a great opportunity for basic and translational studies, once it is possible to isolate MSCs from human tissues that are usually discarded after surgery procedures, such as skin, adipose tissue, umbilical cord, placenta, dental pulp, and sclerocorneal limbus (Fig. 2) (Dominici *et al.*, 2006; Galgaro *et al.*, 2021; Song *et al.*, 2020).

MSCs have anti-inflammatory, angiogenic, and immune-modulatory properties that play an important role in wound healing and regeneration (Chang *et al.*, 2021). Preclinical and clinical studies have demonstrated their promising potential to treat degenerative diseases, such as Alzheimer's disease, autoimmune diseases, bone and cartilage diseases, as well as, respiratory, cardiovascular, kidney and liver diseases (Brown *et al.*, 2019; Samadi *et al.*, 2021). The therapeutic effects of MSCs can be credited to three key mechanisms of action: 1) "homing", of the cells to the injury site; 2) cell differentiation, to promote repair of the damaged tissue; and 3) the secretion of bioactive factors (Vizoso *et al.*, 2017). MSCs can also modulate the host foreign-body immunogenic reaction toward the engineered constructs. These characteristics make them attractive for tissue engineering applications (Chen and Liu, 2016; Hanson *et al.*, 2014).

The combination of stem cells with biomaterials is a promising strategy for tissue regeneration as evidenced by several studies (Sierra-Sánchez *et al.*, 2021). Thus, our group has also contributed with the literature, evaluating the association among different scaffolds and MSCs. In our studies, we have found that Bioglass 45S5 associated with adipose-derived MSCs (ADSCs) is suitable to be tested in preclinical studies for bone regeneration. MSCs maintained their viability, natural morphology, and osteoinduction potential after exposure to Bioglass 45S5 extract. They also grew attached to the bioglass for a long time *in vitro*. Moreover, the biocompatibility of bioglass samples as scaffolds for allogeneic MSCs was confirmed after subcutaneous implantation in mice (Rodrigues *et al.*, 2019). ADSCs were also evaluated after contact with samples of 99.95% and 99.5% pure iron for cardiovascular stents. The viability, proliferation, and morphology of ADSCs were not affected *in vitro* after contact with iron (Paim *et al.*, 2020).

The use of MSCs isolated or in combination with different scaffolds is another promising strategy to treat cutaneous diseases and injuries (Sierra-Sánchez *et al.*, 2021).

*Address correspondence to: Márcia Rosângela Wink, mwink@ufcspa.edu.br
Received: 30 July 2021; Accepted: 26 September 2021

Doi: 10.32604/biocell.2022.018498

www.techscience.com/journal/biocell

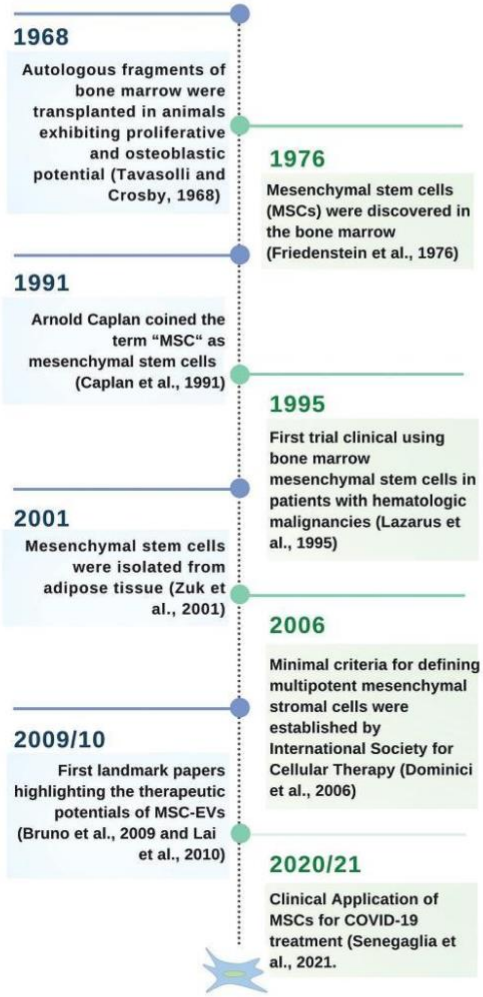

FIGURE 1. A brief timeline of MSCs.

In this setting, our research group evaluated the adhesion, morphology, and viability of ADSCs in a film composed of chitosan, gelatin, and liposomes (Vedovatto *et al.*, 2020). Our results suggested that the biomaterial was suitable for drug delivery and promoted the growth of MSCs without cell damage. In addition, the ADSCs were also studied in combination with CMC (sodium carboxymethylcellulose), a synthetic polymer used in the treatment of skin wounds. There was no significant toxicity or DNA damage on cells cultured with CMC. The association tested as a therapy in a preclinical model contributed to wound healing of skin lesions without overproduction of collagen that could cause a fibrosis (Rodrigues *et al.*, 2014). In addition, ADSCs could also proliferate *in vitro* on the human amniotic membrane (hAM), a biological scaffold generally discarded following the birth. There were no changes in their morphology, as well as, no losses on their potential of multilineage differentiation. These results indicate that hAM can be tested as a scaffold for MSCs in clinical applications (Naasani *et al.*, 2019).

Many efforts have also been put into reproducing the corneal stroma to find an alternative to corneal transplantation (Alió del Barrio *et al.*, 2021). We evaluated decellularized hAM and porcine small intestine submucosa (SIS) as scaffolds for limbal stroma–MSCs (L-MSCs), aiming to compare their performance for application in corneal regeneration. Both biological matrices maintained the cell viability, actin cytoskeleton, nuclei morphology, and mesenchymal phenotype. Nevertheless, there was a slight increase in the percentages of negative markers for L-MSCs grown on the SIS membrane for two weeks, in comparison to hAM, which was able to maintain the MSCs phenotype for a longer time. Besides, the hAM-L-MSCs construct was more transparent, which is an important characteristic to treat corneal injury (Sous Naasani *et al.*, 2018).

In our opinion, while there are many reports in the literature about the MSCs applications, it is not clear yet, whether their regenerative potential is due to the cell itself, their secretome or the combination of both. Regarding the MSCs immunomodulatory properties, researchers have shown that they can be attributed to the secretome (Bruno *et al.*, 2015; Dabrowska *et al.*, 2020). The proteins released into the microenvironment include active factors such as cytokines, chemokines, and growth factors. They can also be released encapsulated in extracellular vesicles (EVs), classified as apoptotic bodies, microvesicles (100–1000 nm), and exosomes (30–200 nm) (Harrell *et al.*, 2019). These EVs are essential to cell-cell communication, once they can carry proteins, lipids, mRNAs, and microRNAs (miRNAs) in the inner core (Groot and Lee, 2020).

Recently, several studies are revealing that extracellular vesicles secreted from MSCs have a critical therapeutic role. MSC-derived EVs have been reported in the treatment of osteoarthritis (Kim *et al.*, 2021; Li *et al.*, 2021), renal injury (Birtwistle *et al.*, 2021), traumatic brain injury (Yang *et al.*, 2017), lung injury (Huang *et al.*, 2019) and liver fibrosis (Chiabotto *et al.*, 2020). The regenerative potential of MSCs-EVs was also shown in cartilage, bone, and periodontium (Cooper *et al.*, 2019; Gholami *et al.*, 2021). The potential of MSCs and their extracellular vesicles, microvesicles, or exosomes is largely explored in clinical trials. Currently, there are over 50 phases III or IV protocols registered in clinicaltrials.gov (ongoing or completed), using MSCs from different sources, a similar proportion of allogeneic and autologous cells, and a range of variable approaches (Table S1).

One specific cargo carried by the MSC-derived EVs are the miRNAs, which are non-coding RNAs (ncRNAs) They act on post-transcriptional regulation of gene expression allowing the restoration of the injured tissue, as other effects (Saliminejad *et al.*, 2019). Several miRNAs are important regulators of gene expression during osteogenic and chondrogenic differentiation. Dysregulation of miRNA mediated mechanisms is related to the development of osteoporosis, bone fractures, and tumors (Iaquinta *et al.*, 2021). Recently, Marupanthorn found that inhibition of

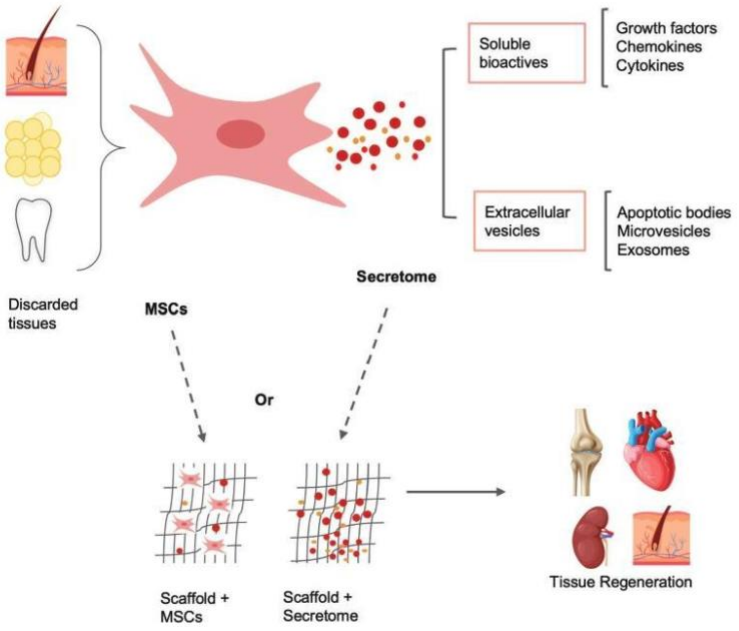

FIGURE 2. MSCs can be isolated from the discarded tissues such as: placenta, umbilical cord, teeth, adipose tissue, skin and sclerocorneal limbus. These cells secrete soluble bioactives and extracellular vesicles. MSCs or their secretome can be associated with biomaterials and promote tissue regeneration.

specific miRNAs (miR-31, miR-106a, and miR-148a) can promote osteogenic differentiation of chorion-derived mesenchymal stem cells (CH-MSCs) and placenta-derived mesenchymal stem cells (PL-MSCs) (Marupanthorn *et al.*, 2021). Likewise, Zhang showed that the silencing of miRNA-132-3p expression in the bone tissues can promote bone marrow-derived mesenchymal stromal cells (BMSC) osteogenic differentiation and osteogenesis in mice with osteopenia (Hu *et al.*, 2020). For this reason, miRNAs can be therapeutic targets to promote bone regeneration in osteogenesis-related disorders.

Currently, the MSCs-EVs have been studied to treat COVID-19 (O'Driscoll, 2020). The analysis of the miRNAs cargo carried by the MSC-EVs showed that they may reduce inflammatory responses, inhibit cell death genes and key factors of the coagulation cascade, preventing tissue damage and coagulation disturbances (Schultz *et al.*, 2021). MSCs can be administered as monotherapy or in association with other treatments. As an example, Tocilizumab, a monoclonal antibody against interleukin-6, in association with an advanced therapy product, based on umbilical cord-derived mesenchymal stromal cells (UC-MSC) was used to treat a severe COVID-19 patient. This therapeutic strategy promoted the decrease of inflammatory cytokines, the increase of regulatory cells, leading to lung repair (Senegaglia *et al.*, 2021). The presence of exosomes derived from UC-MSCs, in combination with Tocilizumab may be responsible for an additive or synergistic anti-inflammatory effect, which was translated in the improvement observed in this COVID-19 patient (Schultz *et al.*, 2021).

Another type of non-coding RNA (ncRNA), also present in MSCs, is the circular RNA (circRNA), which seem to be involved in tissue damage repair. Sun *et al.* (2018) observed an abundant expression and up-regulation of circRNAs, during the repair of human endometrial stromal cells (ESCs) by Wharton's jelly-derived MSCs (WJ-MSCs), leading to the enhance of the endometrial regeneration. Likewise, another recent study from the same group showed that circ6401 was significantly upregulated in WJ-MSCs co-cultured with damaged ESCs. The overexpression of circ6401 increased the levels of VEGFR2 and RAP1B in WJ-MSCs, promoting angiogenesis and proliferation of the damaged ESCs (Shi *et al.*, 2020).

In the recent COVID-19 scenario, the MSCs performance in clinical study protocols was a great surprise. This new open avenue begs the question, what is the next? It is notorious that MSCs have a promising use in different fields of medicine, however basic questions still remain to be answered. While the phenotype of MSCs isolated from different tissues seems very similar, they are not functionally identical (Iser *et al.*, 2014; Naasani *et al.*, 2017). This can explain, for example, the differences in therapeutic potential according to MSC origin (Eiró *et al.*, 2014; Vieira *et al.*, 2010). The secretome composition of stem cells can vary regarding different factors, such as species, tissue source, donor age, protocols for MSCs isolation, culture methods, and therapeutic protocol. Immortalization, an interesting strategy for reducing the need for primary isolation, also changes important characteristics, mainly related to levels of the extracellular adenosine, a potent immunosuppressor (Beckenkamp *et al.*, 2020). Another important aspect to be taken into consideration is the cell microenvironment. It includes the biochemical (e.g., growth factors, small bioactive molecules, and genetic regulators) and biophysical (e.g., pore size, porosity, stiffness, and topography of the

biomaterial) stimuli to which the cells are exposed (Brown *et al*., 2019; Chen and Liu, 2016; Daneshmandi *et al*., 2020). Moreover, the extracellular matrix, one of the most important components of the niche environmental signals, can impact the proliferation and differentiation of MSCs (Assis-Ribas *et al*., 2018; Novoseletskaya *et al*., 2020).

Therefore, there are important questions to be addressed before using MSCs as a cellular therapy to ensure clinical safety and efficacy: (1) Is it better to use autologous MSCs than allogeneic? (2) Are the MSCs from different donors functionally identical? (3) Are there differences between MCSs derived from young or old donors? (4) Is there relevance in the gender of the donor? (5) Can the body mass index (BMI) of donors influence the MCS performance? (6) What is the best tissue for cell isolation? (7) What is the best protocol, cultured MSCs or directly collected? (8) Is there a way of immortalizing MSCs that does not change their key functions? (9) When culturing and expanding MSCs, what is the best growth medium for clinical application? (10) What is the most suitable administration route? (11) How many cells need to be applied? (12) How many cell infusions are necessary? Answering all these variables that can impact clinical success, and other still open questions regarding the MSCs basic cell biology is the key to advance in the next therapeutic challenges.

Acknowledgement: We are grateful to MSc. Iago Carvalho Schultz and Dr. Guido Lenz for critical reading and suggestions to the manuscript. Fig. 2 has elements designed by macrovector/Freepik.

Authors' Contribution: The authors confirm responsibility for the following: viewpoint and manuscript preparation.

Funding Statement: This study was financed in part by the Coordenação de Aperfeiçoamento de Pessoal de Nível Superior —Brasil (CAPES)—Finance Code 001; TCP is fellowship from PhD CAPES (Coordenação de Aperfeiçoamento de Pessoal de Nível Superior); MRW is recipient of 1D level research fellowship from CNPq (Conselho Nacional de Desenvolvimento Científico e Tecnológico); This study was supported by CNPq, MS-SCTIE-Decit/CNPq no 12/2018 (441575/2018-8) and MS-SCTIE-DECIT-DGITIS-CGCIS/CNPq no 26/2020 (442586/2020-5); and by Fundação de Amparo à Pesquisa do Estado do Rio Grande do Sul—Brasil (FAPERGS/CAPES 06/2018—Programa de Internacionalização da pós-graduação no RS (19/2551-0000679-9).

Conflicts of Interest: The authors declare that they have no conflicts of interest to report regarding the present study.

References

Alió Del Barrio JL, Arnalich-Montiel F, de Miguel MP, El Zarif M, Alió JL (2021). Corneal stroma regeneration: Preclinical studies. *Experimental Eye Research* **202**: 108314. DOI 10.1016/j.exer.2020.108314.

Assis-Ribas T, Forni MF, Winnischofer SMB, Sogayar MC, Trombetta-Lima M (2018). Extracellular matrix dynamics during mesenchymal stem cells differentiation. *Developmental Biology* **437**: 63–74. DOI 10.1016/j.ydbio.2018.03.002.

Beckenkamp LR, da Fontoura DMS, Korb VG, de Campos RP, Onzi GR, Iser IC, Bertoni APS, Sévigny J, Lenz G, Wink MR (2020). Immortalization of mesenchymal stromal cells by TERT affects adenosine metabolism and impairs their immunosuppressive capacity. *Stem Cell Reviews and Reports* **16**: 776–791. DOI 10.1007/s12015-020-09986-5.

Birtwistle L, Chen XM, Pollock C (2021). Mesenchymal stem cell-derived extracellular vesicles to the rescue of renal injury. *International Journal of Molecular Sciences* **22**: 6596. DOI 10.3390/ijms22126596.

Brown C, McKee C, Bakshi S, Walker K, Hakman E, Halassy S, Svinarich D, Dodds R, Govind CK, Chaudhry GR (2019). Mesenchymal stem cells: Cell therapy and regeneration potential. *Journal of Tissue Engineering and Regenerative Medicine* **13**: 1738–1755. DOI 10.1002/term.2914.

Bruno S, Deregibus MC, Camussi G (2015). The secretome of mesenchymal stromal cells: Role of extracellular vesicles in immunomodulation. *Immunology Letters* **168**: 154–158. DOI 10.1016/j.imlet.2015.06.007.

Bruno S, Grange C, Deregibus MC, Calogero RA, Saviozzi S et al. (2009). Mesenchymal stem cell-derived microvesicles protect against acute tubular injury. *Journal of the American Society of Nephrology* **20**: 1053–1067. DOI 10.1681/ASN.2008070798.

Caplan AI (1991). Mesenchymal stem cells. *Journal of Orthopaedic Research* **9**: 641–650. DOI 10.1002/jor.1100090504.

Chang C, Yan J, Yao Z, Zhang C, Li X, Mao HQ (2021). Effects of mesenchymal stem cell-derived paracrine signals and their delivery strategies. *Advanced Healthcare Materials* **10**: e2001689. DOI 10.1002/adhm.202001689.

Chen FM, Liu X (2016). Advancing biomaterials of human origin for tissue engineering. *Progress in Polymer Science* **53**: 86–168. DOI 10.1016/j.progpolymsci.2015.02.004.

Chiabotto G, Pasquino C, Camussi G, Bruno S (2020). Molecular pathways modulated by mesenchymal stromal cells and their extracellular vesicles in experimental models of liver fibrosis. *Frontiers in Cell and Developmental Biology* **8**: 594794. DOI 10.3389/fcell.2020.594794.

Cooper LF, Ravindran S, Huang CC, Kang M (2019). A role for exosomes in craniofacial tissue engineering and regeneration. *Frontiers in Physiology* **10**: 1569. DOI 10.3389/fphys.2019.01569.

da Silva ML, Chagastelles PC, Nardi NB (2006). Mesenchymal stem cells reside in virtually all post-natal organs and tissues. *Journal of Cell Science* **119**: 2204–2213. DOI 10.1242/jcs.02932.

Dabrowska S, Andrzejewska A, Janowski M, Lukomska B (2020). Immunomodulatory and regenerative effects of mesenchymal stem cells and extracellular vesicles: Therapeutic outlook for inflammatory and degenerative diseases. *Frontiers in Immunology* **11**: 591065. DOI 10.3389/fimmu.2020.591065.

Daneshmandi L, Shah S, Jafari T, Bhattacharjee M, Momah D, Saveh-Shemshaki N, Lo KWH, Laurencin CT (2020). Emergence of the stem cell secretome in regenerative engineering. *Trends in Biotechnology* **38**: 1373–1384. DOI 10.1016/j.tibtech.2020.04.013.

Dominici M, Le Blanc K, Mueller I, Slaper-Cortenbach I, Marini F, Krause D, Deans R, Keating A, Prockop D, Horwitz E (2006). Minimal criteria for defining multipotent mesenchymal stromal cells. The International Society for Cellular Therapy position statement. *Cytotherapy* **8**: 315–317.

Eiró N, Sendon-Lago J, Seoane S, Bermúdez MA, Lamelas ML, Garcia-Caballero T, Schneider J, Perez-Fernandez R, Vizoso FJ (2014). Potential therapeutic effect of the secretome from human uterine cervical stem cells against both cancer and stromal cells compared with adipose tissue stem cells. *Oncotarget* **5**: 10692–10708. DOI 10.18632/oncotarget.2530.

Friedenstein AJ, Gorskaja JF, Kulagina NN (1976). Fibroblast precursors in normal and irradiated mouse hematopoietic organs. *Experimental Hematology* **4**: 267–274.

Galgaro BC, Beckenkamp LR, Nunnenkamp M, Korb VG, Naasani LIS, Roszek K, Wink MR (2021). The adenosinergic pathway in mesenchymal stem cell fate and functions. *Medicinal Research Reviews* **41**: 2316–2349. DOI 10.1002/med.21796.

Gholami L, Nooshabadi VT, Shahabi S, Jazayeri M, Tarzemany R, Afsartala Z, Khorsandi K (2021). Extracellular vesicles in bone and periodontal regeneration: Current and potential therapeutic applications. *Cell & Bioscience* **11**: 16. DOI 10.1186/s13578-020-00527-8.

Groot M, Lee H (2020). Sorting mechanisms for MicroRNAs into extracellular vesicles and their associated diseases. *Cells* **9**: 1044. DOI 10.3390/cells9041044.

Hanson S, D'Souza RN, Hematti P (2014). Biomaterial-mesenchymal stem cell constructs for immunomodulation in composite tissue engineering. *Tissue Engineering Part A* **20**: 2162–2168. DOI 10.1089/ten.tea.2013.0359.

Harrell CR, Jovicic N, Djonov V, Arsenijevic N, Volarevic V (2019). Mesenchymal stem cell-derived exosomes and other extracellular vesicles as new remedies in the therapy of inflammatory diseases. *Cells* **8**: 1605. DOI 10.3390/cells8121605.

Hu Z, Zhang L, Wang H, Wang Y, Tan Y et al. (2020). Targeted silencing of miRNA-132-3p expression rescues disuse osteopenia by promoting mesenchymal stem cell osteogenic differentiation and osteogenesis in mice. *Stem Cell Research & Therapy* **11**: 58. DOI 10.1186/s13287-020-1581-6.

Huang R, Qin C, Wang J, Hu Y, Zheng G, Qiu G, Ge M, Tao H, Shu Q, Xu J (2019). Differential effects of extracellular vesicles from aging and young mesenchymal stem cells in acute lung injury. *Sedentary Life and Nutrition* **11**: 7996–8014. DOI 10.18632/aging.102314.

Iaquinta MR, Lanzillotti C, Mazziotta C, Bononi I, Frontini F et al. (2021). The role of microRNAs in the osteogenic and chondrogenic differentiation of mesenchymal stem cells and bone pathologies. *Theranostics* **11**: 6573–6591. DOI 10.7150/thno.55664.

Iser IC, Bracco PA, Gonçalves CEI, Zanin RF, Nardi NB, Lenz G, Battastini AMO, Wink MR (2014). Mesenchymal stem cells from different murine tissues have differential capacity to metabolize extracellular nucleotides. *Journal of Cellular Biochemistry* **115**: 1673–1682. DOI 10.1002/jcb.24830.

Kim GB, Shon OJ, Seo MS, Choi Y, Park WT, Lee GW (2021). Mesenchymal stem cell-derived exosomes and their therapeutic potential for osteoarthritis. *Biology* **10**: 285. DOI 10.3390/biology10040285.

Lai RC, Arslan F, Lee MM, Sze NSK, Choo A et al. (2010). Exosome secreted by MSC reduces myocardial ischemia/reperfusion injury. *Stem Cell Research* **4**: 214–222. DOI 10.1016/j.scr.2009.12.003.

Lazarus HM, Haynesworth SE, Gerson SL, Rosenthal NS, Caplan AI (1995). *Ex vivo* expansion and subsequent infusion of human bone marrow-derived stromal progenitor cells (mesenchymal progenitor cells): Implications for therapeutic use. *Bone Marrow Transplantation* **16**: 557–564.

Li S, Liu J, Liu S, Jiao W, Wang X (2021). Mesenchymal stem cell-derived extracellular vesicles prevent the development of osteoarthritis via the circHIPK3/miR-124-3p/MYH9 axis. *Journal of Nanobiotechnology* **19**: 1–20.

Marupanthorn K, Tantrawatpan C, Kheolamai P, Tantikanlayaporn D, Manochantr S (2021). MicroRNA treatment modulates osteogenic differentiation potential of mesenchymal stem cells derived from human chorion and placenta. *Scientific Reports* **11**: 7670. DOI 10.1038/s41598-021-87298-5.

Naasani LIS, Rodrigues C, de Campos RP, Beckenkamp LR, Iser IC, Bertoni APS, Wink MR (2017). Extracellular nucleotide hydrolysis in dermal and limbal mesenchymal stem cells: A source of adenosine production. *Journal of Cellular Biochemistry* **118**: 2430–2442. DOI 10.1002/jcb.25909.

Naasani LIS, Souza AFD, Rodrigues C, Vedovatto S, Azevedo JG, Bertoni APS, da Cruz Fernandes M, Buchner S, Wink MR (2019). Decellularized human amniotic membrane associated with adipose derived mesenchymal stromal cells as a bioscaffold: Physical, histological and molecular analysis. *Biochemical Engineering Journal* **152**: 107366. DOI 10.1016/j.bej.2019.107366.

Novoseletskaya E, Grigorieva O, Nimiritsky P, Basalova N, Eremichev R et al. (2020). Mesenchymal stromal cell-produced components of extracellular matrix potentiate multipotent stem cell response to differentiation stimuli. *Frontiers in Cell and Developmental Biology* **8**: 555378. DOI 10.3389/fcell.2020.555378.

O'Driscoll L (2020). Extracellular vesicles from mesenchymal stem cells as a COVID-19 treatment. *Drug Discovery Today* **25**: 1124–1125. DOI 10.1016/j.drudis.2020.04.022.

Paim TC, Wermuth DP, Bertaco I, Zanatelli C, Naasani LIS, Slaviero M, Driemeier D, Schaeffer L, Wink MR (2020). Evaluation of *in vitro* and *in vivo* biocompatibility of iron produced by powder metallurgy. *Materials Science & Engineering: C* **115**. DOI 10.1016/j.msec.2020.111129.

Rodrigues C, de Assis AM, Moura DJ, Halmenschlager G, Saffi J, Xavier LL, da Cruz Fernandes M, Wink MR (2014). New therapy of skin repair combining adipose-derived mesenchymal stem cells with sodium carboxymethylcellulose scaffold in a pre-clinical rat model. *PLoS One* **9**: e96241. DOI 10.1371/journal.pone.0096241.

Rodrigues C, Naasani LIS, Zanatelli C, Paim TC, Azevedo JG, de Lima JC, da Cruz Fernandes M, Buchner S, Wink MR (2019). Bioglass 45S5: Structural characterization of short range order and analysis of biocompatibility with adipose-derived mesenchymal stromal cells *in vitro* and *in vivo*. *Materials Science & Engineering C, Materials for Biological Applications* **103**: 109781. DOI 10.1016/j.msec.2019.109781.

Saliminejad K, Khorram Khorshid HR, Soleymani Fard S, Ghaffari SH (2019). An overview of microRNAs: Biology, functions, therapeutics, and analysis methods. *Journal of Cellular Physiology* **234**: 5451–5465. DOI 10.1002/jcp.27486.

Samadi P, Saki S, Manoochehri H, Sheykhhasan M (2021). Therapeutic applications of mesenchymal stem cells: A comprehensive review. *Current Stem Cell Research & Therapy* **16**: 323–353. DOI 10.2174/1574888X15666200914142709.

Schultz IC, Bertoni APS, Wink MR (2021). Mesenchymal stem cell-derived extracellular vesicles carrying miRNA as a potential multi target therapy to COVID-19: An *in silico* analysis. *Stem Cell Reviews and Reports* **17**: 341–356. DOI 10.1007/s12015-021-10122-0.

Senegaglia AC, Rebelatto CLK, Franck CL, Lima JS, Boldrini-Leite LM et al. (2021). Combined use of tocilizumab and mesenchymal stromal cells in the treatment of severe COVID-19: Case report. *Cell Transplantation* **30**: 9636897211021008.

Shi Q, Sun B, Wang D, Zhu Y, Zhao X, Yang X, Zhang Y (2020). Circ6401, a novel circular RNA, is implicated in repair of the damaged endometrium by Wharton's jelly-derived

mesenchymal stem cells through regulation of the miR-29b-1-5p/RAP1B axis. *Stem Cell Research & Therapy* **11**: 1–16.

Sierra-Sánchez Á., Montero-Vilchez T, Quiñones-Vico MI, Sanchez-Diaz M, Arias-Santiago S (2021). Current advanced therapies based on human mesenchymal stem cells for skin diseases. *Frontiers in Cell and Developmental Biology* **9**: 643125. DOI 10.3389/fcell.2021.643125.

Song N, Scholtemeijer M, Shah K (2020). Mesenchymal stem cell immunomodulation: Mechanisms and therapeutic potential. *Trends in Pharmacological Sciences* **41**: 653–664. DOI 10.1016/j.tips.2020.06.009.

Sous Naasani LI, Rodrigues C, Azevedo JG, Damo Souza AF, Buchner S, Wink MR (2018). Comparison of human denuded amniotic membrane and porcine small intestine submucosa as scaffolds for limbal mesenchymal stem cells. *Stem Cell Reviews and Reports* **14**: 744–754. DOI 10.1007/s12015-018-9819-8.

Sun B, Shi L, Shi Q, Jiang Y, Su Z, Yang X, Zhang Y (2018). Circular RNAs are abundantly expressed and upregulated during repair of the damaged endometrium by Wharton's jelly-derived mesenchymal stem cells. *Stem Cell Research & Therapy* **9**: 314. DOI 10.1186/s13287-018-1046-3.

Tavassoli M, Crosby WH (1968). Transplantation of marrow to extramedullary sites. *Science* **161**: 54–56. DOI 10.1126/science.161.3836.54.

Vedovatto S, Facchini JC, Batista RK, Paim TC, Lionzo MIZ, Wink MR (2020). Development of chitosan, gelatin and liposome film and analysis of its biocompatibility *in vitro*. *International Journal of Biological Macromolecules* **160**: 750–757. DOI 10.1016/j.ijbiomac.2020.05.229.

Vieira NM, Zucconi E, Bueno CR Jr, Secco M, Suzuki MF, Bartolini P, Vainzof M, Zatz M (2010). Human multipotent mesenchymal stromal cells from distinct sources show different *in vivo* potential to differentiate into muscle cells when injected in dystrophic mice. *Stem Cell Reviews and Reports* **6**: 560–566. DOI 10.1007/s12015-010-9187-5.

Vizoso FJ, Eiro N, Cid S, Schneider J, Perez-Fernandez R (2017). Mesenchymal stem cell secretome: Toward cell-free therapeutic strategies in regenerative medicine. *International Journal of Molecular Sciences* **18**: 9. DOI 10.3390/ijms18091852.

Yang Y, Ye Y, Su X, He J, Bai W, He X (2017). MSCs-derived exosomes and neuroinflammation, neurogenesis and therapy of traumatic brain injury. *Frontiers in Cellular Neuroscience* **11**: 55. DOI 10.3389/fncel.2017.00055.

Zuk PA, Zhu M, Mizuno H, Huang J, William Futrell J, Katz AJ, Benhaim P, Peter Lorenz H, Hedrick MH (2001). Multilineage cells from human adipose tissue: Implications for cell-based therapies. *Tissue Engineering* **7**: 211–228. DOI 10.1089/107632701300062859.

TABLE S1

Clinical trials with mesenchymal stem cells.

Cell type/ source	Study brief title	Condition	Interventions	Phase status	Reference
Autologous Bone Marrow-derived MSCs	Combination of autologous MSC and HSC infusion in patients with decompensated cirrhosis	Cirrhosis	- CD34 and MSC infusion - Standard of care for cirrhosis management	Phase 4 Completed	NCT0424368
	Bone regeneration with mesenchymal stem cells	Mandibular Fractures	- Application of MSCs	Phase 3 Completed	NCT02755922
	Safety and efficacy of autologous mesenchymal stem cells in chronic spinal cord injury	Spinal Cord Injury	- Posterior cervical laminectomy and MSCs transplantation	Phase 2/3 Completed	NCT01676441
	Safety and efficacy of intracoronary adult human mesenchymal stem cells after acute myocardial infarction	Acute Myocardial Infarction	- Intracoronary injection of MSCs - Control (aspirin and clopidogrel)	Phase 2/3 Completed	NCT01392105
	A comparative study of 2 doses of BM autologous H-MSC + biomaterial *vs.* iliac crest autograft for bone healing in non-union	Non-Union Fracture	- MSCs low dose + biphasic calcium phosphate (BCP) - MSCs high dose + BCP - Control (Autologous iliac crest graft)	Phase 3 Recruiting	NCT03325504
	To evaluate the efficacy and safety of HEARTICELGRAM®-AMI in patients with acute myocardial infarction	Acute Myocardial Infarction	- MSCs and contemporary drug treatment - Control (contemporary drug treatment)	Phase 3 Recruiting	NCT01652209
	Clinical trial to evaluate the efficacy and safety of Cellgram-LC administration in patients with alcoholic cirrhosis	Alcoholic Cirrhosis	- Injection of MSCs in hepatic artery - Best supportive care	Phase 3 Not yet recruiting	NCT04689152
	Bone marrow mesenchymal stem cells transfer in patients with ST-segment elevation myocardial infarction	Myocardial Infarction	- Bone marrow MSC transfer - Best medical treatment - Percutaneous coronary intervention	Phase 2/3 Completed	NCT04421274

(Continued)

Table S1 (continued).

Cell type/ source	Study brief title	Condition	Interventions	Phase status	Reference
	Parkinson's disease therapy using cell technology	Transplantation: Mesenchymal Stem Cell	- MSCs transplantation - Placebo	Phase 2/3 Recruiting	NCT04146519
	Bone marrow derived stem cell transplantation in T2DM	Type 2 Diabetes Mellitus	- MSCs transplantation - MNC's transplantation - Control	Phase 3 Recruiting	NCT01759823
	Efficacy in alveolar bone regeneration with autologous mscs and biomaterial in comparison to autologous bone grafting	Alveolar Bone Atrophy	- MSC combined with BCP - Autologous bone graft	Phase 3 Recruiting	NCT04297813
	Evaluatiton the efficacy and safety of mutiple lenzumestrocel (neuronata-r® inj.) Treatment in patients with ALS	Amyotrophic Lateral Sclerosis	- Lenzumestrocel - Riluzole - Placebo	Phase 3 Recruiting	NCT04745299
	Cardiovascular clinical project to evaluate the regenerative capacity of cardiocell in patients with acute myocardial infarction (AMI)	Myocardial Infarction	- MSCs administration - Placebo	Phases 2 and 3 Completed	NCT03404063
	Safety and efficacy of repeated administrations of NurOwn® in ALS patients	Amyotrophic Lateral Sclerosis (ALS)	- NurOwn® (MSC-NTF cells) - Placebo	Phase 3 Completed	NCT03280056
	Stem cell therapy for treatment of female stress urinary incontinence	Urinary Incontinence, Stress	- MSCs injection - Surgery (TVT)	Phase 3 Completed	NCT02334878
	Transplantation of bone marrow derived mesenchymal stem cells in affected knee osteoarthritis by rheumatoid arthritis	Rheumatoid Arthritis	- MSCs transplantation - Placebo	Phase 2/3 Completed	NCT01873625
	Bone marrow *vs.* adipose autologous mesenchymal stem cells for the treatment of knee osteoarthritis*	Knee Osteoarthritis	- Bone marrow derived MSC - Adipose derived MSC - Bone marrow & adipose derived MSC injection	Phase 3 Not yet recruiting	NCT04351932
	Multicenter trial of stem cell therapy for osteoarthritis (miles)*	Osteoarthritis	- Autologous Bone Marrow Concentrate - Adipose-derived Stromal Vascular Fraction - Umbilical Cord Tissue - Corticosteroid injection	Phase 3 Active, not recruiting	NCT03818737
Allogeneic Bone Marrow-derived MSCs	Mesenchymal stem cell infusion in haploidentical hematopoietic stem cell transplantation in patients with hematological malignancies	Hematopoietic Stem Cell Transplantation	- MSCs infusion - Cyclophosphamide administration	Phase 3 Completed	NCT03106662
	A study of allogeneic low oxygen mesenchymal bone marrow cells in subjects with myocardial infarction	Myocardial Infarction	- MSCs administration - Placebo	Phase 3 Completed	NCT02672267
	Left ventricular assist device combined with allogeneic mesenchymal stem cells implantation in patients with end-stage heart failure.	Heart Failure Ischemic Cardiomyopathy	- MSCs implantation	Phase 2/3 Active, not recruiting	NCT01759212
	MSCS in COVID-19 ARDS	Acute Respiratory Distress Syndrom, COVID	- MSCs infusion - Placebo	Phase 3 Active, not recruiting	NCT04371393
	Evaluation of PROCHYMAL® adult human stem cells for treatment-resistant moderate-to-severe crohn's disease	Crohn's Disease	- *Ex Vivo* Cultured Adult Human Mesenchymal Stem Cells-Prochymal® - Placebo	Phase 3 Completed	NCT00482092

(Continued)

Table S1 (continued).

Cell type/ source	Study brief title	Condition	Interventions	Phase status	Reference
	Extended evaluation of PROCHYMAL® adult human stem cells for treatment-resistant moderate-to-severe crohn's disease	Crohn's Disease	- Placebo - *Ex Vivo* Cultured Adult Human Mesenchymal Stem Cells- Prochymal®	Phase 3 Completed	NCT00543374
	Evaluation of PROCHYMAL® for treatment-refractory moderate-to-severe crohn's disease	Crohn's Disease	- *Ex Vivo* Cultured Adult Human Mesenchymal Stem Cells- Prochymal®	Phase 3 Completed	NCT01233960
	Efficacy and safety of PROCHYMAL™ infusion in combination with corticosteroids for the treatment of newly diagnosed acute graft *versus* host disease (GVHD)	Graft *vs.* Host Disease	- *Ex Vivo* Cultured Adult Human Mesenchymal Stem Cells- Prochymal® - Placebo	Phase 3 Completed	NCT00562497
Autologous Adipose-derived MSCs	Clinical study to evaluate efficacy and safety of ASC and fibringlue or fibringlue in patients with crohn's fistula	Crohn's Fistula	- MSCs injection - Fibrin Glue	Phase 3 Recruiting	NCT04612465
	A phase 2b/3a study to evaluate the efficacy and safety of JOINTSTEM in patients diagnosed as knee osteoarthritis	Osteoarthritis, Knee	- JOINTSTEM - Placebo Control	Phases 2 and 3 Recruiting	NCT04368806
	A phase 3 study to evaluate the efficacy and safety of JOINTSTEM in treatment of osteoarthritis	Degenerative Arthritis Knee Osteoarthritis	- JOINTSTEM - Saline	Phase 3 Completed	NCT03990805
	Clinical trial to evaluate the efficacy and safety of stem cells	Anal Fistula	- MSCs + fibrin glue - fibrin glue	Phase 3 Completed	NCT01803347
	Effects of α mat *versus* steroid injection in knee osteoarthritis (stα mat-knee study)	Knee Osteoarthritis	-Microfragmented Adipose Tissue Transplant - Corticosteroid injection	Phase 3 Recruiting	NCT04230902
	Follow-up study for participants of JOINTSTEM	Knee Osteoarthritis	- JOINTSTEM - Saline	Phase 3 Enrolling by invitation	NCT04427930
	Bone marrow *versus* adipose autologous mesenchymal stem cells for the treatment of knee osteoarthritis*	Knee Osteoarthritis	- Bone marrow derived-MSC - Adipose derived MSC - Bone marrow & adipose derived MSC injection	Phase 3 Not yet recruiting	NCT04351932
	Multicenter trial of stem cell therapy for osteoarthritis (miles)*	Osteoarthritis	- Autologous Bone Marrow Concentrate - Adipose-derived Stromal Vascular Fraction - Umbilical Cord Tissue - Corticosteroid injection	Phase 3 Active, not recruiting	NCT03818737
Allogeneic Adipose-derived MSC	Clinical study to evaluate efficacy and safety of ALLO-ASC-DFU in patients with diabetic foot ulcers.	Diabetic Foot Ulcer	- ALLO-ASC-DFU - Vehicle sheet	Phase 3 Active, not recruiting	NCT03370874
	Adipose derived mesenchymal stem cells for induction of remission in perianal fistulizing crohn's disease	Crohn's Disease	- MSCs injection - Saline solution	Phase 3 Completed	NCT01541579
	Clinical study to evaluate efficacy and safety of ALLO-ASC-DFU in patients with diabetic wagner grade 2 foot ulcers	Diabetic Foot Ulcer	- Hydrogel sheet containing MSC - Vehicle Sheet without MSCs	Phase 3 Recruiting	NCT04569409

(Continued)

Table S1 (continued).

Cell type/ source	Study brief title	Condition	Interventions	Phase status	Reference
Allogeneic Umbilical Cord-derived MSCs	Different efficacy between rehabilitation therapy and stem cells transplantation in patients with sci in China	Spinal Cord Injury	- Cell therapy - Cehabilitation	Phase 3 Completed	NCT01873547
	The effectiveness of adding allogenic stem cells after traditional treatment of osteochondral lesions of the talus	Osteochondral Fracture of Talus	- Platelet-poor plasma scaffold embedded in MSCs added to the traditional treatment for osteochondral lesions - Traditional treatment (debridement and microfracture)	Phase 3 Recruiting	NCT03905824
	Efficacy of stem cell transplantation compared to rehabilitation treatment of patients with cerebral paralysis	Cerebral Palsy	- Rehabilitation - MSCs injection	Phase 3 Completed	NCT01929434
	Efficacy and safety of UC-MSCS for the treatment of steroid-resistant agvhd following allo-hsct	Graft *vs.* Host Disease	- MSCs and Anti-CD25 mAb - Anti-CD25 mAb	Phase 3 Not yet Recruiting	NCT04738981
Allogeneic Wharton's Jelly derived MSCs	Management of retinitis pigmentosa by mesenchymal stem cells by Wharton's jelly derived mesenchymal stem cells	Retinitis Pigmentosa Inherited Retinal Dystrophy	- MSCs administration	Phase 3 Completed	NCT04224207
	Randomized clinical trial to evaluate the regenerative capacity of cardiocell in patients with chronic ischaemic heart failure (CIHF)	Heart Failure	- CardioCell - Placebos	Phases 2 and 3 Completed	NCT03418233
	Therapy of toxic optic neuropathy via combination of stem cells with electromagnetic stimulation	Methanol Poisoning Toxic Optic Neuropathy Stem Cell Tyrosine Kinase 1 Y842X Magnetic Field Exposure	- MSCs and repetitive electromagnetic stimulation - MSCs injection - Repetitive electromagnetic stimulation	Phase 3 Completed	NCT04877067
	Cardiovascular clinical project to evaluate the regenerative capacity of cardiocell in patients with no-option critical limb ischemia (n-o cli)	Critical Limb Ischemia	- CardioCell - Placebos	Phases 2 and 3 Active, not recruiting	NCT03423732
Allogeneic Human Umbilical Cord Blood-derived MSCs	Efficacy and safety of allogenic stem cell product (CARTISTEM®) for osteochondral lesion of talus	Chondral or Osteochondral Lesion of Talus	- CARTISTEM® (product based MSCs) - Microfracture	Phase 3 Active, not recruiting	NCT04310215
	Follow-up study of CARTISTEM® *versus* microfracture for the treatment of knee articular cartilage injury or defect	Degenerative Osteoarthritis Defect of Articular Cartilage	- CARTISTEM - Microfracture	Phase 3 Completed	NCT01626677
	Multicenter trial of stem cell therapy for osteoarthritis (MILES)	Osteoarthritis	- Autologous Bone Marrow Concentrate - Adipose-derived Stromal Vascular Fraction - Umbilical Cord Tissue - Corticosteroid injection	Phase 3 Active, not recruiting	NCT03818737
	Study to compare efficacy and safety of CARTISTEM and microfracture in patients with knee articular cartilage injury	Cartilage Injury Osteoarthritis	- Cartistem - Microfracture treatment	Phase 3 Completed	NCT01041001

(Continued)

Table S1 (continued).

Cell type/ source	Study brief title	Condition	Interventions	Phase status	Reference
Autologous Deciduous Dental Pulp-derived MSCs	Bone tissue engineering with dental pulp stem cells for alveolar cleft repair	Cleft Lip and Palate	- MSCs associated with hydroxyapatita/collagen - Iliac crest autogenous bone graft	Phase 3 Completed	NCT03766217
Non-Informed	Comparative study of strategies for management of Duchenne Myopathy (DM)	Myopathy	- Sildenafil (Phosphodiesterase inhibitors - Prednisolone (Steroids) - MSC transplantation	Phase 4 Not yet recruiting	NCT03633565
	Mesenchymal stem cell therapy for SARS-CoV-2-related Acute Respiratory Distress Syndrome	COVID-19	- MSC therapy protocol 1 -MSC therapy protocol 2	Phase 2/3 Recruiting	NCT04366063
	MSC for Severe aGVHD	Steroid-resistant Severe aGVHD	- MSCs	Phase 2/3 Recruiting	NCT03631589
	Clinical extension study for safety and efficacy evaluation of Cellavita-HD Administration in Huntington's patients	Huntington Disease	- Injection of Cellavita-HD	Phase 2/3 Active, not Recruiting	NCT04219241

Notes: Free text terms searched in ClinicalTrials.gov on August 2021: "Mesenchymal stem cells" or "Mesenchymal stromal cells" and "extracellular vesicles" or Exosomes or microvesicles, with no language or time restrictions. Studies with status Recruiting, not yet recruiting, active, not recruiting, completed, enrolling by invitation and terminated studies were included. *Studies involving 2 or more MSCs types.

5 CAPÍTULO 2

Os biomateriais desempenham um papel crucial na engenharia de tecidos, por isso este e os próximos capítulos versam sobre novos biomateriais desenvolvidos e testados quanto às suas características físicas e biocompatibilidade. Neste capítulo apresentamos um material composto por metacaulinita e hidroxiapatita que se mostrou promissor para o uso em implantes ósseos. A metacaulinita é um aluminossilicato natural, barato e conhecido por suas propriedades mecânicas, enquanto a hidroxiapatita se destaca pela biocompatibilidade devido à estrutura química semelhante à matriz óssea.

Applied Materials Today 33 (2023) 101875

Contents lists available at ScienceDirect

Applied Materials Today

journal homepage: www.elsevier.com/locate/apmt

Hierarchically porous bioceramics based on geopolymer-hydroxyapatite composite as a novel biomaterial: Structure, mechanical properties and biocompatibility evaluation

Rafaela de Andrade [a,1], Thaís Casagrande Paim [b,1], Isadora Bertaco [b], Liliana Sous Naasani [b], Silvio Buchner [c], Tomáš Kovářík [d,e,2], Jiří Hájek [d], Márcia Rosângela Wink [b,2,*]

[a] Universidade Federal do Rio Grande do Sul (UFRGS), Av. Bento Gonçalves 9500, 91501-970, Porto Alegre, RS, Brazil
[b] Laboratório de Biologia Celular, Departamento de Ciências Básicas da Saúde, Universidade Federal de Ciências da Saúde de Porto Alegre (UFCSPA), Rua Sarmento Leite 245, 90050-170, Porto Alegre, RS, Brazil
[c] LAPMA, Laboratório de Altas Pressões e Materiais Avançados, Instituto de Física, Universidade Federal do Rio Grande do Sul, IF/UFRGS, Porto Alegre, RS
[d] University of West Bohemia, New Technologies – Research Centre, 8 Univerzitní, Pilsen 301 00, Czechia
[e] University of West Bohemia, Department of Material Science and Technology, Faculty of Mechanical Engineering, 8 Univerzitní, Pilsen 301 00, Czechia

ARTICLE INFO

Keywords:
Porous ceramics
Geopolymer
Metakaolin
Hydroxyapatite
Mesenchymal stem cells

ABSTRACT

In this study, open-cell porous bioceramics based on geopolymers were synthesized by the replica technique. The composition consisted of a mixture of metakaolin (MK) and hydroxyapatite (HA) that combined are suitable for application in bone tissue engineering. Metakaolin is a cheap natural aluminosilicate known for its mechanical properties, while hydroxyapatite stands out for its biocompatibility due to the chemical structure similar to the bone matrix. After undergoing heat treatment (HT), the geopolymer-hydroxyapatite (GMK-HA) synthesized materials, referred to as GMK-HA-HT, presented pores in the range from 1 to 5 mm. In the compressive strength tests, they exhibited values between 1.18 and 2.9 MPa. These ranges of values signify a proper balance between mechanical strength and porosity. X-ray diffraction analysis showed phosphate and/or calcium crystalline phases in all heat-treated samples, indicating HA's successful incorporation in the geopolymer structure. In vitro tests using human adipose-derived mesenchymal stem cells (ADSCs) were conducted to evaluate the biocompatibility of the synthesized materials. The extracts obtained from the GMK-HA-HT were found to be non-cytotoxic. ADSCs in contact with extracts have no morphological changes and when cultured on the GMK-HA-HT surface, the cells interacted with the scaffold and formed a monolayer. Here, for the first time, we provide insights into this new class of materials as a promising biomaterial candidate which could be associated with ADSCs to promote bone healing.

1. Introduction

Geopolymers were first described in 1970 by Joseph Davidots [1,2]. They can be classified as a class of cementitious materials that are formed by mixing aluminosilicate materials with an alkali or an alkali-silicate solution [3]. The dominant step in geopolymerization is the dissolution of aluminosilicate materials to form a gel phase. When the gel phase hardens, the separate aluminosilicate particles are bonded together with the gel that acts as the coupling agent [4], geopolymers are then formed with a compact polycrystalline structure. Because of that, this material has good mechanical properties, fire resistance, and durability at ambient temperatures for a long time, which are properties of interest in the construction industry. Moreover, the geopolymers' synthesis is considered a green synthesis and the materials formed are environmentally friendly [2]. It is possible to use recyclable materials such as fly ash, dune and river sand [1,5], blast furnace slag, glass waste and flue gas desulfurization without loss in their essential properties to the construction industry. Nowadays, additive manufacturing technology (3D printing) is also expanding as a way of geopolymers' synthesis because the rheological behavior of geopolymers is suitable for

* Corresponding author.
E-mail address: mwink@ufcspa.edu.br (M.R. Wink).
[1] These authors contributed equally to this work.
[2] These authors shared senior authorship.

https://doi.org/10.1016/j.apmt.2023.101875
Received 27 March 2023; Received in revised form 12 June 2023; Accepted 26 June 2023

Table 1
Chemical composition and particle size of raw metakaolins.

Metakaolins	Oxides (Wt. %)	MK1	MK2	MK3	HA
Chemical Composition	SiO_2	58.20	54.41	52.33	0.08
	Al_2O_3	39.38	29.55	45.00	–
	K_2O	0.82	2.00	0.61	–
	Na_2O	–	9.82	–	–
	Fe_2O_3	0.62	0.38	0.90	–
	MgO	0.42	0.46	0.28	0.52
	TiO_2	0.42	0.22	0.46	–
	CaO	0.14	2.68	0.24	52.82
	P_2O_5	0.05	0.27	–	46.31
	Rh_2O_3	–	–	0.11	0.18
	PbO	–	0.11	–	–
	SO_3	–	0.06	–	0.04
	ZrO	0.01	–	0.03	–
	SrO	–	–	0.01	0.01
	Ga_2O_3			0.01	–
	ZnO	–	0.02	–	–
L.O.I. (loss on ignition) at 1000 °C		3.39	0.92	1.36	1.72
Median size D50 (μm)		8.33	6.64	8.31	9.74
D10 (μm)		4.83	3.25	4.07	5.29
D90 (μm)		13.96	11.48	18.46	18.12

extrusion and it is a time and material-saving technology [6,7].

Among the aluminosilicate materials that could be used in geopolymerization, metakaolin (MK) stands out as a cheap natural material [8]. MK is the amorphous phase of kaolinite - which is the major component of kaolin-obtained by dehydroxylation reaction under heating. Kaolin is a clay mineral formed mostly by the decomposition of feldspars, granite, and aluminum silicates [9].

Currently, there is an expansion in the research of new geopolymers to many applications, such as heavy metal remover [10], catalyst support [11], CO_2 capture [12], wastewater treatment [13,14], energy storage [15], drug delivery systems [16] and bone tissue applications [17]. However, the geopolymers' low bioactivity is a challenge to use these materials in biological applications [18]. Based on their chemical and phase composition, geopolymer composites are assigned to the group of inorganic materials that are widely used in the field of regenerative medicine. In this context, inorganic composites are usually represented in the form of bone cements where key parameters such as Ca^{+2}/PO_4^{3-} ion ratio, viscosity, and solubility kinetics dictate the interaction in the biological system [19]. Geopolymers containing MK were reported to have potential applications in bone tissue engineering (BTE) [9,20].

In this sense, Hydroxyapatite (HA) can be incorporated into the gel phase to increase the biocompatibility of geopolymers [21]. The biocompatibility of HA, whose chemical formula is $Ca_{10}(OH)_2(PO4)_6$, has been attributed to its chemical similarity to the inorganic component of the bone matrix [22]. However, hydroxyapatite can not be used as a prosthesis material due to its brittleness and low fracture toughness. HA has already been reinforced with aluminum oxide, carbon nanotubes, and other materials, although it is crucial to keep the HA biocompatible when doing these modifications [8,23].

The evaluation of biocompatibility in vitro is a valuable method used for materials intended for medical use. Regulatory agencies provide guidelines for testing the cytotoxicity of materials, one important set of guidelines is the ISO 10,993 series [24]. Mesenchymal stem cells (MSCs) are considered for cytotoxicity evaluation due to their presence in various tissues, immune-modulatory, anti-inflammatory, and angiogenic properties, and self-renewal and differentiation capabilities [25]. Besides, these characteristics make them also suitable to be associated with biomaterials, promoting the regeneration of tissue [26,27]. MSCs are important regulators of bone modeling, remodeling, and bone fracture repair; their migration and differentiation into osteogenic progenitors are pivotal in these processes [28]. To improve their therapeutic potential, MSCs have been combined with different materials, such as bioceramics [29], biodegradable polymers [30,31], and composite biomaterials [25,32–34].

Ceramics and ceramic-composite materials applied to bone fractures or joint replacements are called "bioceramics", which have to form a stable interface with the living host tissue [22]. A wide range of materials is used in operating theaters, such as the patented Bioglass and Ceravital [17,29,35]. The geopolymers' mechanical performance can be improved by the transformation of the geopolymer matrix to a ceramic phase using thermal calcination [36,37]. In addition, high temperatures decrease the alkaline pH of materials, which is high due to the synthesis conditions, and affects the biocompatibility [17,38]. Besides chemical composition, size, shape, and surface charge, the type of porosity plays an important role in the functionality of these biomaterials because it increases bone ingrowth [39–41]. Moreover, the variability of porosity-forming techniques that can be implemented to create foams with adjustable size, distribution, and type of pores is also a great advantage [42]. However, porous structures can decrease the materials' mechanical strength [5,42]. In this regard, bone ceramics based on hydroxyapatite and geopolymers can be promising candidates in regenerative medicine due to their mechanical strength, low cost, chemical composition variability, and wide processing window [43].

Herein, we report the synthesis of a novel biocompatible open-cell porous bioceramics based on geopolymers made of the combination of metakaolin and hydroxyapatite, which are non-cytotoxic and have a large porous structure while maintaining the compressive strength. Mechanical properties were evaluated by mechanical compressive strength, X-Ray diffraction analysis showed the crystalline phases, rheology behavior was evaluated by viscosity measurements and scanning electron microscopy was used to show microstructure properties. The biocompatibility of synthesized materials was evaluated with mesenchymal stem cells derived from adipose tissue, which have an important role in tissue regeneration and can be associated with biomaterials to enhance the bone repair process. This study opens up possibilities for further exploration of the synergistic effects between the GMK-HA-HT and the MSCs, with the aim of improving bone tissue engineering strategies.

2. Materials and methods

In this work, three different types of metakaolins (MK) and hydroxyapatite (HA) p.a., ≥90% $3Ca_3(PO_4)_2{\cdot}Ca(OH)_2$ (Sigma-Aldrich) were used. Their chemical composition, loss of ignition and particle sizes are shown in Table 1.

MK1: *Mefisto K05* was supplied by České lupkové závody, a.s., Czech Republic, MK2: *Metapor* was purchased from Dennert Poraver GmbH, Germany and MK3: *Sedlec Rapid* was supplied by Sedlecký Kaolin a.s., Czech Republic.

The measurements show a very similar particle size distribution of metakaolins with an average particle size ranging from 6.5 to 8.5 μm. The volume median values are defined as the value where half of the population resides above this point and half resides below this point. In this context, the smallest particle size distribution is seen in MK2 where 10% of particles are smaller than 3.25 μm.

2.1. Geopolymer design and fabrication route

2.1.1. Geopolymer filler

The geopolymer slurry was prepared as a two-component system based on sodium silicate solution (Silica modulus Ms = 1.6) and metakaolin in a solid-to-liquid weight ratio of 1.5. The raw materials were mixed for 20 min (500 rpm). Curing and solidification took place in a closed container under laboratory conditions (20–25 °C) for 21 days.

The geopolymer body was then crushed and ground in a laboratory agate bowl. This was followed by grinding with a ball mill. The geopolymer filler (GF) served as a particulate filler in the geopolymer-

Table 2
Volume particle size distribution of geopolymer fillers (GF).

Size distribution	Mean size (μm)	Median size D50 (μm)	Dv10 (μm)	Dv90 (μm)
GF1	62.79	24.01	6.17	179.91
GF2	136.96	44.00	5.58	372.42
GF3	79.16	17.46	4.81	255.45

hydroxyapatite (GMK-HA) mixture in the further preparation of the mixtures. The intention was to reinforce the matrix against internal stress during impregnation and heat treatment. The advantage lies in the modification of materials with fillers with the same chemical and mineralogical composition.

Accordingly, 3 types of geopolymeric fillers based on 3 types of metakaolin (MK1, MK2, and MK3) were prepared and labeled GF1, GF2, and GF3. The particle size distribution after mechanical grinding is given in Table 2.

2.1.2. Geopolymer-hydroxyapatite mixture

The geopolymer-hydroxyapatite mixture was prepared on the basis of the same protocol given in paragraph 2.1.1. After mixing the two-component geopolymer system for 10 min. (500 rpm), GF filler (belonging to the same type of metakaolin system) was added in a weight fraction of 15 wt% of the geopolymer system. The mixture was further mixed for 10 min, then HA was added with stirring for another 10 min. HA was added in a weight fraction of 15 wt% of the two-component geopolymer system.

Geopolymer-hydroxyapatite mixtures reinforced with GF and modified by HA were labeled according to the type of metakaolin GMK1-HA, GMK2-HA, and GMK3-HA.

2.1.3. Fabrication route

Experimental mixtures were prepared according to the above-mentioned protocol. In general, the fabrication route is based on the work of the authors published elsewhere [44–46]. Polyurethane (PU) foam with dimensions of 25 × 25 × 25 mm (porosity 7–15 PPI, bulk density 19–22 kg/m^3) was used as the polymer template. PU foam was immersed into the geopolymer mixture so that the polymeric foam was uniformly impregnated. The coated polyurethane was heated in a sealed vessel at 70 °C for 60 min to accelerate the polycondensation reaction and obtain a solid structure [47]. Subsequently, a heat treatment step is made, which decreases the material alkalinity, a crucial factor in the biocompatibility [17,38]. With regard to the heat treatment step, the samples were subsequently marked HT (heat-treated). Samples for biological testing were prepared in the same chemical composition and

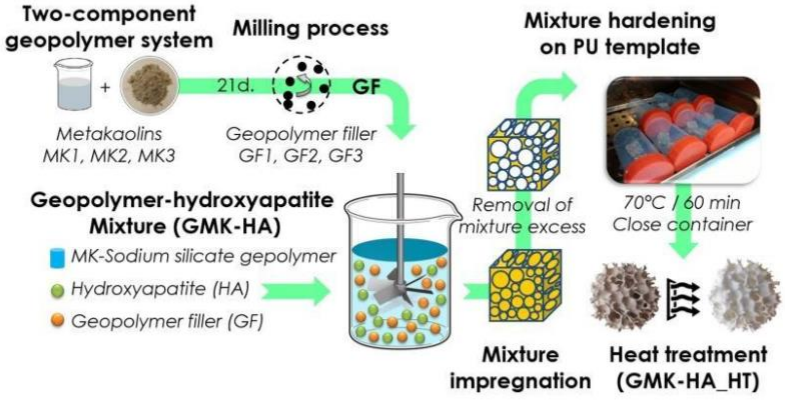

Fig. 1. A schematic illustration of the fabrication route.

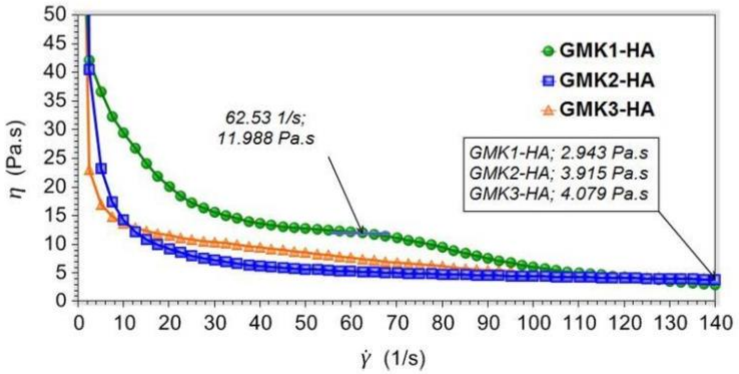

Fig 2. Viscosity curves as a function of shear rate for GMK1-HA, GMK2-HA and GMK3-HA mixtures.

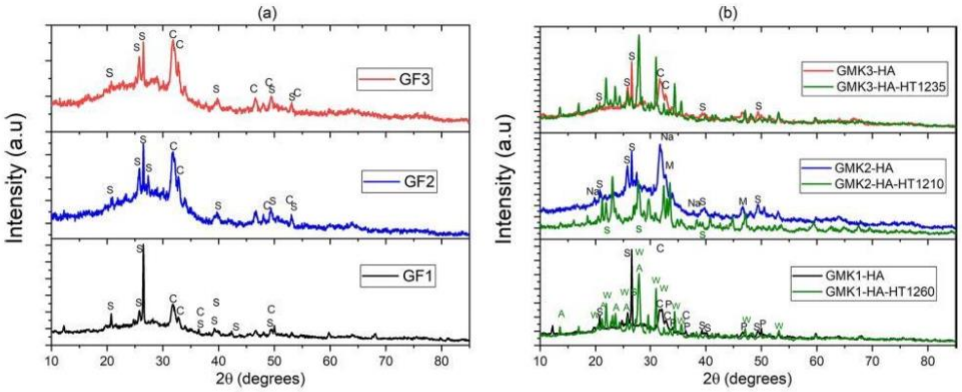

Fig. 3. X-ray diffraction patterns for all samples: a) GF1, GF2, GF3. b) GMK1-HA, MK2-HA, MK3-HA, in comparison of GMK1-HA-HT1260, MK2-HA-HT1210, MK3-HA-HT1235. PS: The symbols (S, C, P, W, A, M, Na|) identify the phase, see Table 3.

Table 3
Identified phases in DRX analysis.

	Sample	Composition of phase formed	Additional information of phase
Fig.3. a	GF1 GF2 GF3	S → SiO_2 C → Ca_2SiO_4	- alpha-Silicon Oxide PDF-number 010–89–8937 - Calcium Silicate PDF-number 000–24–0234
Fig.3. b	GMK1-HA	S → SiO_2 C → Ca_2SiO_4 P → $Ca_{10}(PO_4)_6O$	- alpha-Silicon Oxide PDF-number 010–89–8937 - Calcium Silicate PDF-number 000–24–0234 - Calcium Phosphate Oxide PDF-number 010–89–649
	GMK1-HA-HT1260	S → SiO_2 W → $Ca_{2.06}Mg_{0.14}(PO_4)_2$ A → $Ca_{0.89}O_{12}Al_{1.77}Si_{2.23}O_8$	- alpha-Silicon Oxide PDF-number 010–89–8937 - beta-Whitlockite, syn, PDF-number 010–77–0692 - Calcium Aluminum Silicate PDF-number 000–52–1344
	MK2-HA	S → SiO_2 Na → $Na_2(SO_4)$ M → $Mg_3Al_4Ti_3O_{25}$	- alpha-Silicon Oxide PDF-number 010–89–8937 - Sodium Sulfate PDF-number 010–79–1553 - Magnesium Aluminum Titanium Oxide PDF-number 000–05–0636
	MK2-HA-HT1210	S → SiO_2 Other peaks → $K_3Fe(PO_4)_2$	- alpha-Silicon Oxide PDF-number 010–89–8937 - alpha-Potassium Iron Phosphate phase, PDF-number 000–54–1235, which corresponds to the other peaks.
	MK3-HA	S → SiO_2 C → Ca_2SiO_4	- alpha-Silicon Oxide PDF-number 010–89–8937 - Calcium Silicate PDF-number 000–24–0234
	MK3-HA-HT1235	Only → $Ca(Al_2Si_2O_8)$	one phase: Calcium Aluminum Silicate PDF number 010–73–0265 *All samples present the amorphous halo

technological procedure in a cylindrical size of 25 mm in diameter and 30 mm height. The applied fabrication route is schematically presented in Fig. 1.

The applied heat treatment modes were determined based on firing tests of geopolymer cones. From the experimental mixtures GMK1-HA, GMK2-HA and GMK3-HA, test bodies were prepared and thermally annealed according to the modified methodology of the international standard ASTM C24–09 (2022) [40]. The heating of the specimens (geopolymer cones) was carried out in order to mimic the firing conditions of the experimental specimens ($GMK_{1,2,3}$–HA) and to define the correct firing regime. The motivation was to find the optimum regime to perform sintering of the porous matrix while maintaining the porosity of the foams.

A standard test method has been adopted for the determination of the pyrometric cone equivalent of fireclay and high-alloy refractories which defines the deformation and end point of the cone corresponding to certain conditions of thermal work due to time, temperature and atmosphere.

The test firings were carried out in the interval of 1210, 1235, 1260 °C with different soaking times of 1–4 h (isothermal process). The evolution of the deformation angle of the experimental cone was monitored by optical measurements. It was determined the onset of viscous flow of the experimental specimens ($GMK_{1,2,3}$–HA) would correspond to softening of the top of the cones in the form of a 20% deformation. It was found that different compositions (depending on the type of metakaolin, see Table 1) require slightly different heat treatment regimes.

Based on experimental data, the following regimes were applied: heating ramp of 1 °C/min to 600 °C (30 min. soak), 3 °C/min to 1000 °C (60 minutes' soak time), and 5 °C/min to 1260 °C (4 h soak) for GMK1-HA-HT, 1210 °C (4 h soak) for GMK2-HA-HT and 1235 °C (4 h soak) for GMK3-HA-HT. The slow temperature ramp (1 °C/min to 600 °C) was intentionally designed for the stepwise drying of the geopolymer composite and the gradual thermal decomposition of the PU substrate as a form of the lost template technique. The microstructural and morphological state can be seen in Section 3.3 Microstructural Properties.

2.2. *Adipose-derived mesenchymal stem cells: isolation and characterization*

Adipose-derived mesenchymal stem cells (ADSCs) were isolated and characterized as previously described [48,49]. ADSCs were extracted from the abdominal adipose tissue of a healthy adult donor undergoing tumescent liposuction. The experimental protocol was approved by the Research Ethics Committees of Santa Casa de Misericórdia of Porto Alegre and the Federal University of Health Sciences of Porto Alegre (UFCSPA) and the informed consent was obtained (REC- 3029.141 and 3.734.612), respectively. Briefly, the adipose tissue was washed with phosphate-buffered saline (PBS) and its extracellular matrix was

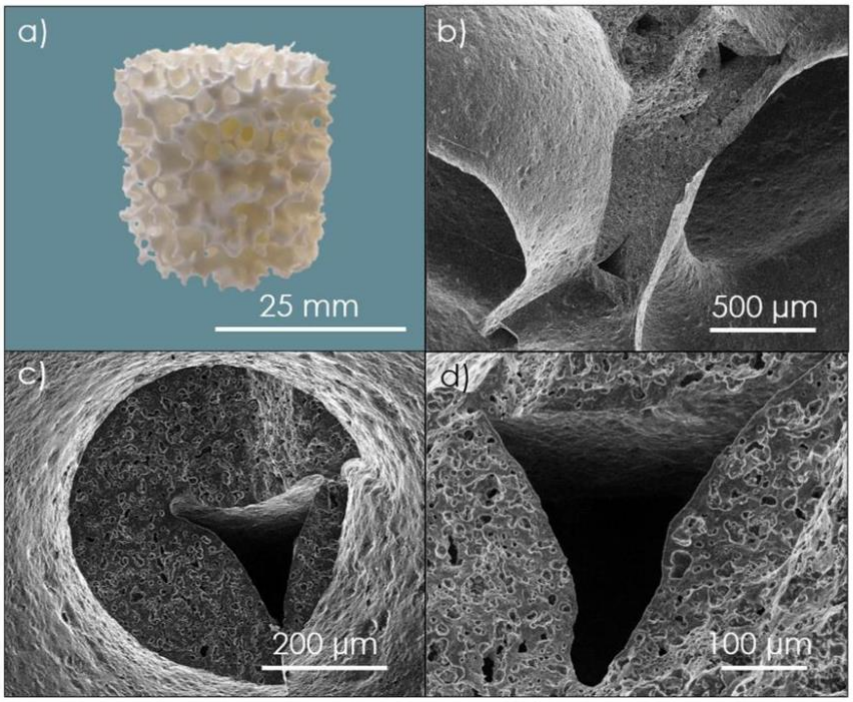

Fig. 4. Macro-photo of the cylindrical ceramic foam specimen GMK1-HA-HT (a); Fracture area of matrix body across ceramic struts (b); Cross section of single strut (c); SEM detail of ceramic strut ending (d).

digested with type I collagenase. Dulbecco's modified Eagle's Medium standard (DMEM) - low glucose supplemented with 10% FBS (Fetal Bovine Serum) was added to inactivate the collagenase. Erythrocytes were lysed with a lysis buffer (150 mM NH_4Cl, 10 mM $NaHCO_3$, and 1 mM EDTA). Cells were cultured with DMEM low 10% FBS, 100 UL^{-1} penicillin, and 100 mg/L streptomycin and they were kept in an aseptic and humidified environment at 37 ± 0.1 °C and 5% CO_2. For the experiments, cell cultures were used in passages from 4 to 10. These cells were tested for adipogenic, chondrogenic and osteogenic differentiation capacity. For this, ADSCs were grown in a 6-well plate at 37 °C with 5% CO_2 with an adipogenic induction medium containing DMEM- high glucose, 10% FBS, 10^{-6} M dexamethasone, 10 µg/mL insulin, 200 µM indomethacin, osteogenesis induction medium consisting of DMEM-high glucose, 10% FBS, 0.1 µM dexamethasone, 10 mM β-glycerol phosphate, and 200 µM ascorbic acid. Chondrogenic differentiation was inducted with the Chondrogenesis Differentiation Kit (Gibco®; Invitrogen, Grand Island, NY).

Two weeks after induction, the adipocyte differentiation was confirmed by oil red O staining and the chondrogenic differentiation by alcian blue staining. After forty days of culture, the osteogenic differentiation was verified by alizarin red staining. Cells in the control group were treated with the standard medium.

The BX-50 microscope (Olympus, Tokyo, Japan) was used to evaluate the staining results. Cells were characterized by immunophenotyping on the FACSCalibur flow cytometer (BD Bioscience, USA) using the antibodies anti CD14, CD34, CD44, CD45, CD90, CD73 and CD105 proteins.

2.3. GMK-HA-HT extracts

GMK-HA-HT extracts were prepared in accordance with EN ISO 10,993–12. Samples were autoclaved and incubated with DMEM-Low supplemented with 10% fetal bovine serum for 24 h under cell culture conditions (5% CO_2, 95% humidity, 37 °C) with a fixed mass ratio to medium volume (0.2 g/ml) [29].

2.4. Cell viability (MTT assay)

ADSCs were used for in vitro cell cytotoxicity experiments. Cells were pre-cultivated in a 96-well plate at a ratio of 3.0×10^3 cells per well and incubated at 37 ± 0.1 °C and 5% CO_2. After 24 h, the culture media was replaced with 100%, 10%, and 1% GMK-HA-HT extract media and cells were further incubated. ADSCs with standard media were used as control. After 24 h, the supernatant was discarded and the cells were incubated with MTT (3-(4,5-dimethylthiazol-2-yl)−2,5-diphenyltetrazolium bromide) at 37 ± 0.1 °C and 5% CO_2 for 3 h. After this, the medium was removed, and the formazan crystals were dissolved in DMSO (dimethyl sulfoxide). The absorbance of the samples was measured by a microplate reader at 560 nm. Statistical analyses were performed using Two-way ANOVA, followed by Tukey post hoc test in the GraphPad Prism 5.0. Differences were considered significant when $P < 0.05$.

2.5. DAPI (4′,6-diamidino-2-phenylindole) and phalloidin staining

Cells were cultured with GMK-HA-HT extracts in a ratio of 6×10^3 24-well. After 24 h, they were fixed with 4% paraformaldehyde,

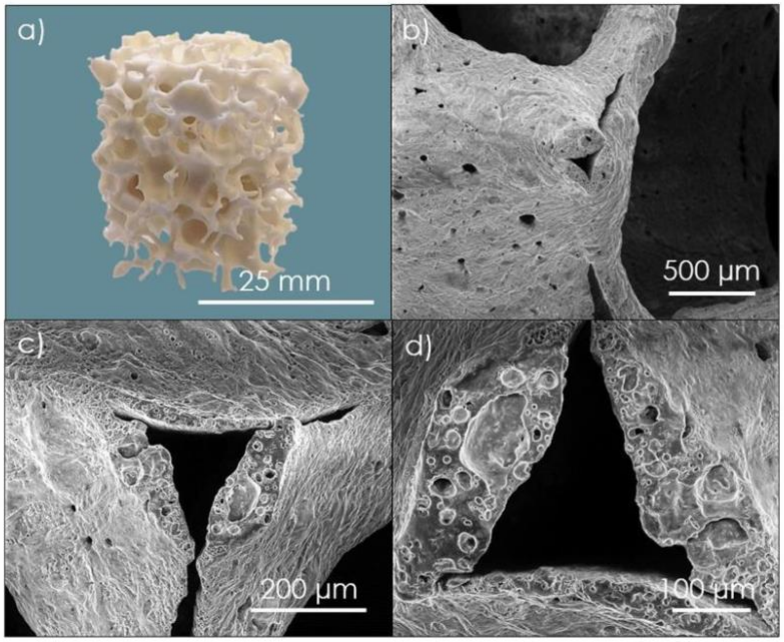

Fig. 5. Macro-photo of the cylindrical ceramic foam specimen GMK2-HA-HT (a); Macro-scale photo of ceramic strut (b) and its fracture area (c); SEM detail of ceramic strut ending (d).

permeabilized with 0.1% Triton X-100, and stained with DAPI (4′,6-diamidino-2-phenylindole) and Alexa Fluor™ 488 Phalloidin. Images were captured on the EVOS FL Auto 2 Cell Imaging System.

2.6. Scanning electron microscopy

The morphology of the cells on the GMK-HA-HT samples was observed by scanning electron microscopy (SEM). ADSCs were cultured on the surface GMK-HA (5 days), fixed in 2.5% glutaraldehyde, and prepared for SEM as previously described [50]. Briefly, ADSCs were cultured on GMK-HA-HT samples for 5 days. After that, the samples were rinsed using PBS and fixed with 2.5% glutaraldehyde for 96 h at 4 °C. Subsequently, they underwent three PBS washes (30 min each). Dehydration of the samples was achieved by exposing them to increasing concentrations of propanone (30%, 50%, and 70% for 10 min; 90% for 10 and 20 min and 100% for 10 and 20 min). To complete the process, a Balzers CPD030 critical point dryer was used for desiccation. The samples were mounted on aluminum stubs and coated with gold. Finally, images were captured using a Jeol JSM-6060 scanning electron microscope.

3. Results and discussion

3.1. Rheology behavior

Dynamic viscosity curves for the geopolymers mixtures are presented in Fig. 2. Decreasing viscosity with increasing shear strain indicates rheological behavior for non-Newtonian fluids [51]. Geopolymer mixtures demonstrate shear-thinning behavior, thus providing good flow behavior at low strains during the mixing step. However, differences are evident from the course of increasing shear strain.

The GMK1-HA mixture shows higher dynamic viscosity above 10 Pa. s in the shear strain range of 0–65 s^{-1}. This implies a longer dispersion and dissolution of the lamellar-packed grains of metakaolin MK1 in the alkaline environment of sodium silicate. GMK2-HA and GMK3-HA showed similar shear-thinning behavior with an as-plateau viscosity curve above 100 s^{-1}. The experimental mixtures showed consistent low viscosity between 3 and 4 Pa.s at higher shear strains. This result indicates suitable flow behavior and good workability of the systems for impregnation of polymer replica in the porous foam formation step. [46]

3.2. X-ray characterization

The X-ray diffraction pattern of all samples is shown in Fig. 3 and *Supplementary file S1*. The XRD patterns shown in Fig. 3 confirm that all samples present the amorphous and crystalline phases.

In Fig 3a. samples GF1, GF2 and GF3, we can see that the crystalline peaks are equivalent for the three samples, associated with the alpha-Silicon Oxide (SiO_2) and Calcium Silicate Ca_2SiO_4 crystalline phase. Of these three samples, GF1 has the smallest amorphous hallo. In Fig. 3b we still observe a small amorphous halo, but with the thermal treatments, this hallo decreases and increases the new peak of the crystalline phase. There is a structural change depending on the sample and mainly on the heat treatment applied. It is worth noting that in the sample GMK3-HA-HT, only a single phase was identified, which is reported as Calcium Aluminum Silicate $Ca(Al_2Si_2O_8)$. In the case of the GMK2-HA-HT sample, we still have some SiO_2 peaks, but most of the sample evolves towards alpha-Potassium Iron Phosphate phase, $K_3Fe(PO_4)_2$. Table 3 summarizes the crystallographic information of all the samples that were shown in Fig. 3.

Additionally, the XRD patterns shown in *Supplementary file S1* for MK1, MK2 and MK3 samples present the amorphous and crystalline fraction phases. Sample MK2 has the highest number of peaks in the crystalline phases, but the intensity of these peaks is small in comparison

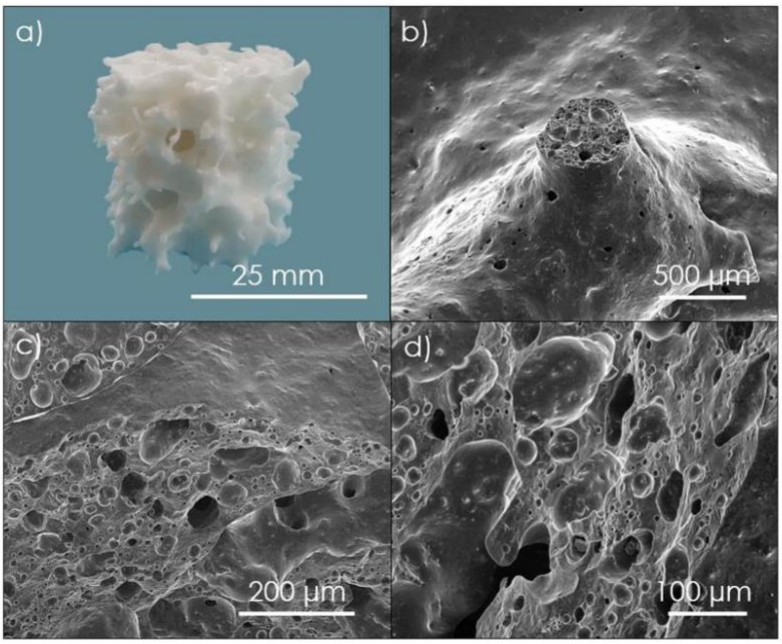

Fig. 6. Macro-photo of the cylindrical ceramic foam specimen GMK3-HA-HT (a); Macro-scale photo of ceramic strut (b); SEM detail of ceramic strut ending (c,d).

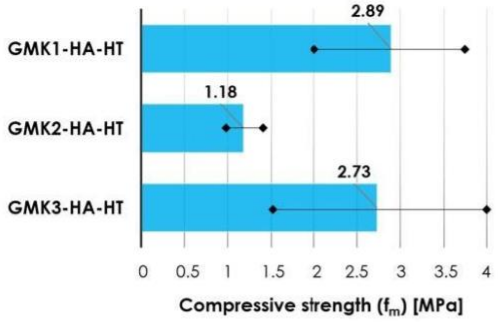

Fig. 7. Compressive strength evaluation of thermally treated samples GMK1-HA-HT, GMK2-HA-HT, GMK3-HA-HT.

to the other two samples, MK1 and MK3, which can explain the compressive strength tests results. The predominant phase in these three samples is alpha-Silicon Oxide (SiO_2). In addition to the SiO_2 phase, peaks of the following phases were identified: MK1 (Zirconium Phosphate and Titanium Oxide), MK2 (Aluminum Silicate and Microcline $KAlSi_3O_8$) and MK3 only SiO_2.

The results shown in Fig. 3 and summarized in table 3 indicated the evolution of phase in function of composition and thermal treatment. Due to the variety of metakaolin chemical composition, it is expected to be a mixture of crystalline phases after heat treatment [45,46,52]. The presence of calcium and phosphate phases indicates the successful incorporation of HA in the materials, forming new crystalline phases during the curing process. The amorphous phase continues to be observed in Fig. 3 for these experimental conditions, but it decreases after heat treatment.

3.3. Microstructural properties

Glass-ceramic foams were studied using visualization techniques with the intention of describing the microstructural state of the matrix, struts and pore distribution. It was observed that the GMK1-HA-HT ceramic foam (HT: after heat treatment) has a compact porous structure with open pores up to 3 mm in size (Fig. 4a). The interconnected cellular structure can be seen in Fig. 4b, where triangular holes form the hollow part of the strut. The correct implementation of the thermal regime is demonstrated by the compact surface of the ceramic body, where no cracks were identified. Multi-level porosity is evident from the visualization of the strut cross-section (Fig. 4c), which is formed by oval pores of less than 20 µm in size. In addition, a high distribution of very fine pores (1–10 µm) was found across the glass-ceramic matrix, as seen in Fig. 4d.

The findings confirm the morphological and microstructural suitability of the geopolymer-based glass-ceramic composite. The interconnected porosity and high specific surface area provide a favorable precondition for positive cell proliferation.

GMK2-HA-HT showed a distinct organization of the macroporous structure with dominant large pores up to 5 mm (Fig. 5a). It is evident that the solid phase shows higher heterogeneity with isolated surface pores. Thin struts with a triangular cross-section and small edge cracks are typical, as seen in Fig. 5b,c. The walls of the struts, with a maximum thickness of 100–150 µm, are formed by randomly organized micrometric pores in the range of 1–50 µm. In this context, it is worth noting that a lower degree of PU substrate coverage and thin shell formation occurs after heat treatment (Fig. 5d).

GMK3-HA-HT represents a compact porous matrix with a lower

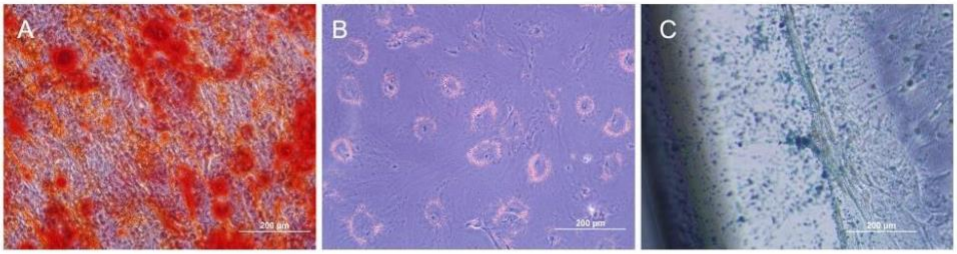

Fig. 8. Characterization of adipose-derived mesenchymal stem cells (ADSCs). (A) Osteogenic differentiation (B) Adipogenic differentiation (C) Chondrogenic differentiation.

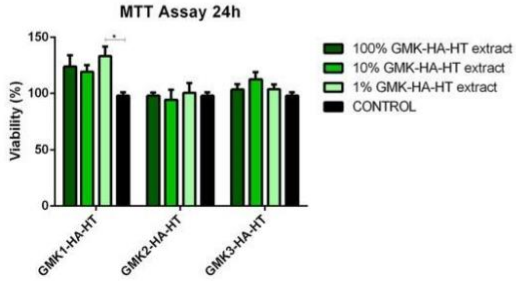

Fig. 9. Viability of ADSCs cultured for 24 h in GMK-HA-HT extracts with 100%, 10% and 1% concentration. Bars represent mean +- SEM ($n = 3$). * P-value < 0.05 (Two way ANOVA, Tukey post-hoc test).

proportion of macroporosity and higher proportion of solid phase (Fig. 6a,b). The compact surface forms a continuous structure with thicker struts composed of heterogeneous micro- to macroporosity in the range from 1 to 200 µm.

It is proven that the ceramic body forms a predominantly porous structure with a close surface without any fibrillary cracks. The porosity of the ceramic matrix consists of oval pores in a wide range of sizes from 1 to 100 µm (Fig. 6c,d).

In conclusion, GMK1-HA-HT foam showed the most preferred morphological properties and interconnected pore distribution including compact surface integrity compared to the other series.

Interpretation of the structural evolution leads to the understanding of the dependence of surface integrity and porosity organization on the mechanical strength of foam composites, as presented in Section 3.5.

3.4. Mechanical strength

The results of compressive mechanical strength scattered with confidence intervals are expressed by error bars, as seen in Fig. 7. The data show a strong dependence of mechanical integrity on the surface compactness of glass-ceramic foams. Although the size of open macropores for all types of composite foams occurs in the range from 1 to 5 mm, GMK2-HA-HT shows the lowest strength ~ 1 MPa with a coefficient of variation of compressive strength of 30.26%. This result can be attributed to the presence of thin wall struts (<100 µm) and incomplete sintering of the ceramic matrix body. The coefficient of variation (Cv), is based on the standard Gaussian distribution reported as a percentage and is defined as the ratio of the standard deviation (σ) to the mean (µ).

The compressive strengths of the GMK1-HA-HT and GMK3-HA-HT composite foams show average values 2.7 and 2.89 MPa however with high data variation of 33.57% and 46.86%, respectively. This trend is indicative of the presence of a larger volume of solid phase including presence of high mico- /macroporosity. Thus, a high coefficient of variation can be interpreted by the increased presence of stress concentrators.

These values are greater than those obtained for similar open-cell macroporous systems [45,52–54], which shows that the hydroxyapatite addition increases the mechanical compressive strength. The values are also greater than the reported for ceramic foams with different compositions [55–58] thus, the compressive strength obtained to the samples is suitable for its use in BTE.

3.5. In vitro cytocompatibility

A cytotoxicity evaluation is necessary for all medical devices and their biomaterials components. Most of these cytotoxicity tests use fibroblasts in vitro to determine whether a biomaterial is noncytotoxic. It is important to consider other cells and tissues that may be specifically affected by the medical device or biomaterial in question [59]. Mesenchymal stem cells (MSCs) have gained significant attention in biocompatibility testing due to their unique properties and potential for therapeutic applications [60]. By employing MSCs in biocompatibility testing, we gain a more comprehensive understanding of how the biomaterial interacts with these cells, which are intricately involved in tissue repair and regeneration.

In this study, we isolated and characterized mesenchymal stem cells from adipose tissue to evaluate biocompatibility in vitro of GMK-HA-HT samples and a possible association of the biomaterial with these cells in bone tissue engineering [61].

Cells isolated from adipose tissue were able to adhere to plastic and differentiate into three lineages (adipogenic, chondrogenic, and osteogenic). This capability was evidenced by staining the cells after culture with an induction medium (Fig. 8). Flow cytometric phenotype analysis showed that the cells are positive for CD44, CD105, CD90, and CD73 and negative for CD14, CD34, and CD45, which is indicative of a typical MSC phenotype. These results indicate that ADSCs were successfully isolated [62].

ADSCs showed good compatibility with 100%, 10%, and 1% extracts in 24 h, as shown in Fig. 9. Cells treated with 1% GMK1-HA-HT extract showed statistically higher viability than its control. According to ISO 10993-5, if viability is reduced by >30% in comparison to control, the biomaterial has a cytotoxic potential. There was no significant change in ADSCs viability, so GMK-HA-HT is cytocompatible [24].

Cells cultured with GMK-HA-HT extracts exhibited good adherence to plastic and the typical morphology of the ADSCs. They preserved the integrity of the actin cytoskeleton and nuclei as observed by DAPI and Phalloidin staining (Fig. 10).

The adherence and morphology of the ADSCs on the surface of GMK-HA-HT samples were observed by SEM after 5 days of culture. The ADSCs showed a fusiform shape and adhered to the surface of the scaffolds. It was possible to observe the cells with cytoplasmic extensions on the scaffolds, which is a sign of biocompatibility of the cells

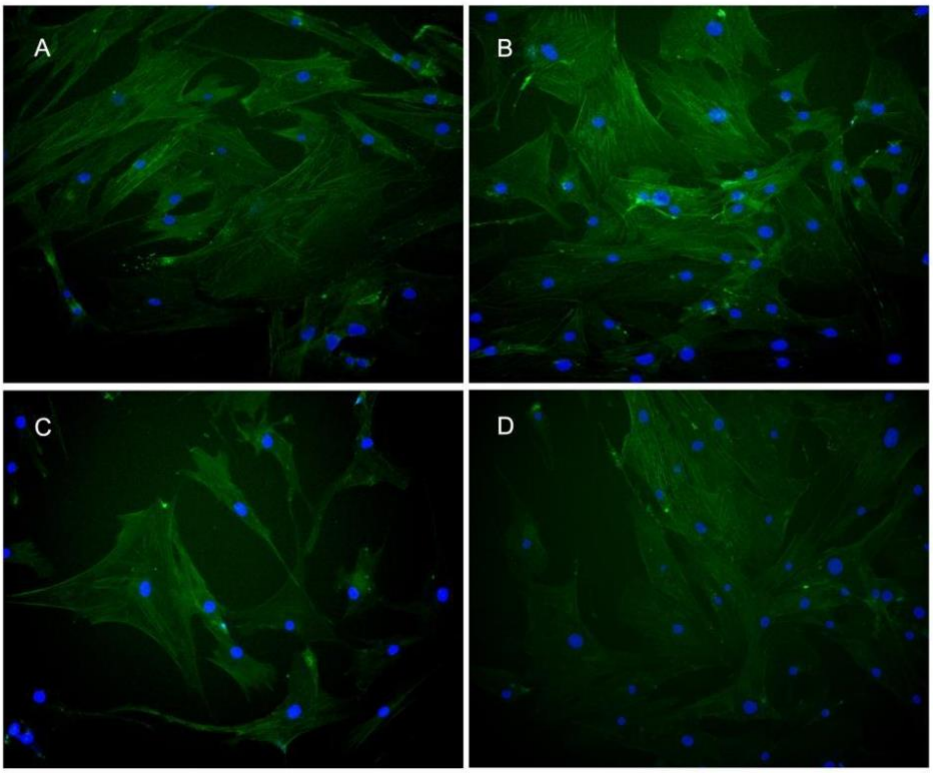

Fig. 10. Micrographs show the F-actin cytoskeleton (green) and nuclei (blue) of the ADSCs treated with GMK-HA-HT extracts for 24 h. (A) Control; (B-D) Samples GMK1-HA-HT, GMK2-HA-HT and GMK3-HA-HT, respectively. Fluorescence microscopy, 200x magnification.

with the material. In addition, cells proliferated and had a significant spreading on the surface of GMK1-HA-HT and GMK3-HA-HT samples. We observed a lower number of cells adhered to the GMK2-HA-HT surface (Fig. 11). Our previous studies show that the interaction between cells and scaffold is a characteristic of biocompatible materials. ADSCs, when adhered to the scaffold, usually show cytoplasmic extensions and form a monolayer [29,63,64].

In literature, cells in contact with biomaterials compounds of hydroxyapatite or geopolymers are described as biocompatible. Quiao et al., (2014) reported that MSCs from the bone marrow co-cultured with nano-hydroxyapatite/polyamide 66/glass fiber (n-HA/PA66/GF) disk have no negative influence on the proliferation and osteogenic differentiation of cells [65]. The association of collagen/hydroxyapatite also promotes the differentiation of ADSC into mature osteoblasts [66].

Geopolymer–carbonated apatite nanocomposites with the addition of Mg and Sr trace elements are not cytotoxics. Fibroblasts showed good spreading, cell viability higher than 80%, and no alterations of the cell morphology and number [67]. Considering that the GMK-HA-HT scaffolds are a novelty, there are no other studies to compare the biocompatibility of biomaterials with the same composition. However, studies with hydroxyapatite or metakaolin corroborate our results that show the biocompatibility of the material developed.

4. Conclusion

In this paper, a novel porous bioceramic based on geopolymer and hydroxyapatite was synthesized by the replica technique. Three types of metakaolin were used and the materials were heat treated. Rheology behavior measurements show that three samples before heat treatment present non-Newtonian fluids behavior with moderate viscosity, which provides a suitable flow behavior for the synthesis process. X-Ray diffraction patterns show that heat treatment increases the crystalline phases and that HA was properly incorporated in the structures. The compressive strengths of GMK1-HA-HT and GMK3-HA-HT foams are, on average, 2.7 and 2.89 MPa. However, GMK2-HA-HT presents the lowest strength (c.a. 1 MPa), which is expected due to the cracks and thin struts observed in microstructural analysis by SEM images. The biocompatibility was evaluated by in vitro tests using mesenchymal stem cells in contact with GMK-HA-HT extracts, which demonstrated the cytocompatible behavior of the foams. Moreover, the adherence and morphology of cells were observed after 5 days of culture by SEM, the images present cell proliferation and spreading in GMK1-HA-HT and GMK3-HA-HT, which are the more resistant and compact structures. Thus, we have introduced and described a new class of biocompatible material that shows promising potential for bone implant applications. Furthermore, this study paves the way for future investigations into the synergistic effects between GMK-HA-HT and MSCs, aiming to enhance bone tissue engineering strategies.

Funding

MRW is recipient of level 1 research productivity fellowship from

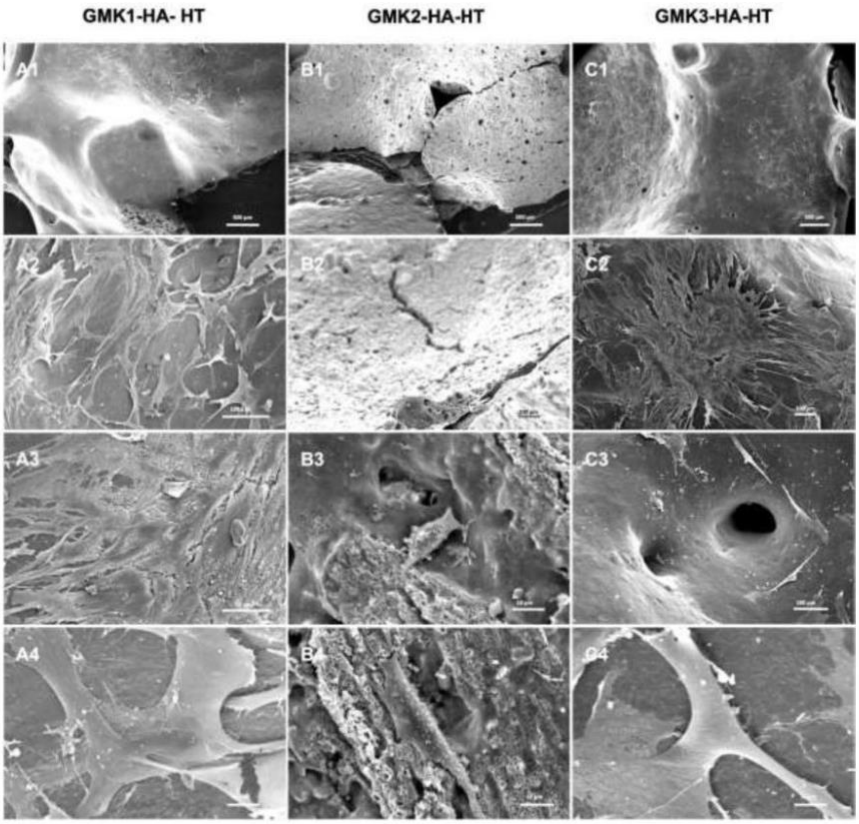

Fig. 11. Scanning electron microscopy of the ADSCs cultured on the GMK-HA-HT scaffolds after 5 days. (A-C) Samples GMK1-HA-HT, GMK2-HA-HT and GMK3-HA-HT, respectively.

Conselho Nacional de Desenvolvimento Científico e Tecnológico – Brasil (CNPq); RA was recipient of Pibic CNPq fellowship; TCP is recipient of PhD fellowship from Coordenação de Aperfeiçoamento de Pessoal de Nível Superior – Brasil (CAPES) – Finance Code 001: LISN is recipient of Postdoc fellowship from CNPq; This study was supported by Fundação de Amparo à Pesquisa do Estado do Rio Grande do Sul - Brasil (FAPERGS) EDITAL 07/2021 - PqG 05/2019 (projects: 19/2551-0001978-5 and 21/2551-0001947-6) and RITES (22/2551-0000385-0); CNPq MS-SCTIE-Decit/CNPq n° 12/2018 (441575/2018-8), MS-SCTIE-DECIT-DGITIS-CGCIS/CNPq n° 26/2020 (442586/2020-5) and National Institute of Science and Technology in 3D printing and Advanced Materials Applied to Human and Veterinary Health - INCT_3D-Saúde, CNPq (406436/2022-3); and UWB university specific research projects NaturTech4 SGS-2022-021.

CRediT authorship contribution statement

Rafaela de Andrade: Conceptualization, Methodology, Investigation, Visualization, Formal analysis, Writing – original draft, Writing – review & editing. **Thaís Casagrande Paim:** Conceptualization, Methodology, Investigation, Visualization, Formal analysis, Writing – original draft, Writing – review & editing. **Isadora Bertaco:** Investigation, Visualization, Validation. **Liliana Sous Naasani:** Conceptualization, Investigation, Visualization, Validation. **Silvio Buchner:** Conceptualization, Funding acquisition, Resources, Methodology, Investigation, Visualization, Formal analysis, Writing – original draft, Writing – review & editing. **Tomáš Kovářík:** Conceptualization, Methodology, Funding acquisition, Project administration, Resources, Supervision, Writing – original draft, Writing – review & editing. **Jiří Hájek:** Conceptualization, Methodology, Investigation, Validation, Formal analysis. **Márcia Rosângela Wink:** Conceptualization, Funding acquisition, Project administration, Resources, Supervision, Writing – original draft, Writing – review & editing.

Declaration of Competing Interest

The authors declare that they have no known competing financial interests or personal relationships that could have appeared to influence the work reported in this paper.

Data availability

Data will be made available on request.

Acknowledgements

The authors would like to thank the INCBAC Institute for the academic internship program (UNIGOU). They would also like to thank Centro de Nanociência e Nanotecnologia at Universidade Federal do Rio Grande do Sul (CNANO - UFRGS), in particular Professor Fabrício Faita for performing the X Ray diffraction measurements, and the prof. Rommulo Conceição and LGI-CPGq-IGEO-UFRGS for MEV facilities.

Supplementary materials

Supplementary material associated with this article can be found, in the online version, at doi:10.1016/j.apmt.2023.101875.

References

[1] K. Korniejenko, B. Figiela, C. Ziejewska, J. Marczyk, P. Bazan, M. Hebda, M. Choińska, W.-T. Lin, Fracture behavior of long fiber reinforced geopolymer composites at different operating temperatures, Materials 15 (2022), https://doi.org/10.3390/ma15020482.

[2] J. Davidovits, Geopolymers: inorganic polymeric new materials, J. Therm. Anal. Calorim. 37 (1991) 1633–1656, https://doi.org/10.1007/BF01912193.

[3] M. Catauro, F. Bollino, I. Lancellotti, E. Kamseu, C. Leonelli, Chemical and biological characterization of geopolymers for potential application as hard tissue prostheses, Adv. Sci. Technol. Water Resour. 69 (2011) 192–197, https://doi.org/10.4028/www.scientific.net/AST.69.192.

[4] R. Cioffi, L. Maffucci, L. Santoro, Optimization of geopolymer synthesis by calcination and polycondensation of a kaolinitic residue, Resour. Conserv. Recycl. 40 (2003) 27–38, https://doi.org/10.1016/S0921-3449(03)00023-5.

[5] S. Chuah, W.H. Duan, Z. Pan, E. Hunter, A.H. Korayem, X.L. Zhao, F. Collins, J. G. Sanjayan, The properties of fly ash based geopolymer mortars made with dune sand, Mater. Des. 92 (2016) 571–578, https://doi.org/10.1016/j.matdes.2015.12.070.

[6] S. Mujeeb, M. Samudrala, B.A. Lanjewar, R. Chippagiri, M. Kamath, R. V. Ralegaonkar, Development of alkali-activated 3D printable concrete: a review, Energies 16 (2023), https://doi.org/10.3390/en16104181.

[7] S.H. Bong, B. Nematollahi, A. Nazari, M. Xia, J. Sanjayan, Method of optimisation for ambient temperature cured sustainable geopolymers for 3D printing construction applications, Materials 12 (2019), https://doi.org/10.3390/ma12060902.

[8] Y. Xiao, T. Gong, S. Zhou, The functionalization of multi-walled carbon nanotubes by in situ deposition of hydroxyapatite, Biomaterials 31 (2010) 5182–5190, https://doi.org/10.1016/j.biomaterials.2010.03.012.

[9] A.W. Bhuiya, M. Hu, K. Sankar, P.F. Keane, D. Ribero, W.M. Kriven, Bone ash reinforced geopolymer composites, J. Am. Ceram. Soc. 104 (2021) 2767–2779, https://doi.org/10.1111/jace.17621.

[10] P.K. Pachana, U. Rattanasak, K. Nuithitikul, P. Jitsangiam, P. Chindaprasirt, Sustainable utilization of water treatment residue as a porous geopolymer for iron and manganese removals from groundwater, J. Environ. Manage. 302 (2021), 114036, https://doi.org/10.1016/j.jenvman.2021.114036.

[11] Elisabetta Maria Cepollaro, Renata Botti, Giorgia Franchin, Luciana Lisi, Paolo Colombo, Stefano Cimino, Cu/ZSM5-geopolymer 3D-printed monoliths for the NH3-SCR of NOx, Catalysts 11 (2021) 1212, https://doi.org/10.3390/catal11101212.

[12] P. Chindaprasirt, U. Rattanasak, Characterization of porous alkali-activated fly ash composite as a solid absorbent, Int. J. Greenh. Gas Control. 85 (2019) 30–35, https://doi.org/10.1016/j.ijggc.2019.03.011.

[13] P. Chindaprasirt, U. Rattanasak, Synthesis of porous alkali-activated materials for high-acidic wastewater treatment, J. Water Process Eng. 33 (2020), 101118, https://doi.org/10.1016/j.jwpe.2019.101118.

[14] X. Zhang, X. Zhou, T.B. Moghaddam, F. Zhang, F. Otto, Synergistic effects of iron (Fe) and biochar on light-weight geopolymers when used in wastewater treatment applications, J. Clean. Prod. 322 (2021), 129033, https://doi.org/10.1016/j.jclepro.2021.129033.

[15] T. Revathi, K. Janani, R. Jeyalakshmi, Synthesis of alkali and acid-mediated rGO–metakaolin nano composites for supercapacitor application, J. Mater. Sci. (2021), https://doi.org/10.1007/s10854-021-07211-8.

[16] H. Piao, N.S. Rejinold, G. Choi, Y.-R. Pei, G.-W. Jin, J.-H. Choy, Niclosamide encapsulated in mesoporous silica and geopolymer: a potential oral formulation for COVID-19, Microporous Mesoporous Mater. 326 (2021), 111394, https://doi.org/10.1016/j.micromeso.2021.111394.

[17] L. Ricciotti, A. Apicella, V. Perrotta, R. Aversa, Geopolymer materials for bone tissue applications: recent advances and future perspectives, Polymers 15 (2023), https://doi.org/10.3390/polym15051087.

[18] S. Pangdaeng, V. Sata, J.B. Aguiar, F. Pacheco-Torgal, J. Chindaprasirt, P. Chindaprasirt, Bioactivity enhancement of calcined kaolin geopolymer with CaCl2 treatment, Sci. Asia. 42 (2016) 407, https://doi.org/10.2306/scienceasia1513-1874.2016.42.407.

[19] A.K. Gaharwar, I. Singh, A. Khademhosseini, Engineered biomaterials for in situ tissue regeneration, Nat. Rev. Mater. 5 (2020) 686–705, https://doi.org/10.1038/s41578-020-0209-x.

[20] D. Gallego-Perez, N. Higuita-Castro, F.G. Quiroz, O.M. Posada, L.E. López, A. S. Litsky, D.J. Hansford, Portland cement for bone tissue engineering: effects of processing and metakaolin blends, J. Biomed. Mater. Res. B 98 (2011) 308–315, https://doi.org/10.1002/jbm.b.31853.

[21] H. Oudadesse, A.C. Derrien, M. Mami, S. Martin, G. Cathelineau, L. Yahia, Aluminosilicates and biphasic HA-TCP composites: studies of properties for bony filling, Biomed. Mater. 2 (2007) S59–S64, https://doi.org/10.1088/1748-6041/2/1/s09.

[22] H. Zhou, J. Lee, Nanoscale hydroxyapatite particles for bone tissue engineering, Acta Biomater. 7 (2011) 2769–2781, https://doi.org/10.1016/j.actbio.2011.03.019.

[23] K. Balani, D. Lahiri, A.K. Keshri, S.R. Bakshi, J.E. Tercero, A. Agarwal, The nano-scratch behavior of biocompatible hydroxyapatite reinforced with aluminum oxide and carbon nanotubes, surfaces for bio-applications, JOM 61 (2009) 63–66, https://doi.org/10.1007/s11837-009-0136-1.

[24] International Organization for Standardization, Biological Evaluation of Medical Devices - Part 5: Tests for in Vitro Cytotoxicity (ISO 10993-5:2009), 2009. https://books.google.com/books/about/Biological_Evaluation_of_Medical_Devices.html?hl=&id=TnA9MwEACAAJ.

[25] S. Stamnitz, A. Klimczak, Mesenchymal stem cells, bioactive factors, and scaffolds in bone repair: from research perspectives to clinical practice, Cells 10 (2021), https://doi.org/10.3390/cells10081925.

[26] U. Ahmed, R. Ahmed, M.S. Masoud, M. Tariq, U.A. Ashfaq, R. Augustine, A. Hasan, Stem cells based in vitro models: trends and prospects in biomaterials cytotoxicity studies, Biomed. Mater. 16 (2021), 042003, https://doi.org/10.1088/1748-605X/abe6d8.

[27] T.C. Paim, M.R. Wink, The versatility of mesenchymal stem cells: from regenerative medicine to COVID, what is next? BIOCELL 46 (2022) 913–922, https://doi.org/10.32604/biocell.2022.018498.

[28] P. Su, Y. Tian, C. Yang, X. Ma, X. Wang, J. Pei, A. Qian, Mesenchymal stem cell migration during bone formation and bone diseases therapy, Int. J. Mol. Sci. 19 (2018), https://doi.org/10.3390/ijms19082343.

[29] C. Rodrigues, L.I.S. Naasani, C. Zanatelli, T.C. Paim, J.G. Azevedo, J.C. de Lima, M. da Cruz Fernandes, S. Buchner, M.R. Wink, Bioglass 45S5: structural characterization of short range order and analysis of biocompatibility with adipose-derived mesenchymal stromal cells in vitro and in vivo, Mater. Sci. Eng. C. 103 (2019), 109781, https://doi.org/10.1016/j.msec.2019.109781.

[30] C. Stutz, M. Strub, F. Clauss, O. Huck, G. Schulz, H. Gegout, N. Benkirane-Jessel, F. Bornert, S. Kuchler-Bopp, A new polycaprolactone-based biomembrane functionalized with BMP-2 and stem cells improves maxillary bone regeneration, Nanomaterials 10 (2020), https://doi.org/10.3390/nano10091774.

[31] X. Ji, X. Yuan, L. Ma, B. Bi, H. Zhu, Z. Lei, W. Liu, H. Pu, J. Jiang, X. Jiang, Y. Zhang, J. Xiao, Mesenchymal stem cell-loaded thermosensitive hydroxypropyl chitin hydrogel combined with a three-dimensional-printed poly(ε-caprolactone) /nano-hydroxyapatite scaffold to repair bone defects via osteogenesis, angiogenesis and immunomodulation, Theranostics 10 (2020) 725–740, https://doi.org/10.7150/thno.39167.

[32] E. Schätzlein, C. Kicker, N. Söhling, U. Ritz, J. Neijhoft, D. Henrich, J. Frank, I. Marzi, A. Blaeser, 3D-Printed PLA-bioglass scaffolds with controllable calcium release and MSC adhesion for bone tissue engineering, Polymers 14 (2022), https://doi.org/10.3390/polym14122389.

[33] R. Detsch, S. Alles, J. Hum, P. Westenberger, F. Sieker, D. Heusinger, C. Kasper, A. R. Boccaccini, Osteogenic differentiation of umbilical cord and adipose derived stem cells onto highly porous 45S5 Bioglass®-based scaffolds, J. Biomed. Mater. Res. A 103 (2015) 1029–1037, https://doi.org/10.1002/jbm.a.35238.

[34] M. Petretta, A. Gambardella, M. Boi, M. Berni, C. Cavallo, G. Marchiori, M. C. Maltarello, D. Bellucci, M. Fini, N. Baldini, B. Grigolo, V. Cannillo, Composite scaffolds for bone tissue regeneration based on PCL and Mg-containing bioactive glasses, Biology 10 (2021), https://doi.org/10.3390/biology10050398.

[35] L.L. Hench, Bioceramics: from concept to clinic, J. Am. Ceram. Soc. 74 (1991) 1487–1510, https://doi.org/10.1111/j.1151-2916.1991.tb07132.x.

[36] N.A. Mohd Mortar, M.M.A.B. Abdullah, R. Abdul Razak, S.Z. Abd Rahim, I.H. Aziz, M. Nabialek, R.P. Jaya, A. Semenescu, R. Mohamed, M.F. Ghazali, Geopolymer ceramic application: a review on mix design, properties and reinforcement enhancement, Materials 15 (2022), https://doi.org/10.3390/ma15217567.

[37] M. Sitarz, B. Figiela, M. Łach, K. Korniejenko, K. Mróz, J. Castro-Gomes, I. Hager, Mechanical response of geopolymer foams to heating—managing coal gangue in fire-resistant materials technology, Energies 15 (2022), https://doi.org/10.3390/en15093363.

[38] M. Sayed, R.A. Gado, S.M. Naga, P. Colombo, H. Elsayed, Influence of the thermal treatment on the characteristics of porous geopolymers as potential biomaterials, Mater. Sci. Eng. C Mater. Biol. Appl. 116 (2020), 111171, https://doi.org/10.1016/j.msec.2020.111171.

[39] G. Ryan, A. Pandit, D.P. Apatsidis, Fabrication methods of porous metals for use in orthopaedic applications, Biomaterials 27 (2006) 2651–2670, https://doi.org/10.1016/j.biomaterials.2005.12.002.

[40] H. Kienapfel, C. Sprey, A. Wilke, P. Griss, Implant fixation by bone ingrowth, J. Arthroplasty. 14 (1999) 355–368, https://doi.org/10.1016/s0883-5403(99)90063-3.

[41] J.J. Klawitter, A.M. Weinstein, The status of porous materials to obtain direct skeletal attachment by tissue ingrowth, Acta Orthop. Belg. 40 (1974) 755–765.

[42] C. Bai, P. Colombo, Processing, properties and applications of highly porous geopolymers: a review, Ceram. Int. 44 (2018) 16103–16118, https://doi.org/10.1016/j.ceramint.2018.05.219.

[43] E. Fiume, G. Magnaterra, A. Rahdar, E. Verné, F. Baino, Hydroxyapatite for biomedical applications: a short overview, Ceramics 4 (2021) 542–563, https://doi.org/10.3390/ceramics4040039.
[44] J.H. Tomáš Kovářík, Porous geopolymers: processing routes and properties, 9 IOP Conf. Ser. 613 (2019) 1–7.
[45] T. Kovářík, T. Křenek, D. Rieger, M. Pola, J. Říha, M. Svoboda, J. Beneš, P. Šutta, P. Bělský, J. Kadlec, Synthesis of open-cell ceramic foam derived from geopolymer precursor via replica technique, Mater. Lett. 209 (2017) 497–500, https://doi.org/10.1016/j.matlet.2017.08.081.
[46] T. Kovářík, J. Hájek, M. Pola, D. Rieger, M. Svoboda, J. Beneš, P. Šutta, K. Deshmukh, V. Jandová, Cellular ceramic foam derived from potassium-based geopolymer composite: thermal, mechanical and structural properties, Mater. Des. 198 (2021), 109355, https://doi.org/10.1016/j.matdes.2020.109355.
[47] L.B. de Oliveira, A.R.G. de Azevedo, M.T. Marvila, E.C. Pereira, R. Fediuk, C.M. F. Vieira, Durability of geopolymers with industrial waste, Case Stud. Construct. Mater. 16 (2022) e00839, https://doi.org/10.1016/j.cscm.2021.e00839.
[48] T.C. Paim, D.P. Wermuth, I. Bertaco, C. Zanatelli, L.I.S. Naasani, M. Slaviero, D. Driemeier, L. Schaeffer, M.R. Wink, Evaluation of in vitro and in vivo biocompatibility of iron produced by powder metallurgy, Mater. Sci. Eng. C 115 (2020), 111129, https://doi.org/10.1016/j.msec.2020.111129.
[49] D.P. Wermuth, T.C. Paim, I. Bertaco, C. Zanatelli, L.I.S. Naasani, M. Slaviero, D. Driemeier, A.C. Tavares, V. Martins, C.F. Escobar, L.A.L. Dos Santos, L. Schaeffer, M.R. Wink, Mechanical properties, in vitro and in vivo biocompatibility analysis of pure iron porous implant produced by metal injection molding: a new eco-friendly feedstock from natural rubber (Hevea brasiliensis), Mater. Sci. Eng. C 131 (2021), 112532, https://doi.org/10.1016/j.msec.2021.112532.
[50] S. Vedovatto, J.C. Facchini, R.K. Batista, T.C. Paim, M.I.Z. Lionzo, M.R. Wink, Development of chitosan, gelatin and liposome film and analysis of its biocompatibility in vitro, Int. J. Biol. Macromol. 160 (2020) 750–757, https://doi.org/10.1016/j.ijbiomac.2020.05.229.
[51] B. Bournonville, A. Nzihou, Rheology of non-Newtonian suspensions of fly ash: effect of concentration, yield stress and hydrodynamic interactions, Powder Technol. 128 (2002) 148–158, https://doi.org/10.1016/s0032-5910(02)00192-4.
[52] C. Bai, A. Conte, P. Colombo, Open-cell phosphate-based geopolymer foams by frothing, Mater. Lett. 188 (2017) 379–382, https://doi.org/10.1016/j.matlet.2016.11.103.
[53] M.S. Cilla, M.R. Morelli, P. Colombo, Open cell geopolymer foams by a novel saponification/peroxide/gelcasting combined route, J. Eur. Ceram. Soc. 34 (2014) 3133–3137, https://doi.org/10.1016/j.jeurceramsoc.2014.04.001.
[54] M. Catauro, F. Bollino, F. Papale, G. Lamanna, Investigation of the sample preparation and curing treatment effects on mechanical properties and bioactivity of silica rich metakaolin geopolymer, Mater. Sci. Eng. C 36 (2014) 20–24, https://doi.org/10.1016/j.msec.2013.11.026.
[55] X. Liang, Y. Li, J. Yang, Q. Wang, S. Sang, Z. He, Influence of template strut morphology on the mechanical performance of SiC reticulated porous ceramics, Ceram. Int. 46 (2020) 16820–16826, https://doi.org/10.1016/j.ceramint.2020.03.257.
[56] X. Liang, Y. Li, Z. He, W. Yan, F. Tan, Q. Wang, T. Zhu, S. Sang, The effect of cellular structure on the strength and combustion properties of SiC porous ceramics, Ceram. Int. 48 (2022) 2538–2545, https://doi.org/10.1016/j.ceramint.2021.10.036.
[57] X. Liang, Y. Li, L. Pan, S. Sang, T. Zhu, B. Li, C.G. Aneziris, Preparation and enhancement of mullite reticulated porous ceramics for porous media combustion, Ceram. Int. 45 (2019) 22226–22232, https://doi.org/10.1016/j.ceramint.2019.07.246.
[58] G. Wang, T. Yang, Preparation of open cell rigid polyurethane foams and modified with organo-kaolin, J. Cell. Plast. 56 (2020) 435–447, https://doi.org/10.1177/0021955X19880507.
[59] J.M. Anderson, Future challenges in the in vitro and in vivo evaluation of biomaterial biocompatibility, Regen. Biomater. 3 (2016) 73–77, https://doi.org/10.1093/rb/rbw001.
[60] Á. Sierra-Sánchez, K.H. Kim, G. Blasco-Morente, S. Arias-Santiago, Cellular human tissue-engineered skin substitutes investigated for deep and difficult to heal injuries, Npj Regener. Med. 6 (2021) 35, https://doi.org/10.1038/s41536-021-00144-0.
[61] Y. Yoshida, H. Matsubara, X. Fang, K. Hayashi, I. Nomura, S. Ugaji, T. Hamada, H. Tsuchiya, Adipose-derived stem cell sheets accelerate bone healing in rat femoral defects, PLoS ONE 14 (2019), e0214488, https://doi.org/10.1371/journal.pone.0214488.
[62] M. Dominici, K.Le Blanc, I. Mueller, I. Slaper-Cortenbach, F. Marini, D. Krause, R. Deans, A. Keating, D. Prockop, E. Horwitz, Minimal criteria for defining multipotent mesenchymal stromal cells. The International Society for Cellular Therapy position statement, Cytotherapy 8 (2006) 315–317, https://doi.org/10.1080/14653240600855905.
[63] L.I. Sous Naasani, A.F. Damo Souza, C. Rodrigues, S. Vedovatto, J.G. Azevedo, A. P. Santin Bertoni, M. Da Cruz Fernandes, S. Buchner, M.R. Wink, Decellularized human amniotic membrane associated with adipose derived mesenchymal stromal cells as a bioscaffold: physical, histological and molecular analysis, Biochem. Eng. J. 152 (2019), 107366, https://doi.org/10.1016/j.bej.2019.107366.
[64] L.I. Sous Naasani, C. Rodrigues, J.G. Azevedo, A.F. Damo Souza, S. Buchner, M. R. Wink, Comparison of human denuded amniotic membrane and porcine small intestine submucosa as scaffolds for limbal mesenchymal stem cells, Stem Cell Rev Rep 14 (2018) 744–754, https://doi.org/10.1007/s12015-018-9819-8.
[65] B. Qiao, J. Li, Q. Zhu, S. Guo, X. Qi, W. Li, J. Wu, Y. Liu, D. Jiang, Bone plate composed of a ternary nano-hydroxyapatite/polyamide 66/glass fiber composite: biomechanical properties and biocompatibility, Int. J. Nanomed. 9 (2014) 1423–1432, https://doi.org/10.2147/IJN.S57353.
[66] G. Calabrese, R. Giuffrida, C. Fabbi, E. Figallo, D. Lo Furno, R. Gulino, C. Colarossi, F. Fullone, R. Giuffrida, R. Parenti, L. Memeo, S. Forte, Collagen-hydroxyapatite scaffolds induce human adipose derived stem cells osteogenic differentiation in vitro, PLoS ONE 11 (2016), e0151181, https://doi.org/10.1371/journal.pone.0151181.
[67] D. Sutanto, M.H. Satari, B.S. Hernowo, B.P. Priosoeryanto, R. Septawendar, L.A.T. W. Asri, B.S. Purwasasmita, Geopolymer–carbonated apatite nanocomposites with magnesium and strontium trace elements for dental restorative materials, J. Korean Ceram. Soc. 11 (2020) 162, https://doi.org/10.1007/s43207-020-00060-x.

6 CAPÍTULO 3

Neste capítulo consta o primeiro estudo que fabricou amostras de implantes porosos de ferro produzidos por moldagem de pós-metálicos por injeção com uma nova matéria-prima feita a partir da borracha natural (*Hevea brasiliensis*). O trabalho avaliou as propriedades mecânicas e a biocompatibilidade do material proposto para uso de dispositivos biomédicos biodegradáveis, tais como *stents*.

Materials Science & Engineering C 131 (2021) 112532

Contents lists available at ScienceDirect

Materials Science & Engineering C

journal homepage: www.elsevier.com/locate/msec

Mechanical properties, *in vitro* and *in vivo* biocompatibility analysis of pure iron porous implant produced by metal injection molding: A new eco-friendly feedstock from natural rubber (*Hevea brasiliensis*)

Diego Pacheco Wermuth [a,1], Thaís Casagrande Paim [b,1], Isadora Bertaco [b], Carla Zanatelli [b], Liliana Ivet Sous Naasani [b], Mônica Slaviero [c], David Driemeier [c], André Carvalho Tavares [a], Vinicius Martins [f], Camila Ferreira Escobar [e], Luis Alberto Loureiro dos Santos [d], Lírio Schaeffer [a,2], Márcia Rosângela Wink [b,*,2]

[a] Laboratório de Transformação Mecânica, Universidade Federal do Rio Grande do Sul (UFRGS), Av. Bento Gonçalves 9500, 91501-970 Porto Alegre, RS, Brazil
[b] Laboratório de Biologia Celular, Departamento de Ciências Básicas da Saúde, Universidade Federal de Ciências da Saúde de Porto Alegre (UFCSPA), Rua Sarmento Leite 245, 90050-170 Porto Alegre, RS, Brazil
[c] Setor de Patologia Veterinária, Faculdade de Veterinária (FAVET), Universidade Federal do Rio Grande do Sul, Av. Bento Gonçalves 9090, 91540-000 Porto Alegre, RS, Brazil
[d] Laboratório de Biomateriais & Cerâmicas Avançadas, Universidade Federal do Rio Grande do Sul (UFRGS), Av. Bento Gonçalves 9500, 91501-970 Porto Alegre, RS, Brazil
[e] Centro de Ciência e Tecnologia em Energia e Sustentabilidade, Universidade Federal do Recôncavo da Bahia, Av. Centenário 697, 44.085-132 Feira de Santana, BA, Brazil
[f] Laboratório de Metalurgia do Pó, Instituto Federal Sul-rio-grandense Campus Sapucaia do Sul, Av. Copacabana 100, 93216-120 Sapucaia do Sul, RS, Brazil

ARTICLE INFO

Keywords:
Pure iron
Metal injection molding (MIM)
Eco-friendly feedstock
Biodegradable implants
Adipose-derived mesenchymal stromal cells (ADSCs)
In vivo model of subcutaneous implant

ABSTRACT

Metal injection molding (MIM) has become an important manufacturing technology for biodegradable medical devices. As a biodegradable metal, pure iron is a promising biomaterial due to its mechanical properties and biocompatibility. In light of this, we performed the first study that manufactured and evaluated the *in vitro* and *in vivo* biocompatibility of samples of iron porous implants produced by MIM with a new eco-friendly feedstock from natural rubber (*Hevea brasiliensis*), a promisor binder that provides elastic property in the green parts. The iron samples were submitted to tests to determine density, microhardness, hardness, yield strength, and stretching. The biocompatibility of the samples was studied *in vitro* with adipose-derived mesenchymal stromal cells (ADSCs) and erythrocytes, and *in vivo* on a preclinical model with Wistar rats, testing the iron samples after subcutaneous implant. Results showed that the manufactured samples have adequate physical, and mechanical characteristics to biomedical devices and they are cytocompatible with ADSCs, hemocompatible and biocompatible with Wistars rats. Therefore, pure iron produced by MIM can be considered a promising material for biomedical applications.

1. Introduction

The study of new degradable biomaterials has been one of the most attractive topics in the materials research field [1]. These materials are expected to safely and gradually degrade in the body after their function is served [2]. Metals comprise an important class of degradable biomaterials, because of their suitable mechanical properties in structural components. Iron (Fe), Magnesium (Mg), Zinc (Zn), Molybdenum (Mo), and Tungsten (W) have been studied to be used as temporary orthopedic, vascular implants, and electronic systems [3].

Previous studies have shown that pure iron can be an appropriate material for biomedical applications [4–6]. Iron has great radial strength due to its high elastic modulus [7] and it is biocompatible. Studies have shown that pure iron stents produced by laser cutting did

* Corresponding author at: Universidade Federal de Ciências da Saúde de Porto Alegre–UFCSPA, 245, Sarmento Leite, Porto Alegre, RS CEP 90050-170, Brazil.
E-mail address: mwink@ufcspa.edu.br (M.R. Wink).
[1] These authors contributed equally to this work
[2] These authors shared senior authorship

https://doi.org/10.1016/j.msec.2021.112532
Received 14 April 2021; Received in revised form 15 October 2021; Accepted 1 November 2021
Available online 5 November 2021

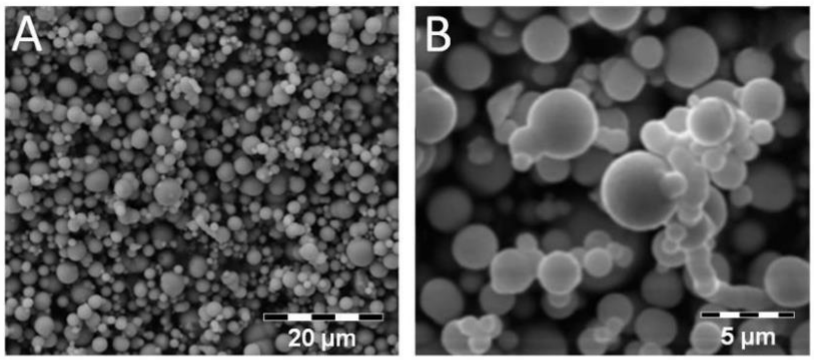

Fig. 1. Iron powder. 99.95% iron powder SEM with a magnification of 3160× (A) and 10,000× (B).

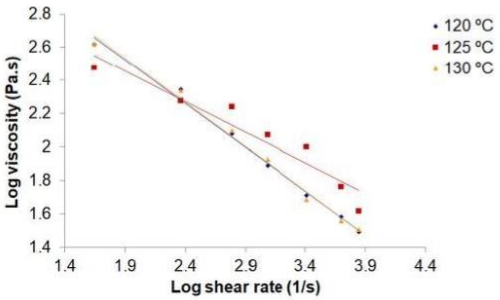

Fig. 2. Rheological evaluation of eco-friendly feedstock. Rheology results at temperatures of 120 °C, 125 °C and 130 °C of feedstock.

Table 1
Rheological results of the feedstock at 120 °C.

Shear rate (1/s)	Viscosity (Pa.s)	Shear stress (Pa)
44	414.2	24,981
230	221.45	50,933
613	119.44	73,217
1210	77.25	93,475
2560	51.44	131,675
5000	38.37	191,875
7000	31.02	232,675

not cause systemic toxicity, iron overload, and significant inflammatory response in animals [4,5,8].

Iron is a biodegradable metal, whose degradation process involves the oxidation of ferrous ions and their dissolution in body fluids [9,10]. Under physiological conditions, the bioavailability of iron is limited because the soluble (Fe^{2+}) (heme) is readily oxidized to (Fe^{3+}) (non-heme iron), which is virtually insoluble. The electrons from the anodic reaction are consumed by a corresponding cathodic reaction (1) and the oxygen is reduced and dissolved in water (2). The metals ions (Fe^{2+}) react with the hydroxyl ion (OH) and form insoluble hydroxides, which are the most common corrosion products (3–4) [11–13]:

(1) $Fe \rightarrow Fe^{2+} + 2e^{-}$ (anodic reaction)
(2) $O_2 + 2H_2O + 4e^{-} \rightarrow 4OH^{-}$ (cathodic reaction)
(3) $Fe^{2+} + 2OH^{-} \rightarrow Fe(OH)_2$
(4) $4\,Fe(OH)_2 + O_2 + 2H_2O \rightarrow 4Fe(OH)_3$ or $2Fe_2O_3.6H_2O$

The ability to donate and accept electrons can lead to significant oxidative damage. The iron overload can produce free radicals and induce damage in different organs such as the pancreas, liver, thyroid, and heart. In the central nervous system, it has been associated with neurodegenerative disorders, such as Parkinson's and Alzheimer's disease [14–16].

An important aspect related to iron is the choice regarding its purity. In a previous study, we compared the mechanical properties and biocompatibility of 99.5% and 99.95% iron samples produced by powder metallurgy. We found that both purity grades have adequate properties to be used in biomedical devices, however, the 99.95% iron had better performance when the biocompatibility was tested *in vitro* [6].

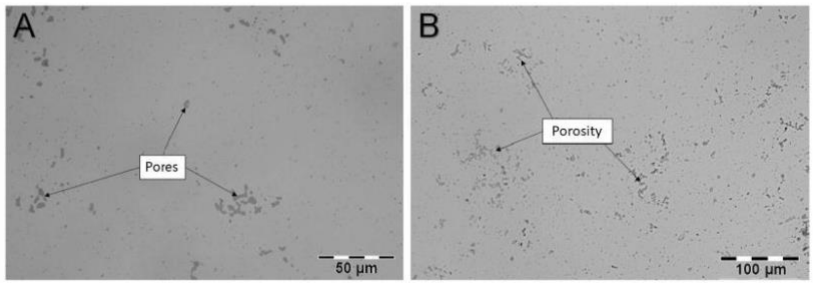

Fig. 3. Porosity. Metallography of sintered pure iron sample with 500× (A) and 200× (B) magnification.

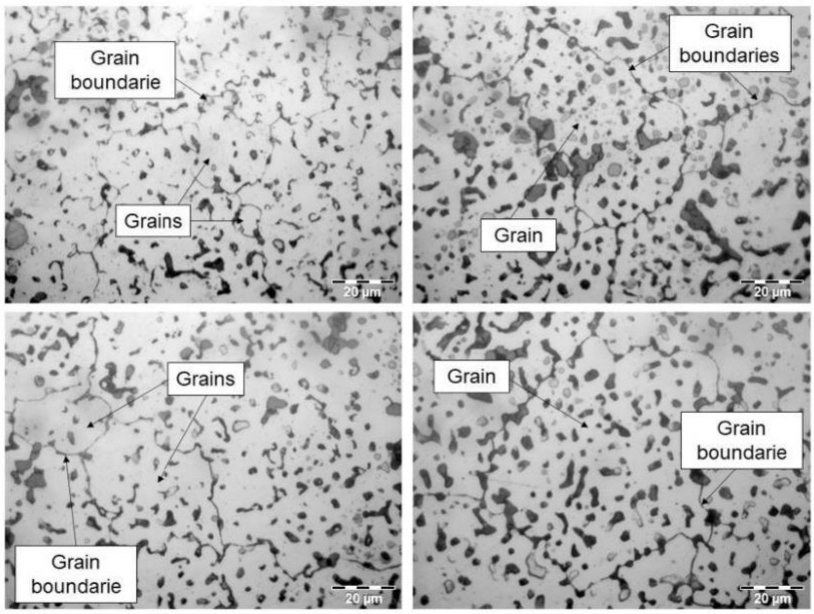

Fig. 4. Grain size. Metallography of sintered pure iron samples after etching 2% Nital.

Table 2
Mechanical properties of pure iron samples obtained by MIM.

Sample	Yield strength (MPa)	Young's modulus (GPa)	Tensile strength (MPa)	Elongation (%)
1	86	113	236	35
2	65	128	312	42
3	96	132	328	53
4	67	138	334	48
Standard deviation	15.02	10.66	45.3	7.77
Average	**78.5**	**127.75**	**302.5**	**44.5**

Corrosion and degradation are also important aspects to be considered in the manufacture of iron. The density has an important role in this process and it needs to be evaluated in biodegradable implants [12]. Thus, we chose the metal injection molding (MIM) process because it allows the control of the porosity that will impact the density. MIM is a metal forming process by which finely-powdered metal is mixed with a binder material to comprise a "feedstock" capable of being handled by plastic processing equipment through a process known as injection molding [17]. The MIM process consists of 4 main steps (1) Mixing: Mixture of binder (polymer + waxes + acids) with the metallic powder to form a feedstock. (2) Injection molding: The feedstock is heated and provides the fluidity of the binder enabling the molding of the green part on an injection machine. (3) Debinding: The binder is removed from the green part and the remaining structure, now called the brown part, is constituted only of metallic powder. (4) Sintering: The metallic structure is heated and the union of metallic powders occurs through diffusion. In this step, the strength in the sintered part is achieved. MIM is characterized for its near net shaping technique that favors the development of complex shapes of high density, promoting great dimensional accuracy. In addition, this process can reduce production costs and allows large production quantities [18].

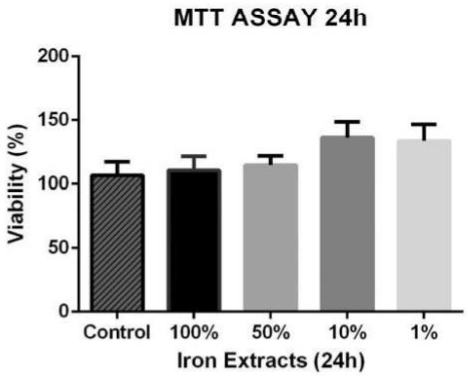

Fig. 5. Cell viability. Viability of ADSCs cultured for 24 h in iron extracts with 100%, 50% 10% and 1% concentration. Control: cells grown in DMEM Low Glucose. Values are means ± SEM, N = 3. There is no statistically significant difference between groups.

The global powder injection molding industry has annual sales of approximately $3 billion, as highlighted in recent applications in the field of micro-miniature medical devices and high added value [19]. MIM is appropriate for the manufacture of materials for medical applications such as stainless steel [20,21], titanium alloys [22], Co\\Cr alloys [23], Bronze [24] as well as biodegradable metals such as zinc and magnesium alloys [25,26]. This process has been used in the healthcare industry for the manufacture of implants and biomedical devices, such as metallic orthodontic brackets, joint replacement surgery devices, medical equipment, and surgical instruments [27]. Iron has been

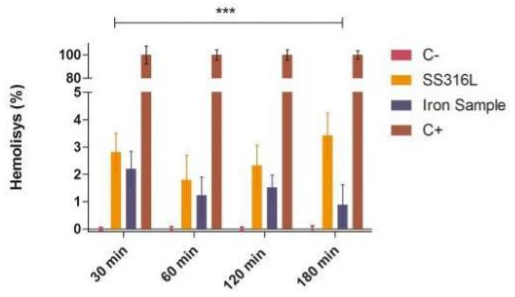

Fig. 6. Hemocompatibility. Hemolysis percentage in the presence of iron, using the SS316L as a golden standard. Negative control (C−): saline; Positive control (C+): distilled water, Values are means ± SEM, N = 3 ***represents $p < 0.001$.

considered to be used in biomedical applications produced by MIM, but the studies are still scarce [28].

The choice of the cell type to assess the biocompatibility of the material *in vitro* is an important step for cytotoxicity evaluation. Mesenchymal stromal cells (MSCs) are an attractive option because they reside virtually in all tissues [29]. Moreover, they have potential to be used in the regenerative medicine field, in cell therapies, or associated with biomaterials [30,31] due to their immune-modulatory, anti-inflammatory, and angiogenic properties [32]. Among several sources of MSCs, adipose tissue has emerged as an attractive source because it contains an abundance of these cells and it is easier to obtain, allowing autologous transplantation [33].

Therefore, considering the advantages of metal injection molding technology and our previous results showing the better performance of 99.95% purity iron in comparison to 99.5% [6], we performed the first study that manufactured and evaluated the *in vitro* and *in vivo* biocompatibility of 99.95% iron samples, produced by MIM through a new eco-friendly feedstock from natural rubber (*Hevea brasiliensis*).

2. Materials and methods

2.1. Iron samples

The limits of the elements contained in the iron powder (lyuelong superfine metal Co., China) used in this research are Fe (≥99.95%), C (≤0.02%), S (≤0.01%), and O (≤0.02%). The 99.95% iron powder, D90 less than 12 μm and average particle size of 6 μm, was evaluated in a scanning electron microscope (Tescan Vega 3, Czech Republic). The material was used to produce samples by metal injection molding with an eco-friendly feedstock containing 60 vol% iron powder. The binder was formulated with 57.5 wt% carnauba wax, 37.5 wt% natural rubber, and 5 wt% stearic acid and dicumyl peroxide. It was prepared according to described in the patent "BR 10 2013 008311-9 A2" [34].

Initially, the rheological test with the feedstock was carried out to obtain preliminary parameters for the metal injection molding process. All samples were injected with the shape of the tensile specimens in an injection molding machine (Thermo Scientific HAAKE MiniJet). The injectable parts, in this step known as green parts, were cut into flat squares with dimensions of approximately 7.5 × 7.5 × 2.5 mm. In the debinding step, a vacuum furnace (Sanchis, Brazil) was used, at a heating rate of 0.1 °C/min up to a temperature of 600 °C maintained for 60 min to remove possible traces of the binder. The remaining structures (brown parts) were constituted only of pure iron powder. After the debinding, the parts were sintered. The sintering step was performed in an electric tube furnace silicon carbide resistor (Sanchis, Brazil) with Argon gas-controlled atmosphere. The sintering cycle started at room temperature and heated up to 1150 °C at a rate of 10 °C/min. The temperature was maintained at 1150 °C for 60 min to guarantee the complete sintering of the samples. After cooling, the parts followed for the physical, mechanical, and biocompatibility tests.

2.2. Physical and mechanical properties

In order to verify the physical properties of the samples, we measured the density of green and sintered parts according to MPIF 42 [35]. For these analyses, the masses of 15 samples were obtained by an analytical balance and the dimensions measured with a micrometer.

The metallographic test was performed to evaluate the morphology, grain size, and pores of the sintered samples. For this purpose, the specimens were mounted using a hot compression thermosetting resin. After mounting, the abrading process was started with aluminum oxide sandpaper of 100, 200, 400, 600, 800, 1000, and 1200 grit. At the end, samples were polished with alumina paste (1 μm) [36] and subjected to etching by 2% Nital. Metallographic analyses were evaluated by optical microscopy (Olympus) before and after the etching process [37]. The measurement of grain size and pores was performed with the ImageJ software according to ASTM E 562-02 standard [37].

The mechanical properties were evaluated by Vickers microhardness, Brinell hardness, and tensile test. Vickers microhardness of 10 samples was determined by the Insize ISH-TDV 1000 durometer with a load of 0.5 kgf, according to ASTM E384 standard [38]. The Brinell hardness of 10 samples was determined by a hardness tester (MRS Fortel) using a 2.5 mm diameter indenter and a load of 62.5 kgf, according to ASTM E10 [39]. Finally, the tensile test of 4 samples was performed on a universal testing machine (Instron, Brazil) with a 50 kN load cell and speed of 1 mm/min at room temperature.

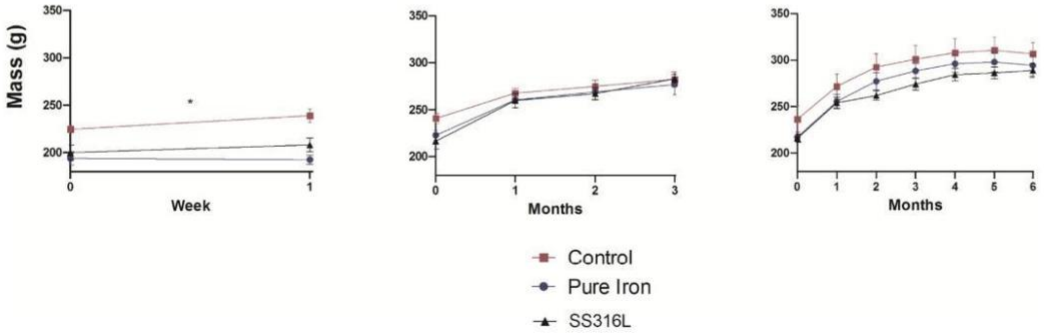

Fig. 7. Body weight. Change of Body Weight of animal groups after 1 week, 3 months and 6 months. Values are means ± SEM *represents $p < 0.05$.

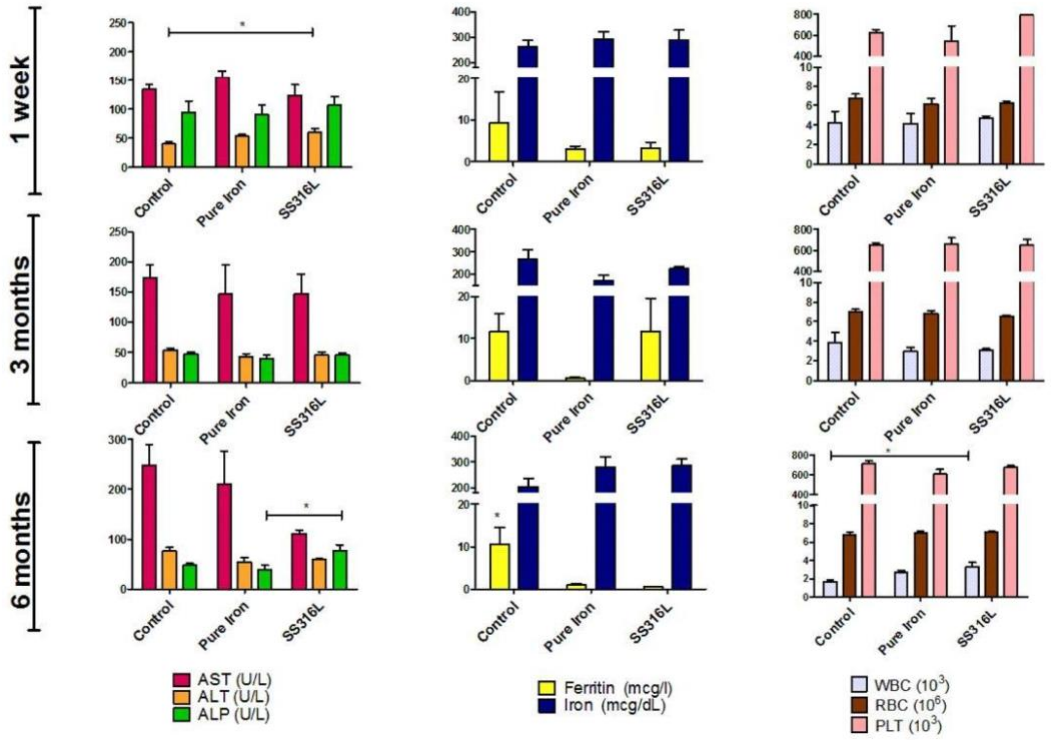

Fig. 8. Blood and serum analysis after 1 week, 3 and 6 months of iron implantation. Control: sham group.Biochemical parameters: iron, ferritin, aspartate aminotransferase (AST), alanine aminotransferase (ALT) and alkaline phosphatase (ALP). Hematological parameters: red blood cell (RBC), white blood cell (WBC) and platelets (PLT) parameters. Values are means ± SEM *represents $p < 0.05$. (For interpretation of the references to colour in this figure legend, the reader is referred to the web version of this article.)

2.3. Indirect cytotoxicity assessment

2.3.1. Adipose-derived stem cells: isolation and characterization

ADSCs were extracted from the abdominal adipose tissue of healthy adult donors during liposuction surgery. The study was conducted with approval from the Research Ethics Committee of Santa Casa de Misericórdia of Porto Alegre (REC-ISCMPA 3029.141) and the Research Ethics Committee of the Federal University of Health Sciences of Porto Alegre (REC-UFCSPA 3.734.612). The cells were isolated and characterized according to the protocol previously described by our research group [40,41].

2.3.2. Indirect cytotoxicity testing (MTT assay)

Cell viability test was conducted by indirect method. For this experiment, the iron extract was prepared according to ISO 10993-5 and 10993-12. Samples were autoclaved and incubated with DMEM Low Glucose supplemented with 10% fetal bovine serum for 24 h under cell culture conditions (5% CO_2, 95% humidity, 37 °C) with a fixed mass ratio to medium volume (0.2 g/mL). The extracts were then collected without any filtration for cytotoxicity tests [42]. A colorimetric test (Bioclin® Kits, Brazil) was performed to evaluate the iron concentration in the extract.

ADSCs were pre-cultivated for 24 h at 37 °C, into 96-well plates at a ratio of 3.0×10^3 cells per well. Next, the medium was removed and replaced by pure, 1:2,1:10 and 1:100 dilutions of iron extract, and incubated. As a control, ADSCs were incubated with a standard medium. The viability of the cells was tested after 24 h of incubation using MTT assay (3-(4,5-dimethylthiazol-2-yl)-2,5-diphenyltetrazolium bromide).

2.4. Hemolysis assay

Healthy human blood from volunteers containing sodium citrate (3.8 wt%) at a ratio of 9:1 was taken and diluted to 10 mL with PBS. The study was approved by the Research Ethics Committee of the Federal University of Health Sciences of Porto Alegre (REC-UFCSPA 3594.874). Pure iron and Stainless Steel (SS316L) specimens were dipped in separate standard tubes containing diluted erythrocytes and incubated for 30, 60, 120, and 180 min at 37 °C. As a positive control for hemolysis, blood was diluted in distilled water, whereas saline diluted blood was added to an empty standard tube which served as a negative control. After this period, specimens were removed and all the tubes were centrifuged at 3300 rpm for 5 min. The supernatant from each tube was transferred to a 96-well plate where the absorbance was measured with a microplate reader (SpectraMax) at 540 nm. Hemolysis was calculated as follows:

$$Hemolysis\ (\%) = \frac{(OD\ sample - OD\ negative\ control)}{(OD\ positive\ control - OD\ negative\ control)} \times 100$$

Where, OD means optical densitiy.

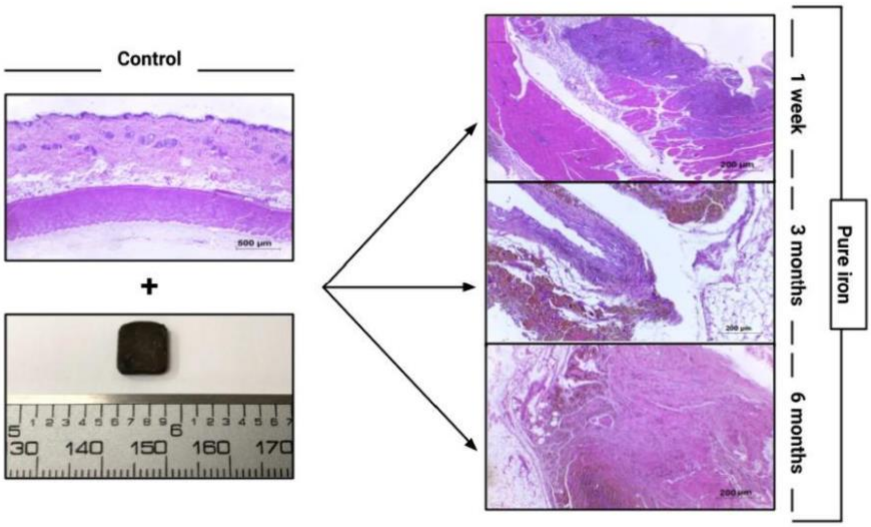

Fig. 9. Histological analysis of subcutaneous tissues located around the iron implants. Hematoxylin and eosin staining of the subcutaneous tissues at 1 week, 3 months and 6 months post-implantation.

2.5. In vivo study

In vivo biocompatibility of pure iron samples was evaluated after a subcutaneous implant in rats as previously described by our research group [6]. All animal procedures are in accordance with the National Council for Animal Experimentation Control and they were approved by UFCSPA Animal Ethics committee (613/19).

A total of 46 Wistar rats (171–262 g; mean: 219 g; ±8 weeks) were randomized into the following 3 groups; pure iron implant; SS316L implant (one of the most common metals used for surgical implants) and sham control (without implant). Prior to surgery, the animals were anesthetized *via* intraperitoneal injection with an association of 90 mg/kg ketamine and 10 mg/kg xylazine. An incision was made through the cutaneous tissue in the dorsal region using a surgical scissor. The pure iron or SS316L implant was inserted into this opening, after which the skin was sutured. The sham control group received the same surgical procedure but no implant.

Tramadol Hydrochloride (5 mg/kg) was administered subcutaneously on rats to provide pain relief. The animals were monitored daily during the first two weeks for surgical wound appearance, locomotion in their cage, and general well-being. The body mass of each rat was monitored monthly during the study.

After 2 weeks, 3 months, and 6 months, one third of the rats in each group was euthanized by cardiac puncture preceded by general anesthesia with 90 mg/kg ketamine and 10 mg/kg xylazine, followed by implant and tissue harvest. Blood was collected in EDTA for complete blood cell, red blood cell (RBC) and white blood cell (WBC) counts and for determining platelets (PLT) levels. The analyzes of non-coagulated blood samples were performed in the BC-5380 auto hematology analyzer (Mindray, Shenzhen, China).

The levels of serum biochemical parameters- iron, ferritin, aspartate aminotransferase (AST), alanine aminotransferase (ALT), and alkaline phosphatase (ALP)- were also assessed using diagnostic kits (Bioclin® Kits, Brazil) in the BS-120 chemistry analyzer (Mindray, Shenzhen, China).

To evaluate the impact of pure iron implants, the tissue around the samples and organs were histologically analyzed. The collected samples were preserved in a 10% buffered formaldehyde solution. After this step, they were trimmed, paraffin embedding, sectioned to a thickness of 4 mm and deparaffinized on microscopy slides. So, tissue samples were stained with hematoxylin and eosin (H&E) and assessed by a veterinary pathologist to identify histological changes.

The degradation study included visual examination, ultrasonication, cleaning, and weighing of the extracted implants to determine the mass variation.

2.6. Statistical analysis

Data samples were statistically compared by *t*-test and ANOVA using GraphPad Prism biostatistics software (GraphPad Inc., USA). Differences between mean values were considered significant when $p < 0.05$.

3. Results

3.1. Feedstock characteristic analysis

Scanning electron microscope (SEM) images of the 99.95% iron powder used in the manufacture of the feedstock were obtained. Fig. 1 presents the images of iron powder, where it is possible to verify spherical shape powder and particle size varying from 1 to 5 μm.

After mixing the eco-friendly feedstock, the rheological test was carried out to check preliminary parameters for setting the injection process. The rheology shear rates were indicated by the capillary rheometer manufacturer due to the high rates that the injection process uses [44]. Fig. 2 shows the results of rheology at temperatures of 120 °C, 125 °C, and 130 °C, within the working range of this eco-friendly feedstock.

Based on the results presented in Fig. 2 and knowing that the injection process uses high shear rates, the temperature range between 120 °C to 130 °C is suitable for the process. It was chosen to use the injection temperature of 120 °C to manufacture the samples since the energy consumption of the equipment is lower. The rheological results obtained at 120 °C are shown in Table 1.

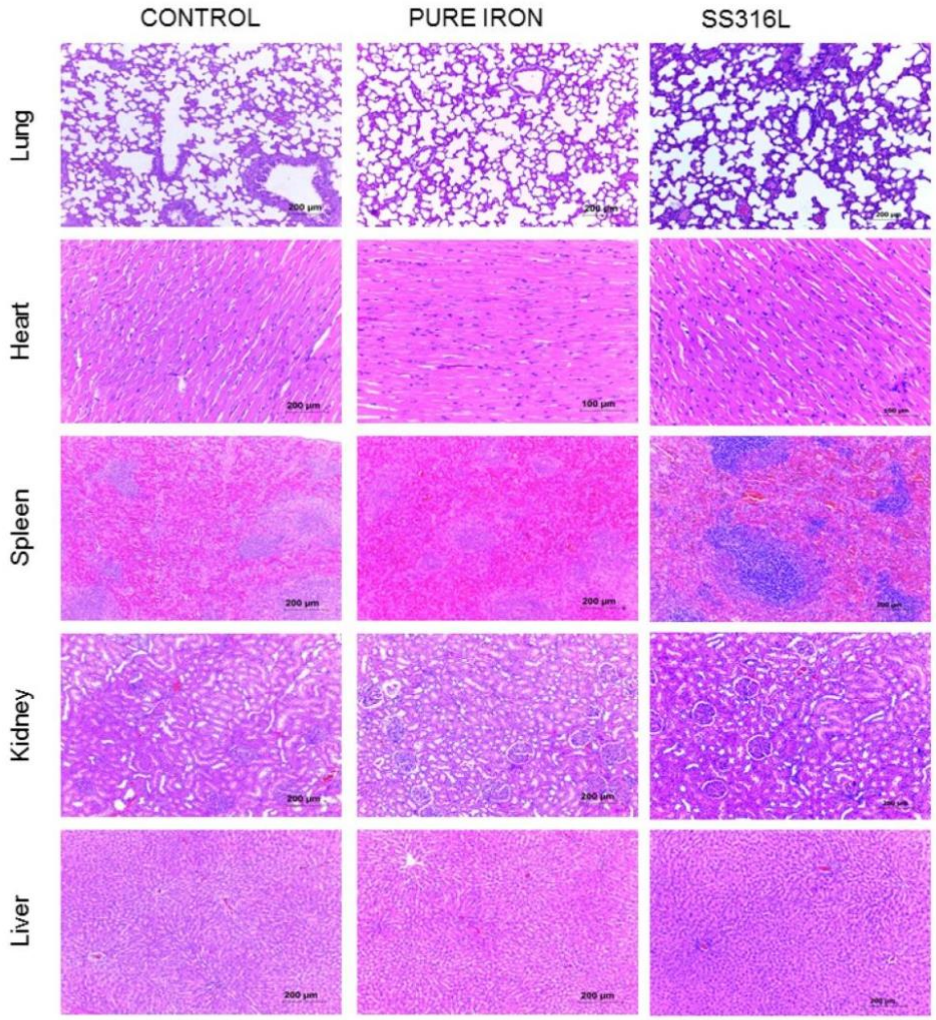

Fig. 10. Histological analysis of the major organs. Hematoxylin and eosin staining of the main organs of rats (lung, heart, kidney, spleen and liver) after 6 months of iron and SS316L implantation in the subcutaneous tissue. Control: sham group.

Table 3
Masses of pure iron samples before and after implantation in the subcutaneous tissue of Wistar rats using paired *t*-test.

	Pure iron implant			
	N	Average pre implantation (g)	Average post implantation (g)	P-value
1 week	6	1.199 ± 0.068	1.207 ± 0.070	$p < 0.05$
3 Months	6	1.267 ± 0.108	1.298 ± 0.108	$p < 0.05$
6 Months	5	1.143 ± 0.025	1.202 ± 0.045	0.064

3.2. *Physical and mechanical properties of iron samples obtained by MIM*

The 99.95% iron injected samples showed a green density of 4.96 g/cm^3 ± 0.16, exhibiting repeatability and stability of mass and volume in the MIM process. After debinding and sintering steps, the samples showed sintered density of 6.61 g/cm^3 ± 0.12.

Metallographic testing was performed to determine the porosity and grain size of the sintered samples. Fig. 3 shows the metallography of the

samples without etching. It is possible to observe that the pores measured between 0.8 and 11.7 μm (average size of 1.5 μm ± 1).

The microstructural grains can be observed in Fig. 4 that shows a sintered pure iron sample after etching with 2% Nital. The samples have grains with 45.14 μm ± 23.20, showing a large variation in size.

The Vickers microhardness on the sintered pure iron samples showed heterogeneity in the measured values, ranging from 57.6 to 77.2 HV, with an average of 61.5 HV. The Brinell hardness values were homogeneous and the samples showed 69.1 HB ± 4.8.

Table 2 shows the results of the tension test of the pure iron samples obtained by the MIM process.

3.3. ADSCs differentiation

MSCs were initially tested for tri-lineage differentiation and expression of MSC surface markers (Supp. Fig. 1). They exhibited osteogenic potential, as demonstrated by marked staining with alizarin red S, adipogenic potential characterized by a higher number of adipocytes stained by oil red O and chondrogenic potential, as evidenced by alcian blue staining. As previously published by our group [6], flow cytometry results showed that the isolated cells expressed CD44, CD105, CD90, and CD73 and they are negative for hematopoietic markers CD14, CD34, and CD45. These results indicate that ADSCs were successfully isolated.

3.4. Viability assay

Fig. 5 shows the relative viabilities of ADSCs cultured in extracts from the pure iron in relation to the negative control (DMEM-Low glucose), after incubation for 1 day. Pure iron extracts maintained the cell viability, morphology and adherence to plastic in comparison with control. The colorimetric test showed that the iron concentration in the extract is 1645 μg/dL ± 75 (N = 2).

3.5. In vitro hemocompatibility

The hemolysis percentage of experimental pure iron and stainless steel 316 L samples is shown in Fig. 6. Iron samples did not exhibit hemolytic activity under the conditions used in this study. The hemolysis ratio of samples tested in the time frame of 30 to 180 min was lower than 5%. Thus, they can be categorized as hemocompatible, according to ASTM-F756-08 [45].

3.6. In vivo biocompatibility

Post-implantation mass gain by rats with iron implants is shown in Fig. 7. All rats with implants gained mass at the same rate that the sham control and SS316L groups. In addition, there were no important alterations in the hematological (RBC, WBC, and PLT) and biochemical parameters (Fe, ferritin, AST, ALT, and ALP) evaluated between the groups (Fig. 8).

The histological analysis of the subcutaneous tissues showed a fibrous encapsulation of implanted material and the presence of macrophages with intracytoplasmic granules of brown pigment. However, there was no evidence of inflammation or necrosis in the subcutaneous tissues located close to the iron implants (Fig. 9). As expected, SS316L also did not cause inflammation or necrosis in the animals (Supp. Fig. 2).

Cells of the lung, kidney, heart and liver also did not present histological changes up to 6 months after the iron implantation in comparison to sham control and SS316L groups (Fig. 10). The iron implants did not show relevant signs of corrosion after 1 week, 3 or 6 months in the subcutaneous tissue of the animals (Table 3).

4. Discussion

Powder metallurgy technology, in specific the MIM, has been recognized as one of the prominent methods to produce components for different fields and industries. Additionally, this technique has also been employed in the medical field for fabricating implants used in surgery and dentistry [18,46]. However, there are only a few studies using pure iron in the production of MIM to biomedical devices. Therefore, in this study we produced pure iron samples by MIM, employing an eco-friendly feedstock extracted from *Hevea brasiliensis*.

The main characteristic of this innovation is the elastic properties of the natural rubber feedstock due to the flexibility of the polymer chains, as well as the restriction to permanent deformation. The elastic factor is an advantage for removing the injected part from the die without compromising its structure. Therefore, natural rubber is a promising alternative to be used as a binder in feedstocks for medical devices and other complex geometry parts.

It is important to highlight that the temperatures for working with natural rubber in the MIM process are different from those used in thermoplastic materials since the crosslinking of natural rubber is temperature-dependent. Because of this, the iron samples show a pseudoplastic behavior that is essential for the MIM process [47]. We also evaluated the physical and mechanical properties, as well as the *in vitro* and *in vivo* biocompatibility of injected iron samples.

The physical properties evaluated were powder morphology, density, porosity and microstructural grain size. SEM images of the iron powder demonstrated a material of spherical morphology due to the atomization process. Particles less than 10 μm and with different distribution sizes become the iron, a suitable feature for use in the injection process [48,49]. The samples showed homogeneous green density variation, ensuring the repeatability and stability of the injection process.

The density of the sintered parts obtained by MIM reached 83.9% of the relative density of the iron, so the average porosity percentage was approximately 16%, in accordance with other studies [28]. In the metallographic analysis, small pores were found. It is necessary to emphasize that porosity is an important feature for a bioabsorbable material, as it would enable a higher rate of corrosion, absorption and facilitate the adhesion of drugs [50]. In addition, samples presented varied grain sizes, a characteristic that results in mechanical properties suitable for medical applications [51].

The mechanical properties of the samples were evaluated by Vickers microhardness, Brinell hardness, and tensile tests. The microhardness of the samples showed heterogeneous values with a range of 31.86% in relation to the average because of high porosity, while Brinell hardness showed low variation (±4.8 HB) indicating that the dispersion of the pores is homogeneous in the sample.

These hardness results are equivalent to those found in biomedical magnesium alloys applied *in vivo* studies [52]. The tensile test showed variation in the maximum displaced tensions, due to the porosity. It is important to note that the elastic deformation in porous materials is different from solid materials [28,53,54]. The tensile test presented the yield strength between 65 MPa and 96 MPa and elongation between 35% and 53%. Specialized literature shows that elongation between 30 and 50% is adequate, for example, to withstand the balloon inflation process, when applied to stents [55,56]. Our results exhibited strengths values between the SS316L and magnesium alloys and high ductility, a required property for cardiovascular materials [27,53,57].

Pure iron samples processed by MIM and by casting were compared. It was found that the porosity retained in the sintered samples has a major effect on the mechanical properties than casting samples [28,53,54]. In addition, it is possible to state that several materials applicable to medical devices have different mechanical behavior. Thus, the results presented in this article are in accordance with values found in the literature [57–59].

Based on the results of the *in vitro* biocompatibility tests, pure iron samples obtained by MIM are biocompatible with ADSCs and hemocompatible. ADSCs did not alter their viability, morphology and adherence to plastic, after iron extract exposition, indicating that they remained viable. The material is considered cytotoxic, according to ISO

10993-5, if cell viability is reduced by more than 30%. Thus, pure iron can be considered compatible with ADSCs [60]. In accordance with our results, Imgrund et al. (2013) produced biodegradable iron-based materials by MIM and characterized its biocompatibility, mechanical and degradation properties. Extracts of Fe and Fe-0.6P samples showed good cytocompatibility after 24 h independent of the sintering conditions [61].

The hemolysis percentage promoted by the pure iron samples produced by MIM was lower than 5%, therefore they can be categorized as hemocompatible. These results are in line with other studies, which found that pure Fe shows adequate cytocompatibility [11,62,63] and good hemocompatibility [63–66].

In vivo assessment of rats containing pure iron implants in respect of well-being, biochemical, hematological and histological analysis of organs were in order with results obtained by the SS316L and control groups, as well as other published studies [6,43]. Animals did now show significant alteration over the follow-up months in weight gain, serum biochemical and hematological parameters in comparison to SS316L and control groups. The histopathological analyses showed that iron implants were not toxic to major organs. Macrophages were observed in the capsule formed around the iron implant, but it was already expected, considering that they are among the first cells to react to any tissue injury or introduced foreign material, such as implants [67,68]. *In vivo* degradation tests of pure iron have shown a rather low biodegradation rate in different studies, a characteristic also found by us [4,69].

5. Conclusions

In this study, pure iron was manufactured by metal injection molding with the new eco-friendly feedstock. We presented that the mechanical and physical properties evaluated, density, microhardness, hardness, yield strength and stretching, are suitable for biomedical devices.

We also showed that the iron samples are biocompatible *in vitro* and *in vivo*. The pure iron samples were cytocompatible with ADSCs, hemocompatible and they did not promote toxicity *in vivo* after subcutaneous implantation in Wistar rats. Therefore, pure iron produced by MIM can be considered a promising material for biomedical applications.

Supplementary data to this article can be found online at https://doi.org/10.1016/j.msec.2021.112532.

Founding

This study was financed in part by the Coordenação de Aperfeiçoamento de Pessoal de Nível Superior – Brasil (CAPES) – Finance Code 001; FAPERGS/MS/CNPq/SESRS n. 03/2017 – PPSUS 17/2551-0001 (Process: 416-2, Marcia R. Wink and 413-8, Lírio Schaeffer); FAPERGS/CNPq/SEBRAE 08/2019 - PDEmp 20/2551-0000207-1 (Diego P. Wermuth) and CNPq MS-SCTIE-Decit/CNPq n° 12/2018 (441575/2018-8).

Thaís Casagrande Paim, Mônica Slaviero and Liliana Ivet Sous Naasani are recipients of fellowships from the Coordenação de Aperfeiçoamento de Pessoal de Nível Superior (CAPES). Diego Pacheco Wermuth is recipient from the Fundação de Amparo à Pesquisa do Estado do Rio Grande do Sul (FAPERGS), Isadora Bertaco and Carla Zanatelli are recipients from Conselho Nacional de Desenvolvimento Científico e Tecnológico (CNPq). Márcia Rosângela Wink, Lírio Schaeffer, Luis Alberto Loureiro dos Santos and David Driemeier are recipients of a research productivity fellowship from the CNPq.

CRediT authorship contribution statement

Diego Pacheco Wermuth: Conceptualization, Data curation, Formal analysis, Methodology; Investigation; Visualization; Funding acquisition; Engineering project administration; Roles/Writing - original draft; Writing - review & editing.

Thaís Casagrande Paim: Conceptualization, Data curation, Formal analysis, Methodology; Investigation; Visualization; Funding acquisition; Roles/Writing - original draft; Writing - review & editing.

Isadora Bertaco dos Santos: Investigation; Validation; Visualization.

Carla Zanatelli: Conceptualization; Investigation.

Liliana Ivet Sous Naasani: Conceptualization; Investigation.

Mônica Slaviero: Pathological investigation and its formal analysis.

David Driemeier: Pathological investigation and its formal analysis.

André Carvalho Tavares: Engineering formal analysis.

Vinicius Martins: Engineering formal analysis.

Camila Ferreira Escobar: Conceptualization of engineering, Formal analysis, Visualization; Investigation; Validation.

Luis Alberto Loureiro dos Santos: Conceptualization of engineering Resources; Supervision.

Lírio Schaeffer: Conceptualization; Funding acquisition; Project administration; Resources; Engineering supervision.

Márcia Rosângela Wink: Conceptualization, Formal analysis; Methodology; Funding acquisition; Project administration; Resources; Cell biology supervision; Roles/Writing - original draft; Writing - review & editing.

Declaration of competing interest

The authors declare that they have no known competing financial interests or personal relationships that could have appeared to influence the work reported in this paper.

Acknowledgments

The authors would like to thank Giuliano Rizzotto Guimarães and Terezinha Stein (Laboratório de Pesquisa em Patologia, UFCSPA), Camila Romero (Laboratório de análises clínicas, UFCSPA), Laura Alencastro de Azevedo (Laboratório de Análises Clínicas e Toxicológicas, UFRGS) and André Rosiak (Laboratório de Transformação Mecânica, UFRGS) for excellent technical support. The authors also gratefully acknowledge both veterinary physicians Dr. Joana Fisch and Dr. Fernanda Bastos de Mello for their assistance in the UFCSPA Animal facility.

References

[1] F. Mahyudin, H. Hermawan, Biomaterials and Medical Devices: A Perspective From an Emerging Country, Springer, 2016.
[2] M. Prakasam, J. Locs, K. Salma-Ancane, D. Loca, A. Largeteau, L. Berzina-Cimdina, Biodegradable materials and metallic implants-a review, J. Funct. Biomater. 8 (2017), https://doi.org/10.3390/jfb8040044.
[3] H. Ryu, M.-H. Seo, J.A. Rogers, Bioresorbable metals for biomedical applications: from mechanical components to electronic devices, Adv. Healthc. Mater. 10 (17) (2021), e2002236, https://doi.org/10.1002/adhm.202002236.
[4] M. Peuster, C. Hesse, T. Schloo, C. Fink, P. Beerbaum, C. von Schnakenburg, Long-term biocompatibility of a corrodible peripheral iron stent in the porcine descending aorta, Biomaterials 27 (2006) 4955–4962.
[5] M. Peuster, P. Wohlsein, M. Brügmann, M. Ehlerding, K. Seidler, C. Fink, H. Brauer, A. Fischer, G. Hausdorf, A novel approach to temporary stenting: degradable cardiovascular stents produced from corrodible metal-results 6–18 months after implantation into New Zealand white rabbits, Heart 86 (2001) 563–569.
[6] T.C. Paim, D.P. Wermuth, I.B. dos Santos, C. Zanatelli, L.I.S. Naasani, M. Slaviero, D. Driemeier, L. Schaeffer, M.R. Wink, Evaluation of in vitro and in vivo biocompatibility of iron produced by powder metallurgy, Mater. Sci. Eng. C 115 (2020), 111129.
[7] S. Garg, P.W. Serruys, Coronary stents: looking forward, J. Am. Coll. Cardiol. 56 (2010) S43–S78.
[8] R. Waksman, R. Pakala, R. Baffour, R. Seabron, D. Hellinga, F.O. Tio, Short-term effects of biocorrodible iron stents in porcine coronary arteries, J. Interv. Cardiol. 21 (2008) 15–20.
[9] G. Mani, M.D. Feldman, D. Patel, C.M. Agrawal, Coronary stents: a materials perspective, Biomaterials 28 (2007) 1689–1710.
[10] L. Zema, G. Loreti, A. Melocchi, A. Maroni, A. Gazzaniga, Injection molding and its application to drug delivery, J. Control. Release 159 (2012) 324–331.
[11] H. Hermawan, A. Purnama, D. Dube, J. Couet, D. Mantovani, Fe-Mn alloys for metallic biodegradable stents: degradation and cell viability studies☆, Acta Biomater. 6 (2010) 1852–1860, https://doi.org/10.1016/j.actbio.2009.11.025.

[12] M. Moravej, A. Purnama, M. Fiset, J. Couet, D. Mantovani, Electroformed pure iron as a new biomaterial for degradable stents: in vitro degradation and preliminary cell viability studies, Acta Biomater. 6 (2010) 1843–1851.
[13] G. Gąsior, J. Szczepański, A. Radtke, Biodegradable iron-based materials—what was done and what more can be done? Materials 14 (2021) 3381, https://doi.org/10.3390/ma14123381.
[14] Z. Luo, X. Zhuang, D. Kumar, X. Wu, C. Yue, C. Han, J. Lv, The correlation of hippocampal T2-mapping with neuropsychology test in patients with Alzheimer's disease, PLoS One 8 (2013), e76203.
[15] S. Ayton, A. Fazlollahi, P. Bourgeat, P. Raniga, A. Ng, Y.Y. Lim, I. Diouf, S. Farquharson, J. Fripp, D. Ames, J. Doecke, P. Desmond, R. Ordidge, C.L. Masters, C.C. Rowe, P. Maruff, V.L. Villemagne, Australian Imaging Biomarkers and Lifestyle (AIBL) Research Group, O. Salvado, A.I. Bush, Cerebral quantitative susceptibility mapping predicts amyloid-β-related cognitive decline, Brain 140 (2017) 2112–2119.
[16] Y. Kohgo, K. Ikuta, T. Ohtake, Y. Torimoto, J. Kato, Body iron metabolism and pathophysiology of iron overload, Int. J. Hematol. 88 (2008) 7–15.
[17] R.M. German, Metal powder injection molding (MIM): key trends and markets, in: Handbook of Metal Injection Molding, Elsevier, 2012, pp. 1–25.
[18] M.F.F.A. Hamidi, W.S.W. Harun, M. Samykano, S.A.C. Ghani, Z. Ghazalli, F. Ahmad, A.B. Sulong, A review of biocompatible metal injection moulding process parameters for biomedical applications, Mater. Sci. Eng. C Mater. Biol. Appl. 78 (2017) 1263–1276.
[19] Professor German updates his views on the present and future outlook for powder injection molding, Met. Powder Rep. 74 (2019) 118–120.
[20] S.-H. Zhu, G.-H. Wang, Y.-Z. Zhao, Y.-M. Li, K.-C. Zhou, B.-Y. Huang, Biocompatibility of MIM 316L stainless steel, J. Cent. S. Univ. Technol. 12 (2005) 9–11, https://doi.org/10.1007/s11771-005-0362-9.
[21] H.O. Gulsoy, H. Ozkan Gulsoy, S. Pazarlioglu, N. Gulsoy, B. Gundede, O. Mutlu, Effect of zr, nb and ti addition on injection molded 316L stainless steel for bio-applications: mechanical, electrochemical and biocompatibility properties, J. Mech. Behav. Biomed. Mater. 51 (2015) 215–224, https://doi.org/10.1016/j.jmbbm.2015.07.016.
[22] A. Dehghan-Manshadi, M.J. Bermingham, M.S. Dargusch, D.H. StJohn, M. Qian, Metal injection moulding of titanium and titanium alloys: challenges and recent development, Powder Technol. 319 (2017) 289–301, https://doi.org/10.1016/j.powtec.2017.06.053.
[23] G. Herranz, C. Berges, J.A. Naranjo, C. García, I. Garrido, Mechanical performance, corrosion and tribological evaluation of a co-cr-mo alloy processed by MIM for biomedical applications, J. Mech. Behav. Biomed. Mater. 105 (2020), 103706.
[24] K.A. Chun, K.-Y. Kum, W.-C. Lee, S.-H. Baek, H.-W. Choi, W.-J. Shon, Evaluation of the safety and efficiency of novel metallic implant scaler tips manufactured by the powder injection molding technique, BMC Oral Health 17 (2017) 110.
[25] M. Wolff, J.G. Schaper, M.R. Suckert, M. Dahms, T. Ebel, R. Willumeit-Römer, T. Klassen, Magnesium powder injection molding (MIM) of orthopedic implants for biomedical applications, JOM 68 (2016) 1191–1197, https://doi.org/10.1007/s11837-016-1837-x.
[26] X. Luo, C. Fang, Z. Fan, B. Huang, J. Yang, Semi-solid powder moulding for preparing medical Mg–3Zn alloy, microstructure evolution and mechanical properties, Mater. Res. Express 6 (2019), 076528, https://doi.org/10.1088/2053-1591/ab14b0.
[27] A. Dehghan-Manshadi, P. Yu, M. Dargusch, D. StJohn, M. Qian, Metal injection moulding of surgical tools, biomaterials and medical devices: a review, Powder Technol. 364 (2020) 189–204, https://doi.org/10.1016/j.powtec.2020.01.073.
[28] P. Mariot, M.A. Leeflang, L. Schaeffer, J. Zhou, An investigation on the properties of injection-molded pure iron potentially for biodegradable stent application, Powder Technol. 294 (2016) 226–235, https://doi.org/10.1016/j.powtec.2016.02.042.
[29] L. da Silva Meirelles, P.C. Chagastelles, N.B. Nardi, Mesenchymal stem cells reside in virtually all post-natal organs and tissues, J. Cell Sci. 119 (2006) 2204–2213.
[30] L. Mazini, L. Rochette, M. Amine, G. Malka, Regenerative capacity of adipose derived stem cells (ADSCs), comparison with mesenchymal stem cells (MSCs), Int. J. Mol. Sci. 20 (2019), https://doi.org/10.3390/ijms20102523.
[31] T. Montero-Vilchez, A. Sierra-Sánchez, M. Sanchez-Diaz, M.I. Quiñones-Vico, R. Sanabria-de-la-Torre, A. Martinez-Lopez, S. Arias-Santiago, Mesenchymal stromal cell-conditioned medium for skin diseases: a systematic review, Front. Cell Dev. Biol. 9 (2021), 654210.
[32] C. Chang, J. Yan, Z. Yao, C. Zhang, X. Li, H.-Q. Mao, Effects of mesenchymal stem cell-derived paracrine signals and their delivery strategies, Adv. Healthc. Mater. 10 (2021), e2001689.
[33] L. Mazini, M. Ezzoubi, G. Malka, Overview of current adipose-derived stem cell (ADSCs) processing involved in therapeutic advancements: flow chart and regulation updates before and after COVID-19, Stem Cell Res Ther 12 (2021) 1.
[34] Escobar, Processo de obtenção de ligante "binder" baseado em poli (isopreno) utilizado na moldagem de pós por injeção (mpi) e uso, BR 10 2013 008311-9 A2, 2013.
[35] Metal Powder Industries Federation, Standard Test Method 42: Method for Determination of Density of Compacted or Sintered Powder Metallurgy (PM) Products Materials, Princeton, 2016.
[36] E04 Committee, Guide for Preparation of Metallographic Specimens, ASTM International, West Conshohocken, PA, 2017, https://doi.org/10.1520/E0003-11R17.
[37] E04 Committee, Test Method for Determining Volume Fraction by Systematic Manual Point Count, ASTM International, West Conshohocken, PA, 2019, https://doi.org/10.1520/E0562-19.
[38] E04 Committee, Test Method for Microindentation Hardness of Materials, ASTM International, West Conshohocken, PA, 2017, https://doi.org/10.1520/E0384-17.
[39] E28 Committee, Test Method for Brinell Hardness of Metallic Materials, ASTM International, West Conshohocken, PA, 2015, https://doi.org/10.1520/E0010-15.
[40] L.I.S. Naasani, A.F.D. Souza, C. Rodrigues, S. Vedovatto, J.G. Azevedo, A.P. S. Bertoni, M. Da Cruz Fernandes, S. Buchner, M.R. Wink, Decellularized human amniotic membrane associated with adipose derived mesenchymal stromal cells as a bioscaffold: physical, histological and molecular analysis, Biochem. Eng. J. 152 (2019), 107366, https://doi.org/10.1016/j.bej.2019.107366.
[41] S. Vedovatto, J.C. Facchini, R.K. Batista, T.C. Paim, M.I.Z. Lionzo, M.R. Wink, Development of chitosan, gelatin and liposome film and analysis of its biocompatibility in vitro, Int. J. Biol. Macromol. 160 (2020) 750–757.
[42] International Organization for Standardization, ISO 10993-12:2012 Biological Evaluation of Medical Devices — Part 12: Sample Preparation and Reference Materials, 2012.
[43] A. Drynda, T. Hassel, F.W. Bach, M. Peuster, In vitro and in vivo corrosion properties of new iron-manganese alloys designed for cardiovascular applications, J Biomed Mater Res B Appl Biomater 103 (2015) 649–660.
[44] R.M. German, Powder Injection Molding, German Metal Powder Industries Federation American Powder Metallurgy, Princeton, 1990.
[45] ASTM International, Standard Practice for Assessment of Hemolytic Properties of Materials, West Conshohocken, PA, 2008, https://doi.org/10.1520/f0756-08.
[46] S. Supriadi, D. Abdussalam, T. Heriyanto, B. Irawan, B. Suharno, Transformation of orthodontics bracket geometry in metal injection molding process, IOP Conf. Ser. Mater. Sci. Eng. 432 (2018), 012002, https://doi.org/10.1088/1757-899x/432/1/012002.
[47] R.M. German, A. Bose, Injection Molding of Metals and Ceramics, Metal Powder Industry, 1997.
[48] P.A. Davies, G.R. Dunstan, D.F. Heaney, T.J. Mueller, Comparison of master alloy and pre-alloyed 316l stainless steel powders for metal injection molding (MIM), in: PM2 TEC 2004 World Congress, Chicago, 2004. https://www.materials.sandvik/globalassets/global/downloads/products_downloads/metal_powders/technical_papers/comparison-of-master-alloy-and-pre-alloyed-316l.pdf.
[49] R.M. German, Powder Metallurgy Science, Metal Powder Industries Federation, Princeton, 1994.
[50] J.J. Elsner, A. Kraitzer, O. Grinberg, M. Zilberman, Highly porous drug-eluting structures: from wound dressings to stents and scaffolds for tissue regeneration, Biomatter 2 (2012) 239–270.
[51] N. Baltzer, T. Copponnex, Precious Metals for Biomedical Applications, Elsevier, 2014.
[52] X. Gu, W.R. Zhou, Y. Zheng, Y. Cheng, S. Wei, S.P. Zhong, T.F. Xi, L.J. Chen, Corrosion fatigue behaviors of two biomedical mg alloys – AZ91D and WE43 – in simulated body fluid, Acta Biomater. 6 (2010) 4605–4613.
[53] P.K. Bowen, J. Drelich, J. Goldman, A new in vitro–in vivo correlation for bioabsorbable magnesium stents from mechanical behavior, Mater. Sci. Eng. C 33 (2013) 5064–5070, https://doi.org/10.1016/j.msec.2013.08.042.
[54] B. Song, S. Dong, S. Deng, H. Liao, C. Coddet, Microstructure and tensile properties of iron parts fabricated by selective laser melting, Opt. Laser Technol. 56 (2014) 451–460, https://doi.org/10.1016/j.optlastec.2013.09.017.
[55] K. Patatas, G. Robinson, V. Shrivastava, R. Lakshminarayan, A novel endovascular technique in the management of a large internal iliac artery aneurysm associated with an arteriovenous fistula, Cardiovasc. Revasc. Med. 14 (2013) 62–65, https://doi.org/10.1016/j.carrev.2012.10.002.
[56] A. Witkowski, W. Ruzyłło, R. Gil, B. Górecka, Z. Purzycki, M. Kośmider, L. Poloński, A. Lekston, M. Gasior, K. Zmudka, P. Pieniazek, P. Buszman, J. Drzewiecki, D. Ciećwierz, Z. Sadowski, A randomized comparison of elective high-pressure stenting with balloon angioplasty: six-month angiographic and two-year clinical follow-up. On behalf of AS (Angioplasty or Stent) trial investigators, Am. Heart J. 140 (2000) 264–271.
[57] B. Al-Mangour, R. Mongrain, S. Yue, Coronary stents fracture: an engineering approach (review), Mater. Sci. Appl. 04 (2013) 606–621, https://doi.org/10.4236/msa.2013.410075.
[58] M. Moravej, D. Mantovani, Biodegradable metals for cardiovascular stent application: interests and new opportunities, Int. J. Mol. Sci. 12 (2011) 4250–4270.
[59] H. Hermawan, D. Dubé, D. Mantovani, Development of degradable fe-35Mn alloy for biomedical application, Adv. Mater. Res. 15–17 (2006) 107–112, https://doi.org/10.4028/www.scientific.net/amr.15-17.107.
[60] International Organization for Standardization, Biological evaluation of medical devices - part 5: tests for in vitro cytotoxicity (ISO 10993-5:2009). https://books.google.com/books/about/Biological_Evaluation_of_Medical_Devices.html?hl=&id=TnA9MwEACAAJ, 2009.
[61] European Powder Metallurgy Association, Euro PM2013 Congress & Exhibition: Compaction, Full Density and Alternative Consolidation, Heat Treatment, European Powder Metallurgy Association, 2013.
[62] N.M. Daud, N.B. Sing, A.H. Yusop, F.A.A. Majid, H. Hermawan, Degradation and in vitro cell–material interaction studies on hydroxyapatite-coated biodegradable porous iron for hard tissue scaffolds, J. Orthop. Trauma Transl. 2 (2014) 177–184, https://doi.org/10.1016/j.jot.2014.07.001.
[63] J. Cheng, T. Huang, Y.F. Zheng, Microstructure, mechanical property, biodegradation behavior, and biocompatibility of biodegradable fe-Fe2O3 composites, J. Biomed. Mater. Res. A 102 (2014) 2277–2287.
[64] E. Zhang, H. Chen, F. Shen, Biocorrosion properties and blood and cell compatibility of pure iron as a biodegradable biomaterial, J. Mater. Sci. Mater. Med. 21 (2010) 2151–2163.
[65] R. Oriňaková, A. Oriňak, M. Giretová, Ľ.ubomír Medvecký, M. Kupková, M. Hrubovčáková, I. Maskaľová, J. Macko, F. Kaľavský, A study of

cytocompatibility and degradation of iron-based biodegradable materials, J. Biomater. Appl. 30 (2016) 1060–1070.
[66] F.L. Nie, Y.F. Zheng, S.C. Wei, C. Hu, G. Yang, In vitro corrosion, cytotoxicity and hemocompatibility of bulk nanocrystalline pure iron, Biomed. Mater. 5 (2010), 065015.
[67] J. Kzhyshkowska, A. Gudima, V. Riabov, C. Dollinger, P. Lavalle, N.E. Vrana, Macrophage responses to implants: prospects for personalized medicine, J. Leukoc. Biol. 98 (2015) 953–962.
[68] B.N. Brown, B.D. Ratner, S.B. Goodman, S. Amar, S.F. Badylak, Macrophage polarization: an opportunity for improved outcomes in biomaterials and regenerative medicine, Biomaterials 33 (2012) 3792–3802.
[69] R. Kardorff, J. Fuchs, M. Peuster, B. Rodeck, Infantile hemangioendothelioma of the liver–sonographic diagnosis and follow-up, Ultraschall Med. 22 (2001) 258–264.

9. CONCLUSÃO

Este estudo visou contribuir para o avanço da engenharia de tecidos, avaliando novos biomateriais para aplicações médicas nas áreas de regeneração óssea, cardiovascular e dérmica. Além disso, abordou a possibilidade do uso das células tronco mesenquimais em diferentes terapias, em especial na medicina regenerativa.

O presente estudo apresentou a associação do geopolímero de metacaulinita com hidroxiapatita como um material biocompatível e promissor para aplicações em implantes ósseos devido às suas propriedades físicas e biocompatibilidade. Essa abordagem abre caminho para futuras investigações sobre os efeitos sinérgicos com células tronco mesenquimais, visando aprimorar as estratégias de engenharia de tecido ósseo.

Os resultados obtidos também destacam o promissor uso da moldagem de pós-metálicos por injeção na fabricação de implantes médicos de ferro puro, como os *stents* cardiovasculares. Amostras foram produzidas através da moldagem de pós-metálicos por injeção utilizando um novo ligante ecológico. As propriedades mecânicas e físicas avaliadas foram consideradas adequadas para dispositivos biomédicos. Além disso, evidenciamos que o ferro produzido é biocompatível in vitro com MSCs e HUVECs (estudo em desenvolvimento) e não promove toxicidade in vivo após implantação subcutânea em ratos *Wistar*.

Ademais, o trabalho traz novas perspectivas no âmbito de desenvolvimento de substitutos dérmicos utilizando células geneticamente modificadas que são potenciais para o uso. Nesta perspectiva foi desenvolvido um substituto com inibição da expressão de CD73 em queratinócitos e fibroblastos para avaliar o papel dessa enzima na regeneração da pele e nos processos de cicatrização de feridas.

Para aumentar a aplicabilidade dos resultados, futuros estudos devem incluir avaliações in vivo da biocompatibilidade e funcionalidade dos biomateriais em modelos animais no local proposto para aplicação. Estudos de longo prazo são necessários para avaliar a degradação e integração dos biomateriais com o tecido hospedeiro. Isso é particularmente importante para implantes ósseos, onde a estabilidade mecânica e a biocompatibilidade a longo prazo são críticas e *stents* biodegradáveis em que o processo corrosivo deve garantir o remodelamento do tecido antes de sua desintegração.

ANEXO A – Parecer de aprovação do comitê de Ética da UFCSPA e da ISCMPA: Isolamento de células a partir de material de descarte humano para o uso em medicina regenerativa

IRMANDADE DA SANTA CASA DE MISERICORDIA DE PORTO ALEGRE - ISCMPA

Plataforma Brasil

PARECER CONSUBSTANCIADO DO CEP

DADOS DO PROJETO DE PESQUISA

Título da Pesquisa: Isolamento de células a partir de material de descarte humano para estudos em medicina regenerativa

Pesquisador: Marcia Rosangela Wink

Área Temática:

Versão: 2

CAAE: 98290318.5.0000.5335

Instituição Proponente: ISCMPA

Patrocinador Principal: Fundação de Amparo a Pesquisa do Estado do Rio Grande do Sul

DADOS DO PARECER

Número do Parecer: 3.029.141

Apresentação do Projeto:

Projeto de pesquisa a ser realizado em parceria com o Laboratório de Biologia Celular da Universidade Federal de Ciências da Saúde de Porto Alegre e as Unidades de Obstetrícia, Oftalmologia e Cirurgia Plástica da Santa Casa de Porto Alegre, utilizando material de descarte hospitalar como lipoaspirado, pele, limbo esclero-corneal, membrana amniótica e cordão umbilical, serão extraídos diferentes tipos celulares humanos (queratinócitos, melanócitos, células estromais mesenquimais e células endoteliais) para o desenvolvimento de novas terapias celulares para medicina regenerativa, como a aplicação de células estromais mesenquimais em sítios lesionados e também para a verificação da biocompatibilidade de materiais propostos para uso clínico, tais como filmes de quitosana e colágeno, stents cardíacos de ferro e geopolímeros.

Objetivo da Pesquisa:

Já referido em parecer anteriormente emitido.

Avaliação dos Riscos e Benefícios:

Já referido em parecer anteriormente emitido.

Comentários e Considerações sobre a Pesquisa:

Já referido em parecer anteriormente emitido.

Endereço: R. Profº Annes Dias,295 Hosp.Dom Vicente Scherer
Bairro: 6º andar - Centro **CEP:** 90.020-090
UF: RS **Município:** PORTO ALEGRE
Telefone: (51)3214-8571 **Fax:** (51)3214-8571 **E-mail:** cep@santacasa.tche.br

IRMANDADE DA SANTA CASA DE MISERICORDIA DE PORTO ALEGRE - ISCMPA

Continuação do Parecer: 3.029.141

Considerações sobre os Termos de apresentação obrigatória:
Já referido em parecer anteriormente emitido.

Recomendações:
Inserido nº do CNPJ na Folha de Rosto para Pesquisa envolvendo seres humanos.

Conclusões ou Pendências e Lista de Inadequações:
As pendências solicitadas foram atendidas conforme carta e documentos anexados, a pesquisa está de acordo com a resolução vigente.

Considerações Finais a critério do CEP:
Após reavaliação do protocolo acima descrito, o presente comitê não encontrou óbices quanto ao desenvolvimento do estudo em nossa Instituição e poderá ser iniciado a partir da data deste parecer.

Obs.: 1 - O pesquisador responsável deve encaminhar à este CEP, Relatórios de Andamento dos Projetos desenvolvidos na ISCMPA. Relatórios Parciais (pesquisas com duração superior à 6 meses), Relatórios Finais (ao término da pesquisa) e os Resultados Obtidos (cópia da publicação).

2 – Para o início do projeto de pesquisa, o investigador deverá apresentar a chefia do serviço (onde será realizada a pesquisa), o Parecer Consubstanciado de aprovação do protocolo pelo Comitê de Ética.

Este parecer foi elaborado baseado nos documentos abaixo relacionados:

Tipo Documento	Arquivo	Postagem	Autor	Situação
Informações Básicas do Projeto	PB_INFORMAÇÕES_BÁSICAS_DO_PROJETO_1200535.pdf	12/11/2018 16:54:02		Aceito
Recurso Anexado pelo Pesquisador	CARTA_RESPOSTA_AO_CEP.pdf	12/11/2018 16:53:24	Samlai Vedovatto	Aceito
Projeto Detalhado / Brochura Investigador	PROJETO_MATERIAIS_DE_DESCARTE.pdf	12/11/2018 16:50:59	Samlai Vedovatto	Aceito
Folha de Rosto	FOLHA_DE_ROSTO.pdf	12/11/2018 16:49:40	Samlai Vedovatto	Aceito
TCLE / Termos de Assentimento / Justificativa de	TCLEs_materiais_descarte_e_justificativas.pdf	12/09/2018 17:57:45	THAIS CASAGRANDE PAIM	Aceito

Endereço: R. Profº Annes Dias,295 Hosp.Dom Vicente Scherer
Bairro: 6º andar - Centro **CEP:** 90.020-090
UF: RS **Município:** PORTO ALEGRE
Telefone: (51)3214-8571 **Fax:** (51)3214-8571 **E-mail:** cep@santacasa.tche.br

IRMANDADE DA SANTA CASA DE MISERICORDIA DE PORTO ALEGRE - ISCMPA

Continuação do Parecer: 3.029.141

Ausência	TCLEs_materiais_descarte_e_justificativas.pdf	12/09/2018 17:57:45	THAIS CASAGRANDE	Aceito
Outros	Formulario_Cadastro_Projetos_Unidade_Pesquisa.pdf	16/08/2018 16:02:38	Samlai Vedovatto	Aceito
Declaração de Instituição e Infraestrutura	Termo_responsavel_setor_onde_realizada_pesquisa.pdf	16/08/2018 16:00:56	Samlai Vedovatto	Aceito
Declaração de Pesquisadores	Termo_entrega_relatorios.pdf	16/08/2018 15:59:54	Samlai Vedovatto	Aceito
Outros	Declaracao_de_autorizacao_da_chefia_responsavel.pdf	16/08/2018 15:56:09	Samlai Vedovatto	Aceito
Outros	Formulario_Inscricao_Projetos_pesquisa.pdf	16/08/2018 15:52:48	Samlai Vedovatto	Aceito
Declaração de Pesquisadores	Declaracao_utilizacao_dados_prontuario.pdf	16/08/2018 15:51:29	Samlai Vedovatto	Aceito
Declaração de Instituição e Infraestrutura	Declaracao_isencao_onus_instituicao.pdf	16/08/2018 15:50:45	Samlai Vedovatto	Aceito
Declaração de Pesquisadores	Declaracao_confidencialidade_sujeito_estudo.pdf	16/08/2018 15:49:41	Samlai Vedovatto	Aceito
Declaração de Manuseio Material Biológico / Biorepositório / Biobanco	Declaracao_utilizacao_dados_material_biologico.pdf	16/08/2018 15:48:11	Samlai Vedovatto	Aceito

Situação do Parecer:
Aprovado

Necessita Apreciação da CONEP:
Não

PORTO ALEGRE, 21 de Novembro de 2018

Assinado por:
ELIZETE KEITEL
(Coordenador(a))

Endereço: R. Profº Annes Dias,295 Hosp.Dom Vicente Scherer
Bairro: 6º andar - Centro **CEP:** 90.020-090
UF: RS **Município:** PORTO ALEGRE
Telefone: (51)3214-8571 **Fax:** (51)3214-8571 **E-mail:** cep@santacasa.tche.br

UNIVERSIDADE FEDERAL DE CIÊNCIAS DA SAÚDE DE PORTO ALEGRE

PARECER CONSUBSTANCIADO DO CEP

Elaborado pela Instituição Coparticipante

DADOS DO PROJETO DE PESQUISA

Título da Pesquisa: Isolamento de células a partir de material de descarte humano para estudos em medicina regenerativa

Pesquisador: Marcia Rosangela Wink

Área Temática:

Versão: 1

CAAE: 98290318.5.3001.5345

Instituição Proponente: Universidade Federal de Ciências da Saúde de Porto Alegre

Patrocinador Principal: Fundação de Amparo a Pesquisa do Estado do Rio Grande do Sul

DADOS DO PARECER

Número do Parecer: 3.214.091

Apresentação do Projeto:

Projeto de pesquisa a ser realizado em parceria com o Laboratório de Biologia Celular da Universidade Federal de Ciências da Saúde de Porto Alegre e as Unidades de Obstetrícia, Oftalmologia e Cirurgia Plástica da Santa Casa de Porto Alegre, utilizando material de descarte hospitalar como lipoaspirado, pele, limbo esclero-corneal, membrana amniótica e cordão umbilical, serão extraídos diferentes tipos celulares humanos (queratinócitos, melanócitos, células estromais mesenquimais e células endoteliais) para o desenvolvimento de novas terapias celulares para medicina regenerativa, como a aplicação de células estromais mesenquimais em sítios lesionados e também para a verificação da biocompatibilidade de materiais propostos para uso clínico, tais como filmes de quitosana e colágeno, stents cardíacos de ferro e geopolímeros.

Objetivo da Pesquisa:

Objetivo Primário:

Isolar células de tecidos humanos, que seriam descartados, para estudos que gerem novas terapias com potencial uso em medicina regenerativa.

Objetivo Secundário:

-Isolar e caracterizar células estromais mesenquimais de tecidos humanos de descarte: pele, cordão umbilical, gordura e limbo esclerocorneal para serem estudadas e testadas em biomateriais

Endereço: Rua Sarmento Leite ,245
Bairro: Sarmento **CEP:** 90.050-170
UF: RS **Município:** PORTO ALEGRE
Telefone: (51)3303-8804 **E-mail:** cep@ufcspa.edu.br

UNIVERSIDADE FEDERAL DE CIÊNCIAS DA SAÚDE DE PORTO ALEGRE

utilizados em regeneração tecidual;-Isolar e caracterizar queratinócitos e melanócitos de pele humana e limbo esclerocorneal, para aplicação em biomateriais;
-Isolar e caracterizar Células Endoteliais da Veia Umbilical Humana (HUVEC) obtidas de cordão umbilical (proveniente de partos a termo) para avaliar a biocompatibilidade in vitro de amostras de ferro, micro moldado por injeção, para uso em stents cardíacos;
-Estudar in vitro a biocompatibilidade de metais biocorrosíveis com células estromais mesenquimais humanas (MSCs);
-Avaliar a biocompatibilidade da membrana amniótica humana e de uma matriz compósita de quitosana e colágeno com células estromais mesenquimais
humanas.

Avaliação dos Riscos e Benefícios:

Riscos: O único risco ao doador de material de descarte é não ser respeitada a confidencialidade das suas informações pessoais, para prevenção deste problema os pesquisadores assinarão a declaração de compromisso para utilização de dados de material biológico e a declaração de confidencialidade do sujeito no estudo.

Benefícios:

Provavelmente não haverá benefício imediato para o paciente doador. A doação dos materiais poderá vir a beneficiar futuramente a população como um todo gerando novas opções de tratamento para a medicina regenerativa.

Comentários e Considerações sobre a Pesquisa:

O projeto foi iniciado conforme parecer emitido anteriormente.

Considerações sobre os Termos de apresentação obrigatória:

Todos os termos apresentados.

Recomendações:

A entrega do relatório final está prevista para março/2019,no entanto está data deverá ser corrigida pois o projeto está sendo aprovado neste mesmo mês/ano.
Lembramos que o projeto deve iniciar apenas após a aprovação do CEP.

Conclusões ou Pendências e Lista de Inadequações:

Projeto em andamento.
Aprovar

Endereço: Rua Sarmento Leite ,245
Bairro: Sarmento **CEP:** 90.050-170
UF: RS **Município:** PORTO ALEGRE
Telefone: (51)3303-8804 **E-mail:** cep@ufcspa.edu.br

UNIVERSIDADE FEDERAL DE CIÊNCIAS DA SAÚDE DE PORTO ALEGRE

Continuação do Parecer: 3.214.091

Considerações Finais a critério do CEP:

De acordo com o parecer do Relator.

Este parecer foi elaborado baseado nos documentos abaixo relacionados:

Tipo Documento	Arquivo	Postagem	Autor	Situação
Informações Básicas do Projeto	PB_INFORMAÇÕES_BÁSICAS_DO_PROJETO_1261653.pdf	15/01/2019 16:57:14		Aceito
Outros	termo.pdf	15/01/2019 16:51:23	Marcia Rosangela Wink	Aceito
Projeto Detalhado / Brochura Investigador	PROJETO_MATERIAIS_DE_DESCARTE.pdf	12/11/2018 16:50:59	Samlai Vedovatto	Aceito
TCLE / Termos de Assentimento / Justificativa de Ausência	TCLEs_materiais_descarte_e_justificativas.pdf	12/09/2018 17:57:45	THAIS CASAGRANDE PAIM	Aceito
Outros	Formulario_Cadastro_Projetos_Unidade_Pesquisa.pdf	16/08/2018 16:02:38	Samlai Vedovatto	Aceito
Outros	Declaracao_de_autorizacao_da_chefia_responsavel.pdf	16/08/2018 15:56:09	Samlai Vedovatto	Aceito
Outros	Formulario_Inscricao_Projetos_pesquisa.pdf	16/08/2018 15:52:48	Samlai Vedovatto	Aceito
Declaração de Manuseio Material Biológico / Biorepositório / Biobanco	Declaracao_utilizacao_dados_material_biologico.pdf	16/08/2018 15:48:11	Samlai Vedovatto	Aceito

Situação do Parecer:

Aprovado

Necessita Apreciação da CONEP:

Não

PORTO ALEGRE, 21 de Março de 2019

Assinado por:
Fernanda Bordignon Nunes
(Coordenador(a))

Endereço: Rua Sarmento Leite ,245
Bairro: Sarmento **CEP:** 90.050-170
UF: RS **Município:** PORTO ALEGRE
Telefone: (51)3303-8804 **E-mail:** cep@ufcspa.edu.br

ANEXO B – Parecer de aprovação do comitê de Ética da UFCSPA: Avaliação da hemocompatibilidade de biomateriais.

UNIVERSIDADE FEDERAL DE CIÊNCIAS DA SAÚDE DE PORTO ALEGRE

Plataforma Brasil

PARECER CONSUBSTANCIADO DO CEP

DADOS DO PROJETO DE PESQUISA

Título da Pesquisa: Avaliação da hemocompatibilidade de biomateriais.
Pesquisador: Marcia Rosangela Wink
Área Temática:
Versão: 2
CAAE: 17626719.6.0000.5345
Instituição Proponente: Universidade Federal de Ciências da Saúde de Porto Alegre
Patrocinador Principal: Fundação de Amparo a Pesquisa do Estado do Rio Grande do Sul

DADOS DO PARECER

Número do Parecer: 3.594.874

Apresentação do Projeto:
Os biomateriais e dispositivos candidatos ao uso clínico necessitam de análises prévias in vitro para demonstrar a sua biocompatibilidade. Os ensaios de hemocompatibilidade dos materiais que entram em contato com sangue é um dos requisitos recomendados pela International Organization for Standardization (ISO) "ISO 10993 – Biological Evaluation of Medical Devices". O presente projeto visa estudar in vitro a hemocompatibilidade dos seguintes biomateriais para uso em medicina regenerativa: biovidro 45s5 e hidroxiapatita/metakaolinita para regeneração óssea, ferro para uso em stents cardiovascular e matriz compósita de quitosana e colágeno para regeneração cutânea. Serão convidados 20 participantes saudáveis para doarem, de forma espontânea, 10 mL de sangue total para a realização do teste de hemólise e de adesão plaquetária dos biomateriais estudados. Os demais testes in vitro que incluem avaliação de citotoxicidade e genotoxicidade com células primárias humanas provenientes de tecido de descarte hospitalar já foram aprovados (CEP-UFCSPA: 3.214.091) e estão em andamento.

Objetivo da Pesquisa:
Objetivo Primário:
Estudar in vitro a hemocompatibilidade de biomateriais para uso em medicina regenerativa.

Objetivos Secundários:
Analisar a hemocompatibilidade do Biovidro 45s5 e hidroxiapatita/metakaolinita para regeneração

Endereço: Rua Sarmento Leite ,245
Bairro: Sarmento **CEP:** 90.050-170
UF: RS **Município:** PORTO ALEGRE
Telefone: (51)3303-8804 **E-mail:** cep@ufcspa.edu.br

UNIVERSIDADE FEDERAL DE CIÊNCIAS DA SAÚDE DE PORTO ALEGRE

óssea;
Verificar a hemocompatibilidade de matriz compósita de quitosana e colágeno para regeneração cutânea;
Investigar a hemocompatibilidade do ferro para uso em stents cardíacos.

Avaliação dos Riscos e Benefícios:

Riscos:

Hematoma temporário e tontura, podendo haver desmaio após a coleta de sangue.

Benefícios:

Não há benefício direto ao participante da pesquisa. No entanto, pode ser que os resultados deste estudo tragam um benefício para uma parcela de pacientes no futuro.

Comentários e Considerações sobre a Pesquisa:

Os participantes serão recrutados por conveniência, sendo membros da comunidade interna UFCSPA, principalmente do Laboratório de Biologia Celular, que se voluntariarem a participar do estudo. Ressalta-se que o nome da instituição não será mencionada, vinculando os doadores, em trabalhos oriundos do referido estudo. SENDO OS MEMBROS DA COMUNIDADE INTERNA HÁ NECESSIDADE DE UM TERMO DE ANUÊNCIA DA REITORIA.

Será utilizada apenas a auto declaração do participante quanto a doença transmissível pelo sangue, uma vez que a presença de alguma doença não afetará a metodologia e o resultado do teste. Para o manuseio de todas as amostras sanguíneas serão utilizados EPIs, evitando intempéries que possam ocorrer.

TCLE ajustado conforme parecer anterior.

A participação no estudo não acarretará custos de deslocamento, uma vez que a coleta ocorrerá no tempo livre do participante na UFCSPA, pois ele já se desloca ao local diariamente para sua atividades de trabalho ou acadêmicas.

Considerações sobre os Termos de apresentação obrigatória:

Folha de rosto devidamente assinada e carimbada.

Termo de anuência assinado e carimbado.

Termo de compromisso para entrega dos relatórios (parcial julho 2021 e final julho 2022).

TCLE ajustado.

Recomendações:

aprovar

Endereço: Rua Sarmento Leite ,245
Bairro: Sarmento **CEP:** 90.050-170
UF: RS **Município:** PORTO ALEGRE
Telefone: (51)3303-8804 **E-mail:** cep@ufcspa.edu.br

UNIVERSIDADE FEDERAL DE CIÊNCIAS DA SAÚDE DE PORTO ALEGRE

Plataforma Brasil

Continuação do Parecer: 3.594.874

Conclusões ou Pendências e Lista de Inadequações:

Aprovar

Considerações Finais a critério do CEP:

De acordo com o parecer do Relator.

Este parecer foi elaborado baseado nos documentos abaixo relacionados:

Tipo Documento	Arquivo	Postagem	Autor	Situação
Informações Básicas do Projeto	PB_INFORMAÇÕES_BÁSICAS_DO_PROJETO_1396631.pdf	25/08/2019 19:59:37		Aceito
TCLE / Termos de Assentimento / Justificativa de Ausência	TCLE_HEMOCOMPATIBILIDADE.pdf	25/08/2019 19:56:15	THAIS CASAGRANDE PAIM	Aceito
Outros	Carta_de_resposta_ao_cep_ufcspa_projeto_hemocompatibilidade.pdf	25/08/2019 19:54:56	THAIS CASAGRANDE	Aceito
Projeto Detalhado / Brochura Investigador	PROJETO_HEMOCOMPATIBILIDADE.docx	25/08/2019 19:52:15	THAIS CASAGRANDE PAIM	Aceito
Declaração de Pesquisadores	Termo_de_compromisso_para_entrega_de_relatorios.pdf	16/07/2019 16:39:03	THAIS CASAGRANDE	Aceito
Declaração de Instituição e Infraestrutura	Termo_de_anuencia_pelo_local_de_pesquisa.pdf	16/07/2019 16:38:21	THAIS CASAGRANDE PAIM	Aceito
Folha de Rosto	Folha_de_rosto.pdf	16/07/2019 14:50:29	THAIS CASAGRANDE	Aceito

Situação do Parecer:

Aprovado

Necessita Apreciação da CONEP:

Não

PORTO ALEGRE, 24 de Setembro de 2019

Assinado por:
Luciane Dalcanale Moussalle
(Coordenador(a))

Endereço: Rua Sarmento Leite ,245
Bairro: Sarmento **CEP:** 90.050-170
UF: RS **Município:** PORTO ALEGRE
Telefone: (51)3303-8804 **E-mail:** cep@ufcspa.edu.br

ANEXO C – Parecer de aprovação do comitê de Ética no uso de animais

UFCSPA

COMISSÃO CIENTÍFICA E COMISSÃO DE PESQUISA E ÉTICA EM SAÚDE

COMISSÃO DE ÉTICA NO USO DE ANIMAIS - CEUA
UFCSPA

A Comissão de Ética no uso de Animais, analisou o Projeto:

Projeto: 18-247 **Versão do Projeto:** **Versão do TCLE:**

Pesquisadores:
MÁRCIA ROSÂNGELA WINK
THAÍS CASAGRANDE PAIM
LILIANA IVET SOUS NAASANI
ISADORA BERTACO
DIEGO PACHECO WERMUTH

Título: AVALIAÇÃO DA COMPATIBILIDADE E DEGRADAÇÃO IN VIVO DO FERRO 99,5 E 99,9%
P.A. PARA APLICAÇÃO BIOMÉDICA

Este projeto foi aprovado em seus aspectos éticos e metodológicos. Todo e qualquer alteração do projeto, assim com eventos adversos graves, deverão ser comunicados a esta CEUA.

Porto Alegre, 26 de março de 2019.

Profa. Fernanda Bastos de Mello
Deptº de Farmacociências
UFCSPA

APENDICE A – PRODUÇÃO CIENTÍFICA DO DOUTORADO – AUTORIA

Artigo publicado durante o doutorado, mas não incluso na tese.

Received: 15 June 2021 | Revised: 26 August 2021 | Accepted: 14 September 2021

DOI: 10.1002/jcp.30594

REVIEW ARTICLE

Journal of Cellular Physiology WILEY

The implications of the purinergic signaling throughout pregnancy

Lucas Sagrillo-Fagundes[1] | Thaís Casagrande Paim[1] | Luiza Pretto[1] | Isadora Bertaco[1] | Carla Zanatelli[1] | Cathy Vaillancourt[2] | Márcia R. Wink[1]

[1]Departamento de Ciências Básicas da Saúde e Laboratório de Biologia Celular, Universidade Federal de Ciências da Saúde de Porto Alegre, Porto Alegre, Rio Grande do Sul, Brazil

[2]Centre Armand Frappier Santé Biotechnologie, INRS, Laval, Quebec, Canada

Correspondence
Márcia R. Wink, Departamento de Ciências Básicas da Saúde e Laboratório de Biologia Celular, Universidade Federal de Ciências da Saúde de Porto Alegre, Porto Alegre, RS 90050-170, Brazil.
Email: mwink@ufcspa.edu.br

Funding information
NSERC/CRSNG, Grant/Award Number: 262011-2009; Fundação de Amparo à Pesquisa do Estado do Rio Grande do Sul; Fonds de Recherche du Québec - Nature et Technologies: B3X postdoc fellowship; Coordenação de Aperfeiçoamento de Pessoal de Nível Superior; Conselho Nacional de Desenvolvimento Científico e Tecnológico, Grant/Award Numbers: MS-SCTIE-Decit-DGITIS-CGCIS/CNPq no 26/2020, and MS-SCTIE-Decit/CNPq no 12/2018

Abstract

Purinergic signaling is a necessary mechanism to trigger or even amplify cell communication. Its ligands, notably adenosine triphosphate (ATP) and adenosine, modulate specific membrane-bound receptors in virtually all human cells. Regardless of the stage of the pregnancy, cellular communication between maternal, placental, and fetal cells is the paramount mechanism to sustain its optimal status. In this review, we describe the crucial role of purinergic signaling on the regulation of the maternal-fetal trophic exchanges, immune control, and endocrine exchanges throughout pregnancy. The nature of the modulation of both ATP and adenosine on the embryo-maternal interface, going through placental invasion until birth delivery depends on the general maternal-fetal health state and consequently on the selective activation of their specific receptors. In addition, an increasing number of studies have been demonstrating the pivotal role of ATP and adenosine in modulating deleterious effects of suboptimal conditions of pregnancy. Here, we discuss the role of purinergic signaling on the balance that coordinates the embryo-maternal exchanges and a promising therapeutic venue in the context of pregnancy disorders.

KEYWORDS
Adenosine, ATP, embryo-maternal interface, placenta, pregnancy

1 | INTRODUCTION

Appropriate fetal development is based on constant high levels of growth and increased metabolism. In a very simplistic view, the placenta's main responsibility is the pursuit of constant optimal materno-fetal exchange, which happens through the external layer of the placental barrier, the syncytiotrophoblast (STB). Proliferative cytotrophoblasts constantly differentiate into two main pathways: either into the villous cytotrophoblasts (vCTB), located at the chorionic trees responsible for the constant replenishment of the homeostatic status of STB; or into extravillous cytotrophoblasts (evCTB), which invade the uterine decidua (including spiral arteries), during the first trimester to increase the maternal blood flow towards the intervillous space (Figure 1; Mor et al., 2011, 2017). The human placental cells present several mechanisms (e.g., endocrine actions, regulation of the maternal immune system, and invasion of uterine arteries) to mediate the best conditions for both mother and fetus during the pregnancy. These mechanisms are constantly under modulation based on signals released in the cellular microenvironment. A plethora of placental ligands are released to modulate specific actions on target cells. These cells are either located in both the maternal and the fetal side (endocrine action), or in closer areas that are modulated by paracrine and autocrine signaling (Cervar et al.,

Lucas Sagrillo-Fagundes and Thaís Casagrande Paim contributed equally to this study.

APENDICE B – PRODUÇÃO CIENTÍFICA DO DOUTORADO – COAUTORIA

Produção científica realizada durante o doutorado - coautoria:

IOP Publishing Biofabrication 15 (2023) 015012 https://doi.org/10.1088/1758-5090/ac9ff4

Biofabrication

PAPER

Bioscaffold developed with decellularized human amniotic membrane seeded with mesenchymal stromal cells: assessment of efficacy and safety profiles in a second-degree burn preclinical model

RECEIVED
27 August 2022

REVISED
18 October 2022

ACCEPTED FOR PUBLICATION
3 November 2022

PUBLISHED
23 November 2022

Liliana Ivet Sous Naasani[1], Luiza Pretto[1], Carla Zanatelli[1], Thaís Casagrande Paim[1], Aline Francielle Damo Souza[2], Pablo Fagundes Pase[3], Marilda Da Cruz Fernandes[4], Jean Sévigny[5] and Márcia Rosângela Wink[1,*]

[1] Departamento de Ciências Básicas da Saúde, Laboratório de Biologia Celular, Universidade Federal de Ciências da Saúde de Porto Alegre—UFCSPA, Porto Alegre, RS, Brazil
[2] Banco de Tecidos Humanos—Pele Dr. Roberto Corrêa Chem, Hospital Irmandade da Santa Casa de Misericórdia de Porto Alegre—ISCMPA, Porto Alegre, RS, Brazil
[3] Cirurgia Plástica—Hospital de Pronto Socorro e Moinhos de Vento, Porto Alegre, RS, Brazil
[4] Departamento de Ciências Básicas da Saúde, Laboratório de Patologia, Universidade Federal de Ciências da Saúde de Porto Alegre—UFCSPA, Porto Alegre, RS, Brazil
[5] Département de Microbiologie-Infectiologie et d'Immunologie, Faculté de Médecine, Université Laval, Québec, QC G1V 0A6, Canada
* Author to whom any correspondence should be addressed.

E-mail: mwink@ufcspa.edu.br and marciawink@yahoo.com.br

Keywords: decellularized human amniotic membrane (DhAM), adipose derived mesenchymal stromal cells (AD-MSCs), deep second degree burn, murine preclinical model, CD73, CD11b

Supplementary material for this article is available online

Abstract

Therapies to deep burn injuries remain a global challenge. Human amniotic membrane (hAM) is a biomaterial that has been increasingly explored by the field of regenerative medicine. A decellularized hAM (DhAM) can be used as scaffold for mesenchymal stromal cells (MSCs) to grow without the loss of their stemness potential, allowing its application as cell therapy for wound healing. In this work, we associated DhAM with adipose-derived MSCs (DhAM + AD-MSCs), as a therapy strategy for second-degree burns in a preclinical model. Animals with induced second-degree burns were divided into four groups: control, which consists of a non-adherent gauze; a synthetic commercial dressing as the positive control (Control+); DhAM; and DhAM plus rat AD-MSCs (DhAM + AD-MSCs), followed by detailed and long term analysis (5 weeks). The macroscopical analysis showed the healing improvement in the wound area after the DhAM + AD-MSC treatment. Histological analysis also showed no alteration in the animal organs and a regular epithelial progression in comparison to the control. This observation was also confirmed by the analysis of suprabasal layers in the neoepidermis with CK10, showing a stratified and differentiated epithelium, when compared to Control and Control+. A strong CD73 (ecto-5′-nucleotidase) labeling was observed in the first 2 weeks postburn in dermis and epidermis. The expression in dermis was stronger in the second week in the middle of the wound, when comparing the Control+ with DhAM + AD-MSCs ($p = 0.0238$). In the epidermis the expression of CD73 was increased in all regions when compared to the control. This data suggests the involvement of this protein on wound healing. A low CD11b labeling was observed in DhAM + AD-MSCs treatment group mainly in the last treatment week, in comparison to Control and Control+ ($p < 0.0001$), which indicates a reduction in the inflammatory process. MSCs

International Journal of Biological Macromolecules 160 (2020) 750–757

Contents lists available at ScienceDirect

International Journal of Biological Macromolecules

journal homepage: http://www.elsevier.com/locate/ijbiomac

Development of chitosan, gelatin and liposome film and analysis of its biocompatibility *in vitro*

Samlai Vedovatto [a], Jordano C. Facchini [b], Raquel K. Batista [a], Thaís C. Paim [a], Maria Ismenia Z. Lionzo [b,1], Márcia R. Wink [a,*,1]

[a] Laboratório de Biologia Celular, Departamento de Ciências Básicas da Saúde, Universidade Federal de Ciências da Saúde de Porto Alegre, Porto Alegre, RS, Brazil
[b] Laboratório de Farmacociências, Departamento de Farmacociências, Universidade Federal de Ciências da Saúde de Porto Alegre, Porto Alegre, RS, Brazil

ARTICLE INFO

Article history:
Received 9 April 2020
Received in revised form 17 May 2020
Accepted 26 May 2020
Available online 29 May 2020

Keywords:
Chitosan
Gelatin
Liposome
Biomaterial
Film
Biocompatibility analysis

ABSTRACT

A film of chitosan, gelatin and liposome has been designed for dermatological applications. Several adaptations were required throughout development to facilitate *in vitro* analysis, physicochemical characterization and biocompatibility evaluation. The final version of the film was characterized by differential scanning calorimetry, evaluation of swelling and scanning electron microscopy. The biocompatibility of the film was assessed by investigating cellular parameters of three types of human cells by direct contact or through films extracts: I) primary culture of adipose-derived mesenchymal stromal cells (ADCSs) and melanoma cell lines were used to test cell adhesion and morphology by direct cell culture on the material; II) ADSCs and immortalized keratinocytes were used in cell viability assay using different films extracts. The film showed physicochemical characteristics that favored cellular input, being suitable for *in vitro* analysis, which allowed its biocompatible characteristics such as the absence of toxicity to be verified without causing significant morphological changes in ADSCs and melanoma cell line. Altogether, these results suggest that the material has a potential application for drug delivery and promotion of skin tissue repair and is therefore worthwhile for further investigations using preclinical models to cover dermal lesions.

1. Introduction

The fields of tissue engineering and regenerative medicine have suggested dermal substitutes of different materials aimed at accelerating wound healing. From natural to synthetic, these matrices with pro-regenerative characteristics are developed through a combination of substances that have the capacity to carry drugs and biomolecules to improve their properties [1]. These structures can be designed to release drugs in a controlled manner, through assembling and/or association with carriers of different origins and configurations. Several combinations can be used to provide different strategies to administer biologically active compounds, acting as delivery systems [2].

Chitosan is a cationic polymer derived from chitin, an abundant polysaccharide extracted from invertebrate skeletons [3]. Due to its biocompatibility, non-toxicity, stability, low allergenicity and biodegradability properties, chitosan is a suitable material for dermal substitutes [4]. In addition to the biological functions, chitosan film architecture enables the creation of a structure which guarantees material's integrity while handling [5]. This polymer has previously been used as a scaffold loaded with bioactive molecules with different applications for epithelial and soft tissues, such as vascularization, nerve regeneration, periodontal tissue repair and others [6]. To accomplish sustained drug release in chitosan scaffolds, nanoparticles and liposomes may be employed to carry and deliver the substance of interest [7].

Many studies have shown that chitosan-based materials promote wound healing and can be utilized for drug delivery. For example, Değim et al. demonstrated that a chitosan gel formulation containing liposomes loaded with epidermal growth factor led to more rapid epithelialization of second-degree burn wounds in treated rats [8]. In another study, Griseofulvin-loaded liposomes in chitosan film were developed with greater efficiency by Bavarsad et al. for topical drug delivery in superficial fungal infections [9]. Additionally, a composite chitosan-based vaginal sheet successfully incorporated drugs to treat vaginal clinical conditions characterized by excessive fluid [10]. Chitosan hydrogels have also been used in mucoadhesive semisolid formulations combined with polymeric nanocarriers for the treatment of human papillomavirus infection. In this study the authors found that nanocapsules incorporated into chitosan hydrogel performed better than chitosan-coated nanocapsules incorporated into hydroxyethylcellulose gel [11]. These studies indicate that chitosan-derived materials are a promising tool for wound therapy and other clinical issues affecting the skin and mucosa.

* Corresponding author.
E-mail address: marciawink@yahoo.com.br (M.R. Wink).
[1] These authors share senior authorship.

https://doi.org/10.1016/j.ijbiomac.2020.05.229
0141-8130/